SULPHUR DIOXIDE CAPTURE UNDER FLUIDISED BED COMBUSTION CONDITIONS USING DOLOMITE AND COAL ASH AS SORBENTS

Steady Mukondiwa

B.Eng Chemical Engineering (NUST Zimbabwe)

This dissertation is presented in partial fulfilment of the requirements for the degree Master of Science (Chemical Engineering) in the School of Chemical and Minerals Engineering at North-West University, Potchefstroom Campus.

Supervisor: Prof. R.C. Everson

Co-Supervisor: Prof. H.W.J.P. Neomagus

November 2007
Potchefstroom

DECLARATION

I, Steady Mukondiwa do hereby declare that the dissertation with the title SULPHUR DIOXIDE CAPTURE UNDER FLUIDISED BED COMBUSTION CONDITIONS USING DOLOMITE AND COAL ASH AS SORBENTS submitted in partial fulfilment of the requirements for the degree Master of Science (Chemical Engineering) is my work and has not been submitted at any other university either in whole or in part.

Signed at Potchefstroom on the ..... day of 2007

.....

S. Mukondiwa

ACKNOWLEDGEMENTS

I would like to convey my heartfelt appreciation to all those who assisted me in making this research a success. Duly thanks to the following:

- Fore-mostly to God be utmost glory for the great things He has done, for making ways where there seemed to be no way and for making all things possible.
- The Government of South Africa for allowing me an opportunity to study at North-West University.
- North-West University's School of Chemical and Minerals Engineering for giving me an opportunity to explore and experience the world of research.
- Professor R.C Everson and Professor H.J.W.P Neomagus for being real mentors giving light when there was darkness and giving hope when the road seemed heavy.
- Dr. Rufaro Kaitano for being a brother, a friend, a colleague and a technical advisor throughout the process of making this research a success.
- Mr Jan Kroeze and Mr Adrian Brock for maintaining the equipment in a world-class standard, giving help when it was needed and assisting in all spheres to the best of their abilities.
- Mr Hertzorg Bissett for taking his valuable time in assisting with characterisation work.
- To my fiancé Letwin Mucharuona who stood by me in prayer and with love.
- My brother Benedict Winsper for the great support, may God bless him.
- To my family for imparting on me the virtues of hard work which made me achieve this.

ABSTRACT

A study was done to investigate sulphur dioxide capture capacities of South African mined dolomites, limestone and coal ash derived from high inertinite coal. The study was carried out under atmospheric and pressurised fluidised bed coal combustion conditions using a thermogravimetric analyser. Temperatures between 750-900°C were used. A typical flue gas mixture composed of 2000ppm SO_2, 5.3% O_2 and CO_2 concentration of 10 and 20% for atmospheric and pressurised sulphation respectively and balance N_2 was used. The performance of the sorbents was examined at atmospheric (0.875 bar) pressure where the active part of the sorbent was CaO and at 10 and 15 bar where the active part of the sorbent was $CaCO_3$. Coal ash had a calcium content of 7% by weight, this was much lower compared to dolomite and limestone which had between 20-30% calcium by weight. The sorbents' structural characterisation was done using nitrogen adsorption and mercury porosimetry. Compared to coal ash, the raw dolomite and limestone had a relatively smaller internal surface area, between 0.4-1.0 m^2/g, for the uncalcined state, then increasing to between 10-15 m^2/g on calcination. Coal ash had a relatively high internal surface area of 11 m^2/g, which is comparable to the calcined sorbents. The porosity of raw sorbents increased from about 0.2 to 0.35 on calcination. Sulphation at atmospheric pressure showed a calcium conversion of between 22-44% for dolomites, 37-49% for limestone and 13-28% for coal ash after 180 minutes. At atmospheric pressure, dolomites and coal ash reactivity started off relatively fast followed by a sudden decline after 20% conversion, this is attributed to the change from kinetic control to product layer control; limestone did not show a decline in reactivity. Under pressurised conditions the reaction started off relatively slow and no signs of reaction decline were observed up to 180 minutes reaction period. Sulphation at 15 bar was higher than at 10 bar. At 15 bar dolomite calcium conversion observed ranged between 16-34%, for limestone it was between 18-36% and coal ash conversion was relatively higher, at 28-35% calcium conversion. The conversion results obtained compare well with results obtained by other researchers. A modified unreacted shrinking core model with variable effective diffusivity accounting for change in diffusion with growing product layer was successfully used to model results at both atmospheric and pressurised conditions.

TABLE OF CONTENTS

LIST OF FIGURES

LIST OF TABLES

NOMENCLATURE

A, B	dimensionless parameters in the extended USC model	-
	-	
C_{SO2}	local concentration of SO_2 in mixture gas	mol/m^3
D	diffusion coefficient	m^2/s
$D_{eff,}$	effective diffusivity of SO_2 in sorbent particle	m^2/s
D_{dif}	effective intraparticle diffusion m^2/s	m^2/s
D_{Kn}	Knudsen diffusivity	m^2/s
D_{mol}	molar diffusion coefficient of SO_2	m^2/s
D_{pl}	product layer diffusivity	m^2/s
D_{pore}	diffusivity in pores	m^2/s
$F(X)$	conversion function for a definite mechanism	-
k_s	reaction rate constant for CaO	m/s
$k_{s,CaO}$	reaction rate constant for CaO	m/s
$k_{s,CaCO3}$	reaction rate constant for $CaCO_3$	m/s
M	molecular weight of CaO or $CaCO_3$	g/mol
M_t	weight of sample at any calcination time	kg
n	reaction order with respect to SO_2 gas	
R_p, R_0	sorbent particle radius	m
Z	molar volume ratio of solid product and reactant	
	(V_{CaSO4}/V_{CaCO3}=1.25)	-
	(V_{CaSO4}/V_{CaO}=2.73)	-
t	time to achieve conversion X	s
T	temperature	K
V	volume enclosed by reaction surface	m^3
W_a	weight of sample after calcination	kg
W_t	weight of sorbent sample at any sulphation time	kg
W_o	weight of oven dried sample before calcination	kg
Vol_{pl}	volume of product layer	m^3
Vol_{pore}	volume of pores	m^3
X	degree of conversion	-

Greek Letters

ε	sorbent particle porosity	m^3/m^3

ε_0	initial porosity of sorbent particle	m^3/m^3
ρ	density of substance of solid reactant	kg/m^3
$\rho_{mol,sample}$	molar density of sample	mol/m^3
$\rho_{mol,CaCO3}$	molar density of solid reactant	mol/m^3
γ, $\gamma(\varepsilon)$	tortuosity	-
ϕ	Thiele modulus	-
τ in USC	time scale	s
τ_{dif}	intraparticle diffusion time scale	s
τ_{kin}	chemical kinetics time scale	s
x_{CaO}	mass fraction of CaO in solid	(-)
x_{CaCO3}	mass fraction of $CaCO_3$ in solid	(-)

Subscripts

0	initial
av	average
dif	intraparticle diffusion
eff	effective
kin	kinetics
Kn	Knudsen
mol	molecular
pl	product layer
p	pore surface

Abbreviations

AFBC	atmospheric fluidised bed combustion
BFBC	bubbling fluidised bed combustion
CCT	clean coal technologies
CFBC	circulating fluidised bed combustion
EDS	energy dispersive x-ray spectrometry
FBC	fluidised bed combustion
FGD	flue gas desulphurisation
TGA	thermogravimetric analyser

ICP	inductively couple plasma
IGCC	integrated gasification combined cycle
PF	pulverised fuel
BET	Brunauer Emmett and Teller
USC	unreacted shrinking core
USC-VED	unreacted shrinking core with variable effective diffusivity
MS	mass spectrometry
NWU	North-West University
IUPAC	International Union of Pure and Applied Chemistry
SOx	sulphur oxides
NOx	nitrogen oxides

CHAPTER 1

INTRODUCTION

1.1 General

In this chapter a preface to the research study is presented. An overview of the current energy scenario regarding coal to electricity power generation and the related environmental challenges and feasible solutions are highlighted in Section 1.2. The motivation for the study is given in Section 1.3 and the objectives of the study are listed in Section 1.4. The project scope, outline and description of the contents of this dissertation are presented in Section 1.5.

1.2 Background

Globally, energy supply organisations face many challenges in this century as they have to continue supplying secure and affordable energy in the face of growing demand (IEA, 2004; WCI, 2005a) while at the same time society expects cleaner energy and less pollution, with an increasing emphasis on environmental sustainability (WCI, 2005b).

Almost 40% of the global electricity generation is currently based on coal (IEA, 2005). Apart from the fact that it is a major source of energy worldwide, coal based electricity generation is a significant generator of pollutants, particularly, emission of particulates, carbon dioxide (CO_2) which is a greenhouse gas, sulphur oxides (SOx) and nitrogen oxides (NOx) which cause acid rain and photochemical smog respectively. Sulphur dioxide (SO_2) resulting from coal combustion forms a very serious danger to human and environmental health and depending on concentration it causes some diseases that may even result in death (The Health Council of The Netherlands, 2003). Despite the pollution and environmental challenges associated with coal mining, beneficiation and combustion, coal has remained an attractive energy option for power generation and the coal prices have remained steady (WCI, 2005a). For South Africa, which is endowed with a large coal resource base, coal usage in generating electricity has been inevitable. About 90% of South Africa's

electricity is generated from coal using pulverised fuel combustors, emitting about 1.9 million tonnes of SO_2 annually (Eskom, 2007)

Over the past decades, the extend of environmental pollution from coal based power generation has led to the greater demand from governments and environmental pressure groups on power companies and boiler manufacturers to progressively meet more stringent regulations on both unit performance and sulphur dioxide (SO_2) emission levels in coal combustion (Curran *et al.,* 1995). Furthermore, the stricter emission standards and use of more low rank coal worldwide have been challenging to the present desulphurisation technologies (Fukasawa, 1997; Carpenter, 1998a,b). Under increasing pressure from environmental concerns, current and future electricity generation systems are expected to have higher thermal efficiencies, be able to burn a wider range of fuels and minimise environmental impact, including CO_2, SOx and NOx emissions without significantly increasing capital or operating costs.

The direct and immediate environmental impact associated with SOx emissions from coal combustion have led to an urgent need in current and future coal combustion systems to control the associated SO_2 emissions. To achieve compliance with the statutory sulphur emission standards, the most common and cost effective option has been to use limestone or dolomite as sorbent, which is either injected into a furnace, where the temperature is in the range of 750–900°C (Basu, 2006), or injected to other auxiliary equipment of boilers to reduce sulphur in flue gases under low temperatures. Although much has been investigated and published on the subject of sulphation, there are no universal applicable findings. Each sorbent tends to behave in a unique way because of different mineralogical, chemical and physical characteristics. Sorbent sulphation capacity depends on various factors including the age of the sorbent, surface characteristics, chemical characteristics, mineralogical composition and operational conditions (Yrjas *et al.,* 1995). It is therefore complex to have a unified interpretation of sulphation capacities of various sorbents, which are different in nature and origin.

1.3 Motivation

"South Africa is an energy intensive country, with a high dependence on electricity and primary energy resources such as coal and imported oil" (Van der Riet *et al.,*

2003). The fact that the country generates and uses about 45% of Africa's total electricity (Eskom, 2007) shows how energy intensive the country is. Eskom, the national power utility uses pulverised coal to produce about 90% of the nation's electricity. Annual coal usage for electricity generation has steadily increased, from 104 million tonnes in 2003, to 119 million tonnes in 2007, an increase attributed to energy demand (Eskom, 2007). The rising coal usage in power generation is likely to remain the situation until substitutes such as nuclear energy, natural gas, hydro or other renewables start to play a more significant role (Van der Riet *et al.,* 2003).

With coal reserves standing at 48.5 billion tonnes, resembling 5.4% of total world coal reserves, South Africa is the world's fifth largest coal producer (BP, 2005). National coal production is about 240 million tonnes per year of which about 66% (160 million tonnes) is for domestic consumption and 33% (80 million tonnes) export (BP, 2005). At the current consumption rate, the country has about 200 years of coal, making it the most abundant indigenous primary energy resource (BP, 2005). As the greater part of export coal is high quality, low sulphur coking coal, the coal mining and beneficiation process results in the generation of a substantial amount of discards and low grade coal on the ground. A survey by The Department of Minerals and Energy in 2001 revealed that about one billion tonnes of coal discard is on the surface in coal rich areas of South Africa, the common characteristics of this coal are high ash content and low calorific value. Studies have shown that South African coal industry produces in excess of 45 million tonnes discard coal per annum of which about 25% with high ash (above 35%) and low calorific value (below 18MJ/kg) is recoverable (Horsfall, 1993; Department of Minerals and Energy Affairs, 2001). Part of the discards and low rank coals can be recovered and used as cheaper option for domestic use in thermal power systems and coal based oil production.

Since the national economy is expected to grow at a rapid pace of 5% per annum for the next three years (Ministry of Finance, 2006), this will result in increased electricity demand due to lifestyle changes. South Africa may have to use inferior quality fuels, the coal discard and the low grade coal which may be available at lower cost for economic electrical power generation to meet the anticipated growth in energy demand.

The low quality coal presents a technological challenge due to its high ash content of up to 45% and sulphur content of about 1.2% (EIA, 2004b) and cannot be combusted economically in the currently used pulverised coal boilers. Coal usage thus needs to

be compatible with the environmental protection drive by use of clean coal technologies (CCTs), which offer a route to a low emissions future, while allowing the continued usage of the most abundant and affordable of all fossil fuels – coal (WCI, 2005a). Some attractive options, which have the potential to meet these requirements for the conversion of coal to electricity, are atmospheric fluidised bed combustion (AFBC) and pressurised fluidised bed combustion (PFBC). PFBC systems which combine the advantages of fluidised beds with advanced combined cycles have potential for burning a wide range of coals (even with high ash and sulphur content) to generate electricity at higher thermal efficiencies and lower emission rates than is possible using conventional (pulverised fuel) coal-fired systems.

The use of low quality coals, which usually have high ash and sulphur content, present immense environmental pressure to control SO_2, NOx and other gaseous emissions from combustion systems. Locally mined limestone and dolomite can be used to control the emission of SO_2 by injecting them as sorbents into the furnace in fluidised bed combustors. Low rank coals may also contain a significant amount of calcium and magnesium in the form of exchanged ions in the coal (Grubor *et al.*, 2003; Manovic *et al.*, 2002; Sheng *et al.*, 2000; Gray, 1986), the ash can contribute to capture of sulphur dioxide from combustion gases. The speculation and uncertainty in use of sorbents present a challenge to sorbent selection for sulphur removal in fluidised beds.

In a bid to keep up with the changing environmental regulation, sustainable resource usage and a need to maintain the electrical energy cost at relatively stable levels, Eskom in partnership with The Coal Technology Research Group of North-West University (Potchefstroom campus) has embarked on research to investigate the most economical ways to utilise the low grade coals without negative environmental impacts. AFBC and PFBC as cleaner coal technologies have been identified as the most feasible options for economical generation of electricity using the coal discards and the poorer type low rank coals in the medium term. The operation of the fluidised bed combustor (FBC) should fall within the range of emission levels as described in the statutory air quality standards (National Environmental Management: Air Quality Act 39 of 2004).

As fluidised bed combustion is the most favoured combustion system to replace pulverised combustion in power generation in South Africa, it is important to consider the performance of the associated environmental process using local sorbents.

1.4 Objectives of Study

The purpose of this study was to investigate sulphur dioxide capture under atmospheric and pressurised combustion conditions using dolomite and limestone originating from South African mines and also to investigate in situ sulphur dioxide capture by coal ash. The investigations were carried out in a thermogravimetric analyser (TGA) using simulated flue gas. Pressures of 0.875, 10 and 15 bar at temperatures between 750 and 900°C resembling carbon dioxide partial pressure of 0.0875, 2.0 and 3.0 bar respectively were used to simulate AFBC and PFBC conditions. The objectives of the investigations were:

1. To characterise the chemical and structural properties of two different locally mined dolomite samples, limestone and coal ash.
2. To investigate the effects of temperature and pressure on full calcination, partial calcination and subsequent sulphation of dolomite, limestone and coal ash under conditions similar to those used in AFBC and PFBC.
3. To evaluate the particle based sulphation reaction kinetic model suitable for inclusion in fluidised bed combustion systems for modelling of sulphur dioxide capture using the locally available dolomite, limestone and coal ash.
4. To investigate the possibility of using coal ash as a sorbent for sulphur dioxide capture in coal combustion systems.

The aim of the proposed research work is to aid in the effort to develop an achievable control technology for SO_2 emission control in the FBC using locally available sorbents.

1.5 Scope of Dissertation

The effective design and operation of coal combustion systems is heavily dependent on the complementary design and operation of efficient gas cleaning systems, including particulates, SOx and NOx capture systems. In line with consideration of

clean coal technologies (CCTs) for use with the deteriorating coal quality, there is great need to investigate the sulphation capacity of locally mined dolomite, limestone and coal ash under atmospheric and pressurised conditions and compare effectiveness of the sorbents.

In chapter 2 an overview of the available literature on fluidised bed combustion and sorbent sulphation is presented. The properties, behaviour of sorbents under varying reaction conditions, mechanisms of sulphur dioxide capture and the experimental apparatus used in the kinetics investigation of sulphation are given.

Experimental apparatus and methods used are described in Chapter 3. The main apparatus used in sulphation is a high pressure thermogravimetric analyser (TGA), where sorbent is calcined and sulphated in a simulated flue gas mixture. The surface characterisation of sorbents was carried out using a scanning electron microscope. Elemental analysis of sorbents was outsourced to Mintek laboratories in Johannesburg. Porosity, and pore size distribution were measured by mercury porosimetry, internal surface area was measured by nitrogen adsorption and a helium pycnometer was used to measure particle density.

In Chapter 4 the sorbent characterisation results are presented whilst in Chapter 5 the sorbent calcination and sulphation results are presented. The results of the experiments are compared and commented on, with respect to findings from other researchers. In Chapter 6 the results of sulphation reaction modelling using the modified unreacted shrinking core model as presented in Appendix A are discussed.

Finally, in Chapter 7 conclusions and recommendations on the results of the study are listed.

CHAPTER 2

LITERATURE SURVEY

2.1 Introduction

In this Chapter, the literature review on sulphur dioxide capture under fluidised bed combustion conditions (FBC) using dolomite, limestone and coal ash is presented. In Section 2.2 the general methods for sulphur dioxide minimisation are presented. In Section 2.3 the fluidised bed combustion (FBC) technology is discussed while Section 2.4 is an overview of the chemical and physical characteristics of sorbents used by other researchers and the calcium conversion results they obtained. The chemistry of calcination and sulphation is given in 2.5. A summary of desulphurisation kinetics and models used for experimental data evaluation are presented in Section 2.6. Conclusions drawn from the literature survey are discussed in Section 2.7

2.2 Coal combustion and removal of sulphur dioxide

During coal combustion, sulphur is converted into gaseous pollutants (i.e. mainly SO_2 and a little SO_3). Owing to global and national clean energy drive, there is need to control emissions from combustion systems, and removal of SO_2 from coal combustion gas is an important environmental management activity.

To minimise the negative environmental impact of coal combustion gases, there are various methods for reducing SO_2 emissions from coal based thermal power systems into the atmosphere. Each method has both advantages and limitations related to capital and operating costs, removal efficiency, operational experience, suitability for specific application and waste products produced. Consequently, the choice of control technology is based on the criteria required for each individual combustion plant. The technologies available are usually differentiated according to whether the acidic SO_2 reacts with a chemical base in solution, slurry or solid form and whether or not the reaction product is set for disposal or converted into useable by-products (Nolan, 2000). A reduction in the atmospheric emissions of sulphur dioxide produced

by fossil fuel combustion processes can be achieved at one of the three stages, before, during or after combustion as discussed below:

2.2.1 Reducing fuel sulphur content before combustion

Emissions of SO_2 are proportional to the sulphur content of the fuel, although with regards to coal, a proportion is retained in the ash (Grubor and Manovic, 2002; Grubor *et al.,* 2003; Ilic *et al.,* 2003; Manovic *et al.,* 2002). Therefore, one of the simplest ways to reduce the amount of SO_2 released from the combustion process can be achieved by switching to a fuel that has lower sulphur content, i.e. burning low sulphur coal or substituting high sulphur coal by gas; this is an expensive option as low sulphur coal is more expensive. Sulphur in coal is found in inorganic and organic forms and sulphates. Inorganic sulphur, in the form of pyrite (FeS_2), can be removed from coal relatively easily by washing the coal; this can result in a reduction of 10 - 50% of total sulphur content (Horsfall, 1993; Shah *et al.,* 2002). The organic sulphur in coal is difficult to remove by just washing. The disadvantage is that coal washing can change the physical characteristics of coal, this might lead to operational problems when combustion takes place (Horsfall, 1993).

2.2.2 Sulphur removal during combustion

Technologies to either prevent the production of SO_2 or reduce its release into the atmosphere during combustion have been developed over the past two decades. The most developed are the fluidised bed combustion (FBC) and the integrated gasification combined cycle (IGCC) process (WEC, 2006). In FBC, SO_2 emissions can be controlled by adding a sorbent to the bed of inert material in the combustion zone and up to 90% SO_2 can be removed as $CaSO_4$ (Nolan, 2000). In IGCC the sulphur in the coal is converted to hydrogen sulphide (H_2S) which can be further converted to other chemicals (e.g. H_2SO_4) and sold for use within the chemical industry and emissions can be reduced by more than 99% (WCI, 2005a,b). FBC evolved from efforts to find a combustion process with good fuel flexibility and ability to control pollutant emissions without employing external emission control systems such as scrubbers and flue gas desulphurisation.

It has been known that not all of the total sulphur in coal is emitted as gases after coal combustion, independent of the combustion process (Sheng *et al.,* 2000). A part of the sulphur will be retained as solid compounds in coal ash due to neutralisation of alkaline components of the parent coal (Sheng *et al.,* 2000), meaning that coal ash

has a sulphur retaining property which apparently makes a contribution in alleviating the problem of SO_2 emissions. The process of sulphur self retention by coal ash is influenced by various factors which depend on coal characteristics and combustion conditions (Conn *et al.,* 1993; Fuertes *et al.,* 1992; Gray, 1986; Raask, 1985; Sheng *et al.,* 2000)

2.2.3 Removal of sulphur after combustion - FGD

Emissions of SO_2 generated during the combustion of fossil fuels can be reduced by treating the flue gases before they are emitted into the atmosphere via the stacks; this is termed flue gas desulphurisation (FGD). Economiser sorbent injection, duct sorbent injection and hybrid sorbent injection are some of the common FGD systems based on sorbent injection. Flue gas desulphurisation systems can be classified as either regenerable or non-regenerable. Commercially available FGD systems include limestone gypsum systems (Nygaard *et al.,* 2004), spray dry systems (Zheng *et al.,* 2002) and seawater scrubbing process (Williams, 1999) which are non-regenerable and the Wellman-Lord Process which is regenerable (Buzek *et al.,* 1998).

Of the above stated SO_2 removal methods, the FBC in situ SO_2 removal by sorbent (limestone and dolomite) injection during combustion is an economical and attractive option as it allows burning of a wider range of coals that can not be handled by the pulverised fuel (PF) technology. Since the FBC system uses in situ SO_2 capture to control SO_2 emission there is usually no need of auxiliary plant for desulphurisation, which makes the plant cost effective. Also mineral matter contained in coal is capable of reacting with SO_2 under FBC conditions and contribute to removal of SO_2 emission (Grubor and Manovic, 2002; Grubor *et al.,* 2003; Ilic *et al.,* 2003; Manovic *et al.,* 2002). Use of high ash coals may substantially contribute to SO_2 capture considering that the ash may contain active calcium oxide that can react with SO_2 to form stable $CaSO_4$. Puff *et al.* (1983) reported that around 60% of sulphur is retained due to sulphur self retention in ash while values near 90% were obtained with fly ash recirculation or combustion of coal rich with tailings.

2.3 Fluidised bed combustion

Commercial FBC units operate at competitive efficiencies, cost less than the currently used conventional PF units, and have SO_2 and NOx emissions below levels mandated by statutory standards (National Energy Laboratory Technology, 2006).

The fluidised movement within the combustion chamber results in a better heat transfer efficiency to the water filled tubes and therefore operating temperatures are lower than in a conventional pulverised fuel (PF) system. The lower combustion temperatures allow efficient combustion to take place without causing the ash to soften, thereby allowing easy removal of the ash containing the adsorbed SO_2. The sorbents effectively adsorb the SO_2 from the combustion gas as it is released from the coal and forms $CaSO_4$ retained within the ash which is removed regularly. Furthermore the lower operating temperature of FBC (about 850°C) leads to lower emission of NOx and improved SO_2 capture given that at these temperatures the $CaSO_4$ formed is more stable than at higher temperatures (about 1300°C) used in pulverised fuel combustors. Under the conditions existing in an FBC boiler, MgO is regarded as an inert desulphurant agent; at temperatures higher than 800°C the formation of $MgSO_4$ is thermodynamically unfavourable (Dennis and Hayhurst 1984; Fuertes *et al.*, 1995).

Limestone and dolomite have successfully been used in bed removal of sulphur dioxide under AFBC and PFBC conditions (Basu, 2006). Any differences in fuel sulphur level is accommodated in FBC by varying the amount of sorbent fed onto the bed (Boskovic *et al.*, 2002) and SO_2 removal of up to 90% can be achieved (Nolan, 2000). Coal ash contribution to SO_2 removal becomes attractive in fluidised bed combustion since the conditions for capture are conducive. The process of SO_2 self retention in ash is influenced by various factors, which depend on coal characteristics and combustion conditions (Conn *et al.*, 1993; Fuertes *et al.*, 1992; Gray, 1986; Sheng *et al.*, 2000). The most investigated coal characteristic is the Ca/S ratio in coal.

2.4 Sorbents for sulphur dioxide capture

2.4.1 Sorbents used by other researchers

A number of sorbents have been tested for SO_2 capture. Phosphate rock has been tested as an alternative for limestone and dolomite in desulphurisation at temperatures between 500-900°C with a calcined sample and 72% conversion was achieved (Ozer *et al.*, 2002). Calcium magnesium acetate (CMA), calcium acetate (CA), calcium formate (CF), calcium benzoate (CB) calcium propionate (CP) and magnesium acetate (MA) have been tested as sorbents for simultaneous reduction of

NOx and SOx; results showed that calcium and magnesium acetate were the best performers with SO_2 reduction above 70% at Ca/S ratios above 2 (Patsias *et al.*, 2005). Calcium acetate synthesised from natural limestone was tested for removal of sulphur in situ (Zhang *et al.*, 2003) and solid sodium carbonate has also been tested as a sorbent for removal of SO_2 in FBC (Wang *et al.*, 2002). Among the many possible sorbents, limestone and dolomite are the most widely used commercial sorbents due to their low cost and availability (Ar *et al.*, 2002).

During coal combustion a part of total sulphur in coal is retained as solid compounds in ash (Sheng *et al.*, 2000) and depending on the coal quality, the inherent sulphur capture can contribute largely to SO_2 capture during combustion. Coal ash has been investigated as a possible in situ sorbent for SO_2 capture in coal combustion (Grubor *et al.*, 2003; Manovic *et al.*, 2002; Sheng *et al.*, 2000; Gray, 1986)

The level of dolomite and limestone utilisation in desulphurisation is relatively low and 30-40% calcium utilisation is considered to be good (Anthony and Granatstein, 2001; Anthony *et al.*, 1997; Iribarne *et al.*, 1997). Some additives such as propionates and acetates (Patsias *et al.*, 2005), sodium chloride (Shearer *et al.*, 1979) have been found to greatly improve sulphation effects of sorbents.

2.4.2 Sorbents' composition and physical characteristics

Different sorbents with different characteristics behave differently under similar conditions. A good sorbent is the one that provides good adsorptive capacity as well as good kinetics (Do, 1998; Yang, 1997; Gregg and Sing, 1982). To satisfy these requirements, the sorbent must have a reasonably large surface area and a relatively large porosity (Do, 1998). McCauley and Johnson (1991) concluded that reaction surface area increases due to formation of cracks along the surface area and fragmentation of dolomite particle as consequence of decrepitation phenomenon. Fuertes *et al.* (1995) showed that an increase in particle size results in a decrease in fractional conversion and reaction rates, the behaviour has been explained to be a consequence of increase of intra particle resistance with particle diameter. Zevenhoven *et al.* (1998b) found that the internal structure, namely porosity, pore size distribution and internal surface of the unreacted solid of sorbent particle changes during reaction. The porosities of calcium based sorbents increase between two and twenty-fold on calcination (Zevenhoven *et al.*, 1998a,b; Alvarez *et al.*, 1999) as shown on Table 2.1.

Hartmann and Coughlin, (1974) suggested that pore size distribution and surface area of the original limestone must be used as criteria for selecting a limestone as a sorbent, Hartmann *et al.* (1979) and Shearer *et al.* (1979) supported the hypothesis. Other researchers (Bogwardt and Bruce, 1986; Bhatia and Perlmutter, 1980; Garcia-Labiano, 1992) supported the idea that physical parameters of CaO account for limestone reaction in the presence of SO_2; on the ground that even though the general features of CaO are determined by certain properties of limestone, the calcination conditions largely affect the properties of CaO which is the species reacting with SO_2. However, Davini (1995) working with sintered CaO samples pointed out that surface area of these samples do not wholly explain their performance in the presence of SO_2.

It is generally considered that the ash sulphur retention is significantly dependent on coal properties, including coal rank, sulphur content in coal and the contents and occurrences of alkaline elements involved in SO_2 capture and the behaviour of these elements during coal combustion (Sheng *et al.,* 2000; Conn *et al.,* 1993; Fuertes *et al.,* 1992).

Chemical and structural properties which are directly measurable characteristics of the solids such as particle density, porosity, pore size distribution and specific surface area of sorbents are important in defining a sorbent. Prior to sulphation of different sorbents it is important to obtain the nature and ranking of the materials used. Table 2.1 gives the important physical and chemical parameters of sorbents used by other researchers and the conversion of calcium achieved after 180 minutes of sulphation in related sulphation experiments.

Table 2.1: Sorbents used by other researchers and their characteristics and performance using thermogravimetric analysis

Researcher	Sorbent	$CaCO_3$ wt%	$MgCO_3$ wt %	Particle density (kg/m^3)	Specific surface area (m^2/g)	Particle porosity (-)	Average pore diameter (µm)	Ca conversion in 180 minutes
Zevenhoven *et al.* (1998a,b)	Faxe Bryozo (L)	98.4	0.90	1681	2.25	0.178	0.323	0.63^{pfbc}
	Stevens Chalk (L)	98.6	0.65	1351	4.63	0.324	0.412	0.89^{pfbc}
	Gotland (L)	90.4	2.87	2786	3.74	0.063	0.074	0.63^{pfbc}
	Sibbo (D)	60.4	47.4	2727^{a}-->2213^{b}	0.930^{a}-->2.85^{b}	0.022^{a}-->0.206^{b}	0.112	0.58^{pfbc}
	Wisconsin Wilbur (D)	47.4	26.0	2855^{a}-->2416^{b}	0.060^{a}-->0.241^{b}	0.010^{a}-->0.162^{b}	0.291	0.41^{pfbc}
Alvarez *et al.* (1999)								
	Maria (L)	99.1	0.10		0.424	0.014	0.250	
	Andorra (D)	55.9	41.31		0.777^{a}-->5.63^{b}	0.066^{a}-->0.175^{b}	0.060	
Ar *et al.* (2002)								
	Kiynik	85.5	3.14		0.558	0.49	0.125	0.67^{afbc}
Trikkel *et al.* (1999)								
	Rummu (L)	92.26	0.80	1925	0.700	0.0716	0.274	0.39^{pfbc}
	Aseri (L)	64.64	1.34	1992	17.15	0.0852	0.306	0.68^{pfbc}
	Karinu (L)	86.93	4.25	2153	1.14	0.0979	0.234	0.42^{pfbc}
	Adavere (D)	46.68	42.57	2277	0.52	0.0871	0.222	0.30^{pfbc}
	Pajusi (D)	35.72	37.11	1888	2.34	0.0916	0.304	0.61^{pfbc}

(D) – dolomite
(L) – limestone
[a] – based on raw sorbent
[b] – based on partially calcined (half calcined) sorbent
[afbc] – atmospheric fluidised bed combustion condition sulphation using a TGA.
[pfbc] – pressurised fluidised bed conditions sulphation using a TGA.

2.5 Chemistry of calcination and sulphation

2.5.1 Sorbent calcination

The thermodynamic equilibrium relationship of the $CaCO_3/CaO$ and $MgCO_3/MgO$ has been adapted from Erdos and Barker's equations of 1962 (cited by Fuertes *et al.*, 1995) given as equation 2.1 and 2.2 respectively and are presented on Figure 2.1.

The dependence of the dissociation of $MgCO_3$ on CO_2 partial pressure and temperature is stated by equation 2.1:

$$P_{CO2}/atm = 1.339x10^{9}e^{-14145/T(K)} \text{ (Fuertes } et\ al.\text{, 1995)} \quad (2.1)$$

The equilibrium dependence of $CaCO_3$ decomposition on CO_2 partial pressure and temperature as stated by equation 2.2:

$$P_{CO2}(atm) = 1.20x10^{7}e^{-19130/T(K)} \text{ (Fuertes } et\ al.\text{, 1995)} \quad (2.2)$$

Figure 2.1 shows typical ranges of $CaCO_3/CaO$ and $MgCO_3/MgO$ equilibrium with regards to temperature and CO_2 partial pressure.

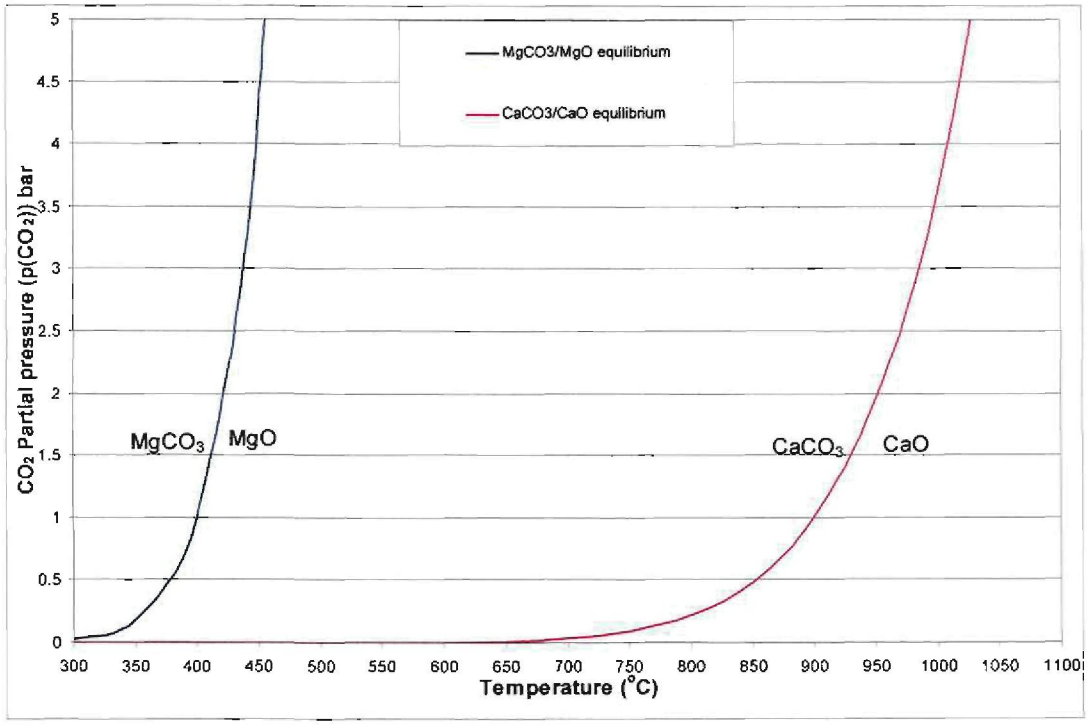

Figure 2.1: $CaCO_3/CaO$ and $MgCO_3/MgO$ equilibrium curves (Fuertes *et al.*, 1995)

When the partial pressure of CO_2 in the combustor is lower than the thermodynamic equilibrium pressure of limestone ($CaCO_3$) or dolomite ($CaCO_3.MgCO_3$), the sorbent calcines to form CaO, MgO and CO_2 (Fuertes *et al.*, 1995; Yrjas *et al.*, 1995; Ngeleka, 2005). Under atmospheric fluidised bed combustion conditions the $CaCO_3$ and $MgCO_3$ in the sorbent calcine as illustrated in equation 2.3 and 2.4:

$$CaCO_3(s) \text{ --------> } CaO(s) + CO_2(g) \quad (2.3)$$

$$CaCO_3.MgCO_3(s) \text{ --------> } CaO(s) + MgO(s) + 2CO_2(g) \quad (2.4)$$

Under pressurised fluidised bed combustion (PFBC) conditions the partial pressure of CO_2 is so high that $CaCO_3$ does not calcine, however $MgCO_3$ does (Yrjas *et al.*, 1995; Iisa, 1990). It is generally agreed (Tullin and Ljungstrom, 1989; Zevenhoven *et al.*, 1998a; Trikkel and Kuusik 2003; Yrjas *et al.*, 1995; Alvarez and Gonzalez, 1999; Fuertes *et al.*, 1995) that the high partial pressure of CO_2 in PFBC prevents the calcination of $CaCO_3$ due to thermodynamic constraints, but the $MgCO_3$ in the dolomite calcines as shown in equation 2.5. So when dolomite is the sorbent in PFBC, a half calcined dolomite will effectively be the sorbent that will undergo sulphation.

$$CaCO_3.MgCO_3(s) \text{ ---------> } CaCO_3.MgO(s) + CO_2(g) \quad (2.5)$$

When lime (CaO) is introduced into the bed at temperature and CO_2 partial pressure that preferentially promote the existence of limestone ($CaCO_3$) as the more stable form of the inorganic calcium, then the CaO will carbonate to $CaCO_3$. Tullin and Ljungstrom, (1989) found that in PFBC ash there is little if any CaO. Sulphation of ash under PFBC conditions is essentially sulphation of $CaCO_3$.

2.5.3 Sorbent sulphation

When limestone is the sorbent under AFBC conditions $CaCO_3$ calcines to CaO and consequently the sulphation reaction is the reaction of CaO with SO_2 in the presence of O_2.

$$CaO(s) + \tfrac{1}{2}\, O_2(g) + SO_2(g) \text{----------> } CaSO_4(s) \quad (2.6)$$

When dolomite is the sorbent under AFBC condition, effectively sulphation will be reaction of CaO with SO_2 and O_2 and the MgO component of the calcined material does not react to a reasonable extent under FBC conditions (Fuertes *et al.,* 1995)

When limestone is the sorbent under PFBC conditions, $CaCO_3$ does not calcine and the sulphation reaction is a direct reaction between $CaCO_3$, SO_2 and O_2.

$$CaCO_3(s) + ½\ O_2(g) + SO_2(g) \text{----------} > CaSO_4(s) + CO_2(g) \qquad (2.7)$$

When dolomite is the sorbent under pressurised fluidised bed combustion conditions the MgO formed does not react with SO_2 (Dennis, 1985) and $CaCO_3$ does not calcine hence sulphation reaction is a direct reaction between $CaCO_3$ and SO_2 in the presence of O_2.

$$CaCO_3.MgO(s) + ½\ O_2(g) + SO_2(g) \text{---------} > CaSO_4(s) + MgO(s) + CO_2(g) \qquad (2.8)$$

Over the past two decades, substantial research effort has been expended at investigating various sorbents' reactivity with SO_2. A summary of some of the sulphation research work done by other researchers with different sorbents is given in Table 2.2.

Ulerich *et al.* (1980); Alvarez and Gonzalez, 1999; Fuertes *et al.* (1995) have shown that sulphation rate and conversion is dependent on sorbent particle size, the smaller the particle size the higher the conversion. Hajaligol *et al.* (1988) confirmed that direct sulphation of $CaCO_3$ achieves higher conversion in isothermal sulphation due to formation of a more porous $CaSO_4$ layer and the porosity of the sample increases with the rate of CO_2 generation, the same findings were also observed by Krishnan and Sortichos (1993a); Snow *et al.* (1988); lisa, (1992) and Yrjas *et al.* (1995).

Table 2.2: Researchers, and the important experimental aspects and parameters of sulphation

Researcher	Adsorbent	Particle size	Pressure	Gas composition	Temperature	Apparatus
lisa *et al.* (1990)	Limestone and dolomite 150-300mg sample per run	125-180μm	1bar, 15bar	3000ppm SO_2, 4% O_2, 15% CO_2, bal N_2 Flow rate 760ml/min at 1bar, 3100ml/min at 15bar	750-950°C	TGA
Zevenhoven *et al.* (1998)	Limestone and dolomite 100mg sample per run	250-300μm	15bar	3000ppm SO_2, 4% O_2, 20% CO_2, bal N_2 Flow rate 3300ml/min	850-950°C	TGA
Fuertes *et al.* (1995)	Dolomite d_p< 200μm 5mg sample mass d_p>200μm 50mg sample mass	20-32μm, 106-150μm 212-300μm,		2600ppmSO_2, 3.6% O_2, high CO_2, N_2 Flow rate 1500ml/min	650-900°C	TGA Shock micro-reactor
Alvarez *et al.* (1999)	Limestone and dolomite 10mg sample per run	100-200μm 500-595μm	12-25bar	5000ppm SO_2, 15% CO_2, 3%O_2, bal N_2 5000ppm SO_2, 12%CO_2, 7% O_2, bal N_2 Flow rate 1000ml/min	800-925°C	TGA
Yrjas *et al.* (1995)	Limestone and dolomite 100mg sample per run	200-400μm	15bar	3000ppm SO_2, 4% O_2, 20% CO_2, bal N_2 Flow rate 3300ml/min	850-950°C	TGA
Zhong, (1995)	Limestone	4.0-5.4μm	1bar	1000-5000ppm SO_2, 70%CO_2, 10%O_2, 20%N_2,	500-800°C	TGA
Ngeleka, (2005)	*Dolomite* 300mg sample per run	212-300μm	0.875bar	2500ppm SO_2, 25%CO_2, 6.8%O_2, bal N_2, 2500ppm SO_2, 8%CO_2, 6.8%O_2, bal N_2, Flow rate 1000ml/min	750-950°C	TGA

The sulphation reaction was found to be zero order with respect to O_2 concentration between 2-11% (Ulerich *et al.,* 1980), which is supported by the finding that sulphation is independent of O_2 in the region of 1-6% (Iisa, 1992). Tests at CO_2 concentrations between 15-90% showed that CO_2 only influences the calcination behaviour and not the sulphation rate (Iisa, 1992). O'Neill *et al.* (1976) showed that isothermal sulphation reactions using TGA with limestone and dolomite is affected by sample size and gas flow rate. Sulphation is dependent on SO_2 concentration with the rate affected by the partial pressure of the SO_2 in the gas mixture (Zhong, 1995; Iisa, 1992) and this is first order with respect to SO_2 (Fuertes *et al.,* 1995). However Qiu and Lindqvist (2000) proved that under conditions favouring direct sulphation of $CaCO_3$ the reaction order is not equal to one, investigations at 13 bar gave a reaction order of 0.58.

Qiu and Lindqvist (2000) also found that an increasing total pressure whilst keeping SO_2 partial pressure constant reduces calcium conversion and reactivity. The rate of direct sulphation was found to be lower than that of calcined limestone (Trikkel and Kuusik, 2003). Yrjas *et al.* (1995) investigated dolomites and limestone sand and found that sulphur capture varied between different sorbents of different qualities, they obtained conversions between 7 and 83%.

Sulphur removal efficiency of limestone in an AFBC improves with increasing temperature between 820-850°C (O'Neill *et al.,* 1976; Ersoy-Mericboyu and Kucukbayrak, 1995). Higher temperatures resulted in higher conversions, with the effect more clearly pronounced for the dolomites than for the limestones. At high CO_2 partial pressure such that $CaCO_3$ does not calcine, no decrease in limestone utilisation was observed at temperature up to 950°C (Alvarez and Gonzalez, 1999; Fuertes *et al.,* 1995; Ulerich *et al.,* 1980).

Kinetic studies of direct sulphation in a tubular isothermal reactor showed that the diffusion of SO_2 through the product $CaSO_4$ layer is rate limiting and the effective diffusivity of SO_2 in the limestone sulphation is two to three orders of magnitude higher than in the sulphation of precalcined limestone (Spartinos and Vayenas, 1991).

2.6 Reaction models

Three categories of heterogeneous (gas solid) reaction models for the sulphation of limestone or dolomite can be distinguished based on the manner in which the sorbent particles are characterised. The models are; unreacted shrinking core model (Szekely and Evans, 1970; Borgwardt *et al.,* 1987), grain models (Szekely and Evans 1970; Ramachandran, 1983) and pore models (Bhatia and Perlmutter, 1980; Kocaefa *et al.,* 1987) and are discussed in section 2.6.1, 2.6.2 and 2.6.3 respectively:

2.6.1 The unreacted shrinking core models

The unreacted shrinking core model assumes that the gas solid reaction occurs at a sharp interface separating the particle's outer product layer and the unreacted core (Szekely and Evans, 1970). As the model does not consider the sorbent particle structure and structural changes during sulphation, it is a relatively simple model mainly used for highly non-porous solid reactants (Wang and Bjerle, 1997). However, the unreacted shrinking core model has been successfully used to model sulphation reaction data for TGA experiments under AFBC and PFBC combustor conditions using dolomite and limestone as sorbents (Zevenhoven *et al.,* 1998a; Zhong, 1995).

Zevenhoven *et al.* (1998a) found that the unreacted shrinking core model alone does not explain differences in conversion of chemically similar but physically different limestone and dolomites and they developed an unreacted shrinking core model with variable effective diffusivity (USC-VED) which has successfully been used to describe limestone and dolomite sulphation under pressure (Zevenhoven *et al.,* 1998a; Trikkel and Kuusik, 2003; Alvarez and Gonzalez, 1999).

2.6.2 Grain models

Grain models consider the sorbent as a collection of non-porous sorbent grains surrounded by inter-granular voids. The rate of reaction of the grains is assumed to be governed by the unreacted shrinking core model and controlled by three resistances in series, diffusion through the voids, diffusion through the product layer and reaction at the surface of the unreacted core.

The grain models differ from the unreacted shrinking core model in the way the particle structural changes during reaction are interpreted. The original grain model which has been referred to as the moving boundary model was developed by

Szekely and Evans (1970), by assuming the porous solid as a semi-infinite solid of macroscopically unidirectional movement of the reaction zone, such that the initial structure is not affected by the progress of the reaction. Pigford and Sliger (1973) modified the original grain model by eliminating the first assumption and considering a mass balance of the gas phase in the spherical particle. The changing grain size model of Hartmann and Coughlin (1976) takes the reduction in porosity due to the larger molar volume of $CaSO_4$ as to that of sorbent (CaO or $CaCO_3$) into account. The grain micro-grain model of Dam-Johansen *et al.* (1991) considers the sorbent particles as made up of a number of individual grains which themselves then consist of micro-grains. The interstices between the grains are considered as forming a system of macro-pores whilst the interstices between grains are considered as forming a system of micro pores. The model assumes that owing to uniform expansion of the micro-grains found in a grain as the reaction progresses, micro pores eventually become blocked; the non porous, partially reacted grains then swell in accordance with a shrinking partially reacted core model. Some modified grain models (Ramachandran and Smith, 1977; Ranade and Harrison, 1981; Lindner and Simonsson, 1981) consider the effect of sorbent sintering caused by high temperature of the calcination/sulphation reaction.

2.6.3 Pore models

Pore models regard the sorbents as a solid continuum penetrated by pores. Since the molar volume of $CaSO_4$ is larger than that of CaO and $CaCO_3$, the radius of the pore decreases as the reaction proceeds so that the solid product eventually fills the pores. Three factors determine reaction rate within the particle, gas phase diffusion through pores, diffusion through product layer of pore walls and chemical reaction at interface between the solid reactant and the product.

There are a number of pore models that differ in the way of describing the pore structure. The original pore model proposed by Szekely and Evans (1970) consider a semi-infinite solid to contain parallel pores with uniform radius and does not consider structural changes.

Ramachandran and Smith (1977) proposed a single pore model that deals with the pore closure phenomenon as a result of the chemical reaction; this model uses an approximate method of mono-dispersed of average pore radius resulting in a simplified model with only a few independent parameters. The pore size distribution

and the intersections of pores are not considered. The distributed pore model of Christman and Edgar (1983) and Kocaefe (1987) assumes the particles as containing numerous pores of a size distribution that can be measured experimentally, and can be represented by a continuous discrete function. Pores are assumed not to intersect internally. The model considers only the loss of pores due to plugging.

The random pore model of Lindner and Simonsson (1981) and the random pore model of Bhatia and Perlmutter, (1980, 1983) regard particles as containing a network of randomly intersecting pores. These models introduce either a structural parameter or parameters relating to porosity and pore size distribution (Lindner and Simonsson, 1981). The reaction rate of the particle is seen as based upon these two parameters.

The tree like model of Simons and Garman (1986) and Simmons *et al.* (1987) postulates that each pore of a particle reaches the surface like the trunk of a tree, the branches and the leaves involving a progressions of pore from maximum to minimum radius. The pore size distribution is modelled by a mathematical function, simplified with respect to the progress of the reaction, making the model easy to use and there are no empirical fitting parameters required. Zevenhoven *et al.* (1998b) obtained a slightly better fit with the random pore based changing internal structure (CIS) model compared to the modified shrinking core model (Zevenhoven *et al.*, 1998a) on direct sulphation data for TGA on natural calcium based sorbents.

2.6.4 The most used kinetic model for sulphation

Of the many models that have been proposed for modelling of sulphation reaction the unreacted shrinking core model with variable effective diffusivity (USC-VED) (Zevenhoven, 1998a) has been one of the most used. The motivation for researchers selecting this model can be summarised as follows:

i. The variation of the effective diffusivity of sorbent is accounted for during reaction by introducing a diffusion resistance that depends on conversion, average pore diameter, initial porosity, pore diffusivity and product layer diffusivity.

ii. The model accounts for reaction and effective diffusion (in pore and product layer) and since sorbents particle are porous as a result of

calcination the consideration of initial porosity has major effect on reactivity.

iii. The model incorporating reaction control and diffusion control can be easily solved numerically to determine different mechanisms under different reaction conditions; also other model parameters can be easily determined using simple characterisation tests.

iv. The model has successfully been used by other researchers to model sulphation data under atmospheric and pressurised conditions.

2.7 Conclusions: Literature survey

Sulphur dioxide capture is an important process in coal based power generation systems. Dolomite and limestone have been the most used sorbents in sulphur dioxide capture in PFBC and AFBC systems. In AFBC CaO is the effective component of the sorbent and in PFBC $CaCO_3$ is the effective component.

Coal ash with reasonable calcium content has been proven to contribute to in situ sulphur dioxide capture.

Different sorbents, even with similar chemical composition behave differently under the same operating conditions and this could be due to different structural parameters with temperature and pressure.

Chemical composition, porosity, pore size distribution and surface area are important parameters of a sorbent in sulphur capture and determine the extent to which a sorbent can react (Zevenhoven *et al.,* 1998a,b) .

Different models have been successfully used to model sulphation reactions. The models are; unreacted shrinking core model (Szekely and Evans, 1970; Borgwardt et al., 1987), grain models (Szekely and Evans 1970; Ramachandran, 1982) and pore models (Bhatia and Perlmutter, 1980; Kocaefa *et al.,* 1987). Of these models the unreacted shrinking core models have been the most used type of model.

CHAPTER 3

EXPERIMENTAL

3.1 Introduction

In this Chapter a description of equipment, materials and the experimental methodology are presented. In Section 3.2 detail of the materials used in the experiments is given. Experimental equipment used is presented in Section 3.3 whereas Section 3.3.1 gives detailed description of the high pressure thermogravimetric analyser (TGA). The experimental conditions and experimental procedures are given and explained in Section 3.4 and 3.5 respectively. In Section 3.6 characterisation techniques are presented.

3.2 Materials

3.2.1 Sorbents

Four natural sorbents were used in this investigation, these were:

1. Dolomite A and dolomite B, supplied by Eskom, and the same sorbents are being used by Eskom's research division in the company's CFBC pilot research project. The samples were crushed and screened to particle size 212-300 μm for use in the characterisation and reactivity tests.
2. Limestone C, independently obtained, mined locally in the Free State, with low magnesium content was used to give a good comparison to the dolomites. The limestone was crushed and screened to particle size 212-300 μm for use in the characterisation and reactivity tests.
3. Coal ash was generated through combusting a coal of 36.3% ash in a packed bed reactor at atmospheric pressure. The coal was crushed and screened to 212-300 μm prior to combustion at 900°C in air for 12 hours, so as to achieve complete combustion (carbon conversion) of the samples. The same coal has been used in coal combustion and gasification studies by Njapha, (2003) and

Kaitano, (2006) in the Coal Technology research group at the North-West University, Potchefstroom Campus.

3.2.2 Gases

Gases used in this study were high purity carbon dioxide, high purity nitrogen and a four component sulphur dioxide mixture gas.

These gases were supplied by Afrox in Johannesburg.

The chemical specifications of the gases used were:

Nitrogen	purity > 99.99%
Carbon dioxide	purity > 99.99%
Sulphur dioxide mixture	3000ppm SO_2, 8% CO_2, 8% O_2, 83.7 N_2

The simulated flue gas mixtures for sorbent preparation and sulphation were prepared by mixing the above gases in the desired proportions.

3.3 Experimental apparatus

The main experimental apparatus used to investigate the reactivity of the sorbents in this study is a thermogravimetric analyser (TGA). The experimental set-up consists of a furnace, gas supply and mass flow controllers, microbalance, data logging system and pressure control as the main units.

3.3.1 Description of TGA

For the simulation of the atmospheric and pressurised sulphation analysis a thermogravimetric analyser (TGA) was used. A schematic diagram of the TGA is presented in Figure 3.1 whilst Figure 3.2 is a schematic diagram of the sample basket. A photograph of the thermogravimetric analyser used in the investigations is given in Figure 3.3. Some of the main features of the TGA shown in the schematic diagram are visible from the photograph of the apparatus given in Figure 3.3.

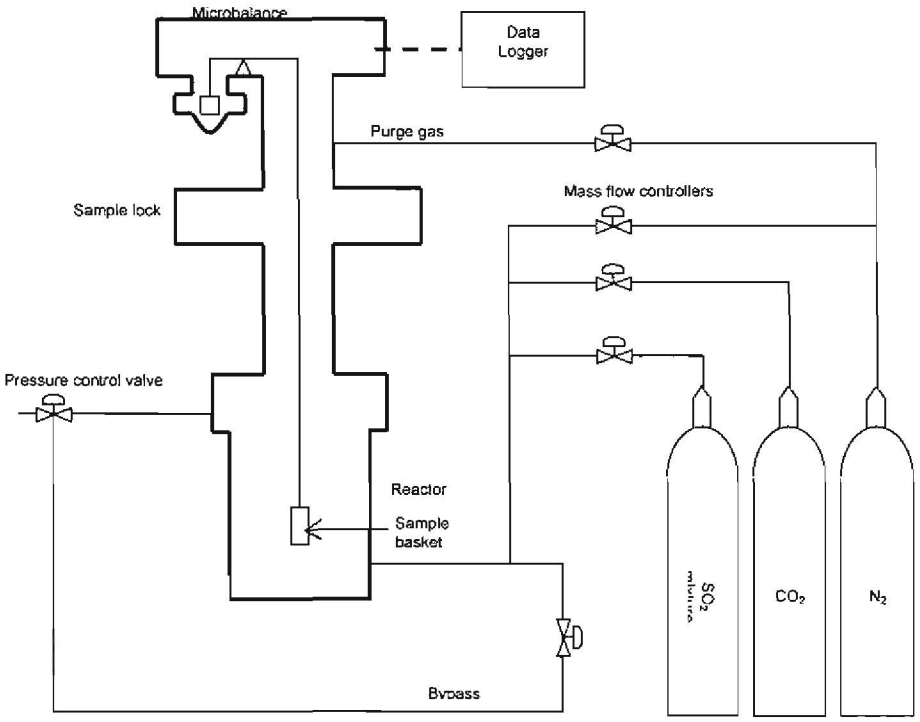

Figure 3.1: Schematic arrangement of experimental equipment (TGA)

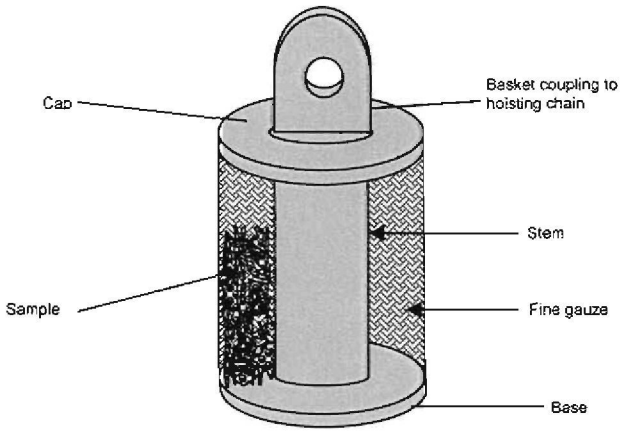

Figure 3.2: Diagram of sample basket

The TGA used in this research is a Bergbau Forshung GMBH 1987 model manufactured by Deutsche Montan Technologie (DMT) in Germany. The TGA can handle solid granules with diameters between 100μm and 5mm and sample mass of up to 800mg. The TGA system is designed for the determination of weight changes

during gas-solid reactions. The reactor can be operated from atmospheric pressure up to 100 bar and temperatures of up to a maximum of 1100°C. The apparatus consists of a microbalance which continuously measure the mass of the sample at controlled temperature and pressure. The microbalance is located above the reactor, in the same chamber and is protected from any corrosive reactive gases by an inert (N_2) gas purge. To avoid the product gases from influencing the reaction rates the reactor is designed as a differential type reactor, meaning that it achieves low gas conversion per pass. Continuous and constant gas flow rates are achieved by a system of calibrated Brooks 5850 TR series thermal mass flow controllers. The experiments can be done isothermally, or the temperature is increased linearly at any desired heating rate between 1-100°C per minute. The stability of the balance requires that a constant gas flow at controlled pressure be maintained to allow for automatic correction of buoyancy and drag forces during experiment. The gas pressure settings on the supply cylinders are set one bar above the required pressure for the TGA hence the gas flow is achieved through pressure difference between the cylinders and the equipment and is automatically controlled through pressure regulators and mass flow controllers.

A computerised data logger allows for the recording of the temperature, pressure, and sample mass at variable sampling rates of up to 10 readings per second. Following a test, the raw data can be stored and plotted showing weight changes as a function of time, pressure or degree of conversion. Different types of reaction rates can be calculated and displayed as a function of time, temperature, or degree of conversion.

The TGA is constructed with a sample lock, located between the microbalance and the reactor and is equipped with an electrically driven winch mechanism for lowering and lifting sample basket into and out of the reaction chamber.

The sample basket shown in Figure 3.2 is suspended from the microbalance with a stainless steel chain. The basket is cylindrical in shape; sample is packed between the inner stem and outer gauze. The sample holder is capable of handling between 100µm and 5mm particle size and sample mass up to 800mg. The basket is made of a platinum frame and platinum gauze which are passive under sulphation reaction conditions.

A photograph of the TGA used in this investigation is shown in Figure 3.3.

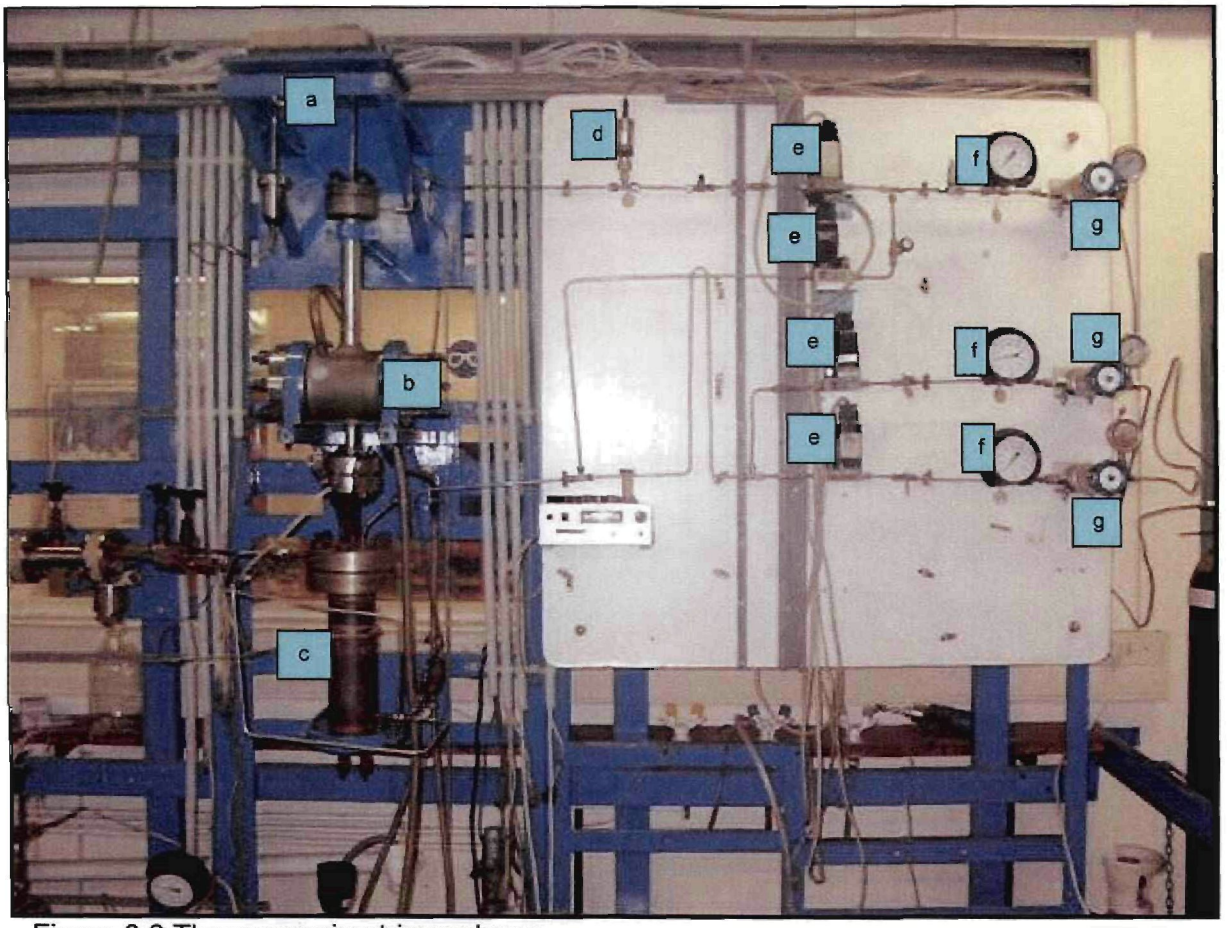

Figure 3.3 Thermogravimetric analyser

Key: a – microbalance
b – sample lock
c – thermal reactor
d – pressure transducer
e – mass flow controller
f – pressure gauge
g – pressure regulator

3.4 Experimental conditions

3.4.1 Solid – gas equilibria

Figure 3.4 gives the experimental zones in relation to $CaCO_3/CaO$ and $MgCO_3/MgO$ phase equilibria with respect to CO_2 partial pressure, these conditions were considered in the design of experiments to simulate atmospheric and pressurised fluidised bed sulphation conditions. Temperatures between 750-900°C are typical of those used in fluidised bed coal combustion (Basu, 2006). The variations in CO_2 equilibrium partial pressure with temperature for the decomposition of $CaCO_3$ and $MgCO_3$ are adapted from Barker (1962) and Erdos (1962) respectively (cited by Fuertes *et al.*, 1995). For dolomite and limestone particles in atmospheric fluidised bed combustors (AFBC) and pulverised coal (PC) combustors operating at CO_2 partial pressures around 0.1-0.2 bar (Fuertes *et al.*, 1995) both $CaCO_3$ and $MgCO_3$ decompose. Atmospheric experiments were done at 0.0875 bar CO_2 partial pressure. In pressurised fluidised bed combustors operating at temperatures up to 900°C with CO_2 partial pressures between 1-2 bar, $MgCO_3$ decompose but $CaCO_3$ does not (Fuertes *et al.*, 1995), if there is CaO it is carbonated by the CO_2 to $CaCO_3$. Pressurised experiments were done at 2 and 3 bar CO_2 partial pressure for the 10 and 15 bar total pressure respectively.

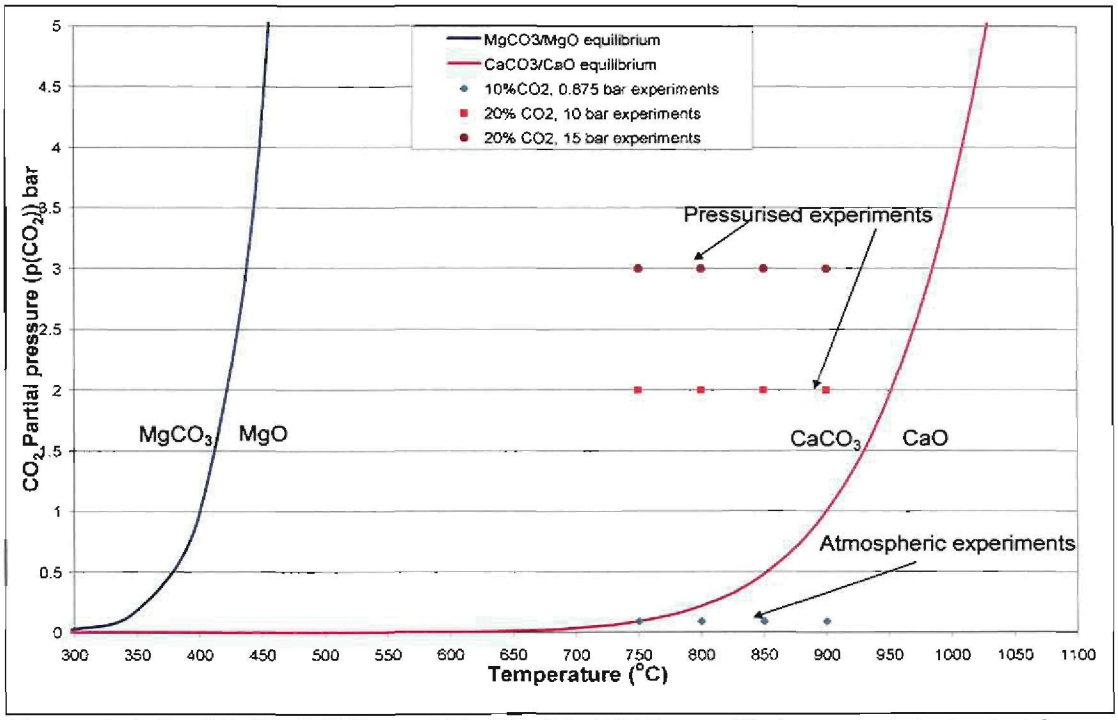

Figure 3.4: $CaCO_3/CaO/CO_2$ and $MgCO_3/MgO/CO_2$ equilibrium curve (adapted from Fuertes *et al.*, 1995)

3.5 Experimental procedure

The calcination and sulphation experiments were carried out in the TGA using simulated flue gas. All sorbent samples were pre-heated for four hours at 150°C in a furnace to drive out free moisture before calcination/carbonation and subsequent sulphation.

3.5.1 Sulphation experimental optimisation

Experimental optimisation was done by varying sample mass and gas flow rate at 850°C. The effect of external diffusion was systematically analysed by varying gas flow rate and sample mass in different sulphation reactions. Figure 3.5 shows mass conversion curves obtained for experimental optimisation using dolomite B under atmospheric (0.875 bar) conditions. The gas composition was 2000ppm SO_2, 5.3% O_2, 10% CO_2 and 84.5% N_2.

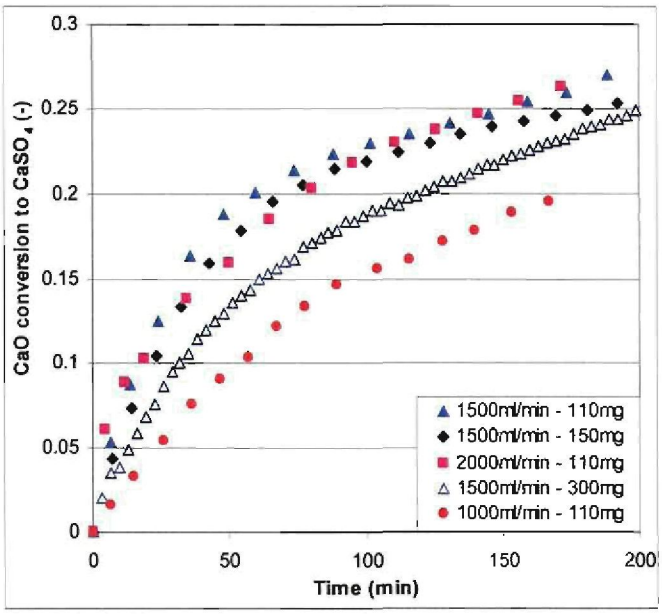

Figure 3.5: Sulphation experimental condition optimisation

Sample size and gas flow rate exert a significant influence on sulphation as shown in Figure 3.5, therefore the determination of sulphation operating conditions in terms of flow rate and sample mass was important. O'Neill *et al.* (1976) also made a similar observation regarding sample mass and flow rate. From these experiments, 100mg sample mass was chosen as the optimum sample weight at a flow rate of 1500 ml/minute for atmospheric experiments and 2000 ml/minute for pressurised experiments to compensate for gas stagnation due to pressurisation.

3.5.2 Sorbent preparation and sulphation under atmospheric conditions

Atmospheric pressure experiments were done at 0.875 bar under isothermal conditions between 750-900°C. Each experiment started with calcination followed by sulphation in simulated flue gas. Temperature, total pressure and CO_2 partial pressure were the same for calcination and sulphation under each set of conditions. The gas composition was selected based on equilibrium partial pressures of decomposition as given in Figure 3.4. Experimentally determined optimum flow rate and sample mass were used to ensure minimal external mass transfer resistance and minimal sample bed diffusion. 100mg sample mass was used per experimental run.

The experimental sequence consisted of the following experimental steps:

1. Sample was first calcined isothermally in a gas consisting of 10% CO_2 and 90% N_2 at atmospheric pressure for reaction temperatures between 750-900°C at a flow rate of 1000 ml/minute. At atmospheric conditions the $MgCO_3$ and $CaCO_3$ in the sorbents calcined to MgO and CaO respectively.
2. After a constant mass had been reached on calcination the experimental temperature and pressure were maintained, the sample basket was raised to the cold non-reaction zone whilst the gas mixture and flow rate were switched over to sulphation gas. During this step the gas flow bypassed the reactor basket. Sulphation gas flow rate was run at 1500 ml/minute.
3. The sulphation gas was run for two minutes before the sample basket was lowered to the reaction zone to allow a homogenous SO_2 gas mixture to fill the reactor system.

The simulation of atmospheric coal combustion gas mixture for use in sulphation was obtained by mixing in the ratio 66.7:4.7:28.6 a sulphur dioxide gas mixture (3000ppm SO_2, 8% CO_2, 8% O_2, 83.7% N_2) with CO_2 (99.99%) and N_2 (99.99%) respectively. The chemical composition of the gas mixture used for atmospheric sulphation constituted of 2000ppm SO_2, 5.3% O_2, 10% CO_2, 84.5% N_2 for atmospheric sulphation.

Table 3.1 shows the experimental conditions used for calcination and sulphation under atmospheric pressure.

Table 3.1: Calcination and sulphation conditions at atmospheric pressure

Parameter	Calcination conditions	Sulphation conditions
Pressure	0.875 bar	0.875 bar
Particle diameter	212-300μm dolomite and limestone 140μm coal ash	212-300μm dolomite and limestone 140μm coal ash
Gas concentration	10% CO_2, 90% N_2	2000ppm SO_2, 5.3% O_2, 10% CO_2, balance N_2
Sample mass	100mg	Product of calcining 100mg
Gas flow rate	1000 $ml_{(stp)}$/min	1500 $ml_{(stp)}$/min
Temperature	750, 800, 850 and 900°C	750, 800, 850 and 900°C

3.5.3 Sorbent preparation and sulphation under pressurised conditions

Pressurised experiments were done at 10 and 15 bar pressures. The gas flow rate for sulphation was 2000 ml/minute for sulphation at both 10 and 15 bar experiments.

The experimental sequence consisted of the following experimental steps:

1. Sample was first calcined isothermally in a gas consisting of 20% CO_2 and 80% N_2 at 10 and 15 bar pressure at temperatures between 750-900°C. The CO_2 partial pressure at pressurised sulphation is such that only $MgCO_3$ will calcine under the range of temperatures used. Coal ash was carbonated in 100% CO_2 gas at temperatures from 750-900°C so as to convert CaO to $CaCO_3$. The flow rate for calcination gas mixture was 1000 ml/minute.
2. After a constant mass had been reached on calcination/carbonation the experimental temperature and pressure were maintained, the sample basket was raised to the cold zone whilst the gas mixture was switched over to sulphation gas. During this step the gas flow bypassed the reactor basket. Sulphation gas flow rate was run at 2000 ml/minute.
3. The sulphation gas was run for ten minutes before the sample basket was lowered to allow a homogenous SO_2 gas mixture to fill the reactor.

The simulation of pressurised sulphation gas mixture was obtained by online mixing in the ratio 66.7:14.6:18.7 of a sulphur dioxide gas mixture (3000ppm SO_2, 8% CO_2, 8% O_2, 83.7% N_2) with CO_2 (99.9%) and N_2 (99.9%) respectively. The final chemical composition of the simulated gas mixture used for pressurised conditions was 2000ppm SO_2, 5.3% O_2, 20% CO_2, and 74.5% N_2.

Table 3.2 shows the experimental conditions used for calcination and sulphation under pressure of either 10 or 15 bar.

Table 3.2: Calcination/carbonation and sulphation conditions under pressure

Parameter	**Calcination/carbonation conditions**	**Sulphation conditions**
Pressure	10 and 15 bar	10 and 15 bar
Particle diameter	212-300μm dolomite and limestone 140μm coal ash	212-300μm dolomite and limestone 140μm coal ash
Gas concentration	20% CO_2, 80% N_2 for calcination 100% CO_2 for coal ash carbonation	2000ppm SO_2, 5.3% O_2, 20% CO_2, balance N_2
Sample mass	100mg	Product of calcining 100mg
Gas flow rate	1000 $ml_{(stp)}$/min	2000 $ml_{(stp)}$/min
Temperature	750, 800, 850 and 900°C	750, 800, 850 and 900°C

3.5.4 Experimental program

Table 3.3 is a summarised list of the sulphation experiments conducted. In all cases the oxygen (O_2) concentration in the gas was 5.3%, SO_2 was 2000ppm, CO_2 was 10 and 20% for atmospheric and pressurised conditions respectively, and the balance constituent of the gas mixture was nitrogen (N_2). Each of the four sorbents was tested at 0.875, 10 and 15 bar total pressure at temperatures 750, 800, 850 and 900°C, therefore a total of 48 experimental runs were done.

Consistence checks were done by repeating a set of experiments at least twice for each sample at one selected temperature to check for repeatability.

Table 3.3: List of experiments done and experimental conditions used.

Experiment No.	Sorbent	Temperature (°C)	Total pressure (bar)	CO_2 conc. (v/v%)	CO_2 partial pressure (bar)	SO_2 conc. (ppm)
OA1-OA4	Dol A	750, 800, 850 and 900	0.875	10	0.0875	2000
OA5-OA8	Dol A	750, 800, 850 and 900	10	20	2.0	2000
OA9-OA12	Dol A	750, 800, 850 and 900	15	20	3.0	2000
OB1-OB4	Dol B	750, 800, 850 and 900	0.875	10	0.0875	2000
OB5-OB8	Dol B	750, 800, 850 and 900	10	20	2.0	2000
OB9-OB12	Dol B	750, 800, 850 and 900	15	20	3.0	2000
OC1-OC4	Limstn C	750, 800, 850 and 900	0.875	10	0.0875	2000
OC5-OC8	Limstn C	750, 800, 850 and 900	10	20	2.0	2000
OC9-OC12	Limstn C	750, 800, 850 and 900	15	20	3.0	2000
OD1-OD4	Coal ash	750, 800, 850 and 900	0.875	10	0.0875	2000
OD5-OD8	Coal ash	750, 800, 850 and 900	10	20	2.0	2000
OD9-OD12	Coal ash	750, 800, 850 and 900	15	20	3.0	2000

Key: Dol A - dolomite A; Dol B - dolomite B. Limstn C - Limestone C

3.5.4 Reproducibility

Reproducibility tests were initially done by repeating three times the sulphation of dolomite B under controlled and fixed reaction conditions as given in table 3.3 at 850°C and 1 bar. The reproducibility was good, within a range of 92-95%. Figure 3.6 shows the results obtained from the reproducibility tests with dolomite B at 850°C and 1 bar using the optimised experimental conditions.

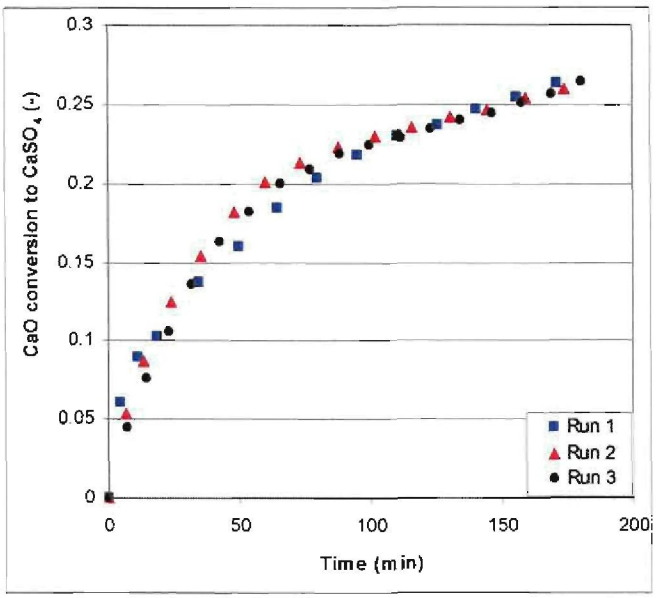

Figure 3.6: Reproducibility tests for experimental set up using dolomite B.

3.6 Sorbent characterisation techniques

Table 3.4 shows the properties determined in the characterisation experiments, the equipment used and the laboratory where the work was conducted.

Table 3.4: Properties determined, analysis equipment and laboratory

Property	**Analysis**	**Equipment used**	**Laboratory**
Porosity Average pore diameter	Mercury porosimetry	Micromeritics Autopore III	NWU
Specific surface area Pore size distribution	Nitrogen Adsorption	Micromeritics ASAP 2010	NWU
Chemical composition, Elemental composition	Spectrometry Combustion for total C	ICP-MS and SEM-EDS	Mintek
Particle size distribution	Laser diffraction	Malvern Mastersizer 2000	NWU
Particle density	Density measurement	Helium stereopycnometer	NWU

NWU - North-West University

3.6.1 Sorbent elemental analysis

The elemental analysis of the sorbent material was done using an inductively coupled plasma mass spectrometer (ICP-MS) at Mintek (S. Africa) laboratory in

Johannesburg, excluding the total carbon content of the material which was determined through combustion.

3.6.2 Sorbent particle density

Skeletal density of each sorbent was measured using a helium pycnometer. The pycnometer used is a Quantachrome Stereopycnometer. Skeletal volume, as applied to discrete pieces of solid material was obtained.

3.6.3 Sorbent surface morphology after reaction

An FEI Quanta 200-SEM was used to obtain images of the morphology of the dolomite, limestone and coal ash surfaces. Despite appearing as three dimensional, true 3-D can only be attained by using two pictures taken at different angles. The images obtained on the dolomite, limestone and coal ash samples were obtained on the back scattered electrons.

3.6.4 Sorbent specific surface area analysis (nitrogen adsorption)

Specific surface area of the sample was measured using a Micromeritics ASAP 2010 Analyser. Samples were prepared by heating to 150°C while simultaneously evacuating to 10^{-6}µmHg in a sample tube to remove the liberated impurities. The evacuated sample was cooled in liquid nitrogen at -196°C, and then exposed to analysis gas, N_2, at a series of precisely controlled pressures up to a relative pressure of one or saturation. The nitrogen adsorption method can be used to characterise material with pore diameter between 0.00035-0.3 µm (Webb, 2001), it is accurate for pore sizes in the micro – meso pore size range.

3.6.5 Sorbent porosity and pore size analysis (mercury porosimetry)

The porosity of the sample was measured using a Micromeritics Auto-pore Analyser III. Mercury porosimetry characterises a material's porosity by applying various levels of pressure to a sample immersed in mercury. The method is suitable for materials with pores in the approximate range of diameter 0.003-400µm (Stanley-Wood and Lines, 1992; Webb, 2001). This method is thus used to determine porosity and pore size distribution in the meso – macro pore size range.

CHAPTER 4

SORBENT CHARACTERISATION

4.1 Introduction

In this Chapter the characterisation results of the sorbents used are presented. In Section 4.2 the particle size distribution results are presented and in Section 4.3 sorbent elemental and chemical composition analysis results are given. Physical properties analysis using nitrogen adsorption, mercury porosimetry and helium pycnometry are presented in Section 4.4. In Section 4.5 the scanning electron microscope images of sorbents surface developments with reaction are presented, whilst in Section 4.6 conclusions from characterisation results are given.

4.2 Sorbent particle size distribution results

The particle size distribution (PSD) of the raw samples and the coal ash are shown in Figures 4.1-4.4. The sorbents particle size distributions were determined using a laser light scattering particle size analyser (Malvern Master Sizer 2000). Particle size distribution of the raw sorbents were relatively similar, showing a normal distribution on a log normal plot, whilst the coal ash sample showed a skewed distribution on a log normal plot. The coal ash particle size distribution shows that there was fragmentation of coal particles in the ashing process.

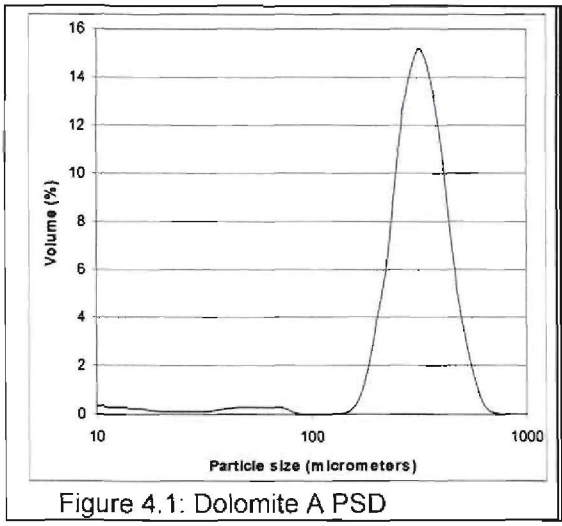

Figure 4.1: Dolomite A PSD

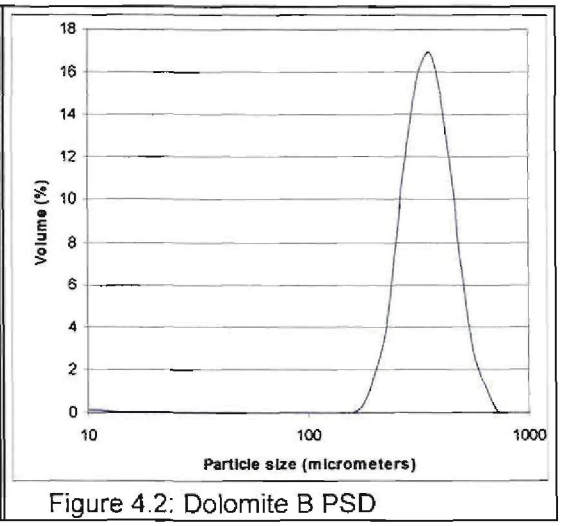

Figure 4.2: Dolomite B PSD

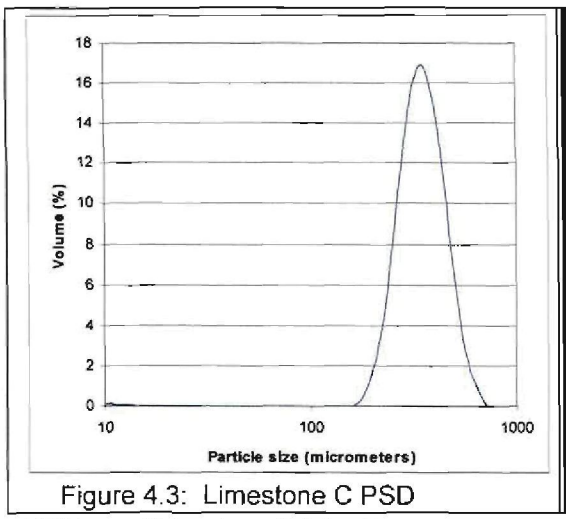

Figure 4.3: Limestone C PSD

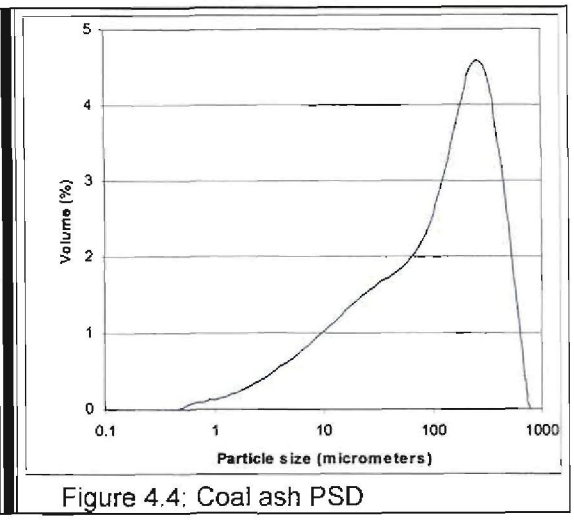

Figure 4.4: Coal ash PSD

PSD- particle size distribution

The average particle size for dolomite A, dolomite B and limestone C was quite similar at about 260μm and coal ash was 140μm.

4.3 Sorbent chemical characterisation results

4.3.1 Proximate and ultimate analysis of coal from which ash was generated

The proximate and ultimate analysis of the coal from which the coal ash was generated is given in Table 4.1.

Table 4.1: Coal proximate and ultimate analysis

Coal proximate analysis				
wt/wt %	% Moisture	% Ash	% Volatiles	% Fixed C
Dry basis	-	37.3	20.9	41.9
As received	2.4	36.3	20.4	40.9

Ultimate analysis					
wt/wt %	Total Sulphur	%Carbon	%Hydrogen	%Oxygen	%Nitrogen
Dry basis	1.7	50.0	2.7	7.1	1.1
As received	1.7	49.1	2.6	6.9	1.1

4.3.2 Elemental and chemical analysis of sorbents

The elemental analysis results of dolomite A, dolomite B, limestone C and coal ash are presented in Table 4.2. Chemical composition deduced from elemental analysis is given in Table 4.3

Elemental and chemical characterisation

Table 4.2: Elemental composition of sorbents done at Mintek (S. Africa) laboratory

Sorbent	C (wt%)	Al (wt%)	Si (wt%)	Ti (wt%)	Mn (wt%)	Fe (wt%)	Ca (wt%)	Mg (wt%)	S (wt%)	O (wt%)
Dolomite A	11.2	0.32	2.84	0.05	0.30	1.56	26.90	5.58	-	47.35
Dolomite B	12.8	0.01	1.43	0.05	0.50	0.59	20.20	11.50	-	48.45
Limestone C	8.97	0.48	9.06	0.04	0.13	0.15	30.05	0.37	-	48.96
Coal ash	1.48	11.60	20.80	0.67	0.07	5.35	7.17	0.92	1.46	n/m

n/m – not measured

Table 4.3: Chemical composition of sorbents (calculated from elemental composition)

Sorbent	Free C (wt%)	Al_2O_3 (wt%)	SiO_2 (wt%)	TiO_2 (wt%)	MnO_2 (wt%)	Fe_2O_3 (wt%)	$CaCO_3$ (wt%)	$MgCO_3$ (wt%)	CaO (wt%)	MgO (wt%)	K_2O (wt%)	Na_2O (wt%)	SO_3 (wt%)	CO_2 (wt%)
Dolomite A	-	0.60	6.00	0.08	0.42	2.20	67.30	19.50	37.71	9.32	-	-	-	39.79
Dolomite B	-	0.09	3.00	0.08	0.69	0.84	50.50	40.30	28.29	19.26	-	-	-	43.24
Limestone C	-	1.81	19.38	0.07	0.20	0.43	75.05	1.28	42.05	0.61	-	-	-	33.69
Coal ash	1.48	21.90	43.70	1.10	0.10	7.70	-	-	10.00	1.50	0.80	0.25	3.64	0.72

Dolomite A with 67.30% $CaCO_3$ and 19.50% $MgCO_3$ is a high-calcium dolomite as its stoichiometric balance is shifted towards calcium. Dolomite B with 50.50% $CaCO_3$ and 40.30% $MgCO_3$ is a balanced dolomite, closer to elemental specifications of a theoretical dolomite. Limestone C with 75.05% $CaCO_3$ and 1.28% $MgCO_3$ is considered a limestone for all purposes.

The $CaCO_3$ and $MgCO_3$ content of dolomite A, dolomite B and limestone C are comparable to the specifications of sorbents used by other researchers (Zevenhoven *et al.*, 1998a,b; Fuertes *et al.*, 1995; Alvarez and Gonzalez, 1999; Trikkel and Kuusik, 2003) in similar work as shown in Table 2.1.

The comparative composition of calcium and magnesium is shown in Figure 4.5. With respect to calcium, limestone C has the lowest relative magnesium content, followed by coal ash then dolomite A and lastly dolomite B. The dominant element in coal ash by composition is silicon which exists in aluminium silicate and silicon dioxide. About 44% weight of coal ash is SiO_2. The coal from which the ash used in the research was produced had 1.7% by weight sulphur and the ash contained 1.46% sulphur, meaning that the ash retained 31.2% of sulphur originally in the coal. In the coal ash 72% of the calcium originally in the coal is unused with regards to sulphur capture; the coal ash shall thus be tested as a raw sulphur capture sorbent.

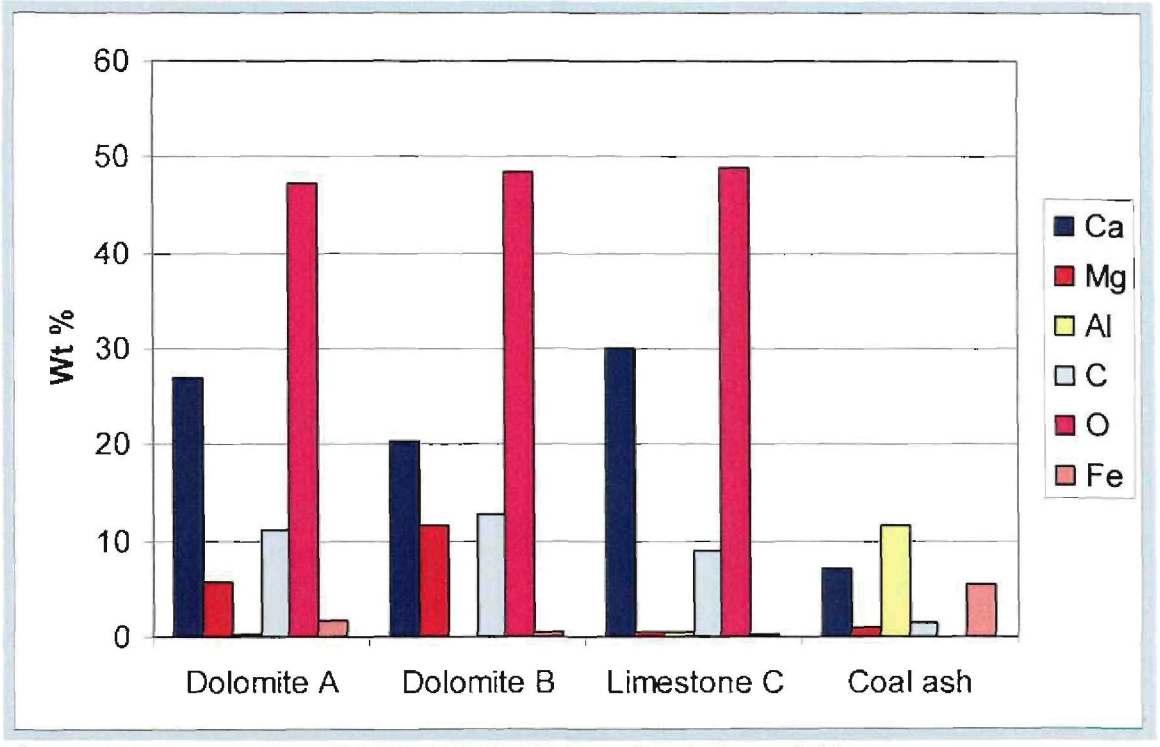

Figure 4.5: Composition of major elements in sorbents by weight.

4.4 Physical properties of raw sorbents

4.4.1 Nitrogen adsorption

The BET (Brunauer, Emmett and Teller) adsorption analysis of the sorbents using nitrogen as the adsorbate gave composite adsorption isotherms shown in Figures 4.6-4.9. The nitrogen adsorption method can be used to characterise material with pore diameter between 0.00035-0.3 μm (Micromeritics, 2001), which is pore size in the micro–meso pore size range. The adsorption isotherms of raw sorbents, dolomite A, dolomite B, limestone C and coal ash generally have similar shape. Half calcined and fully calcined sorbents were also analysed using nitrogen adsorption and the results are presented in Table 4.4.

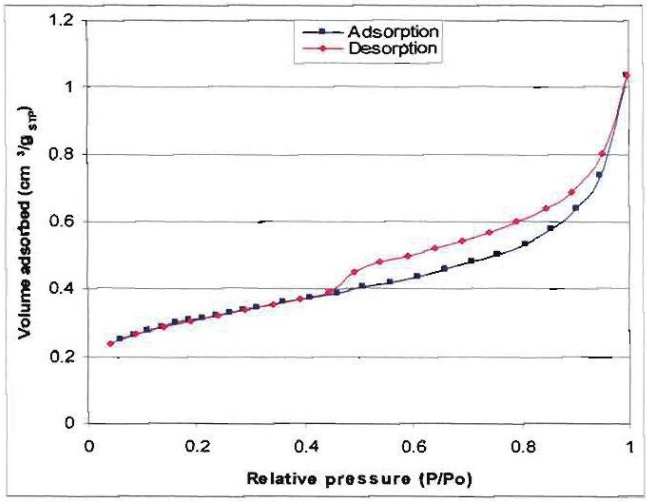

Figure 4.6: Raw dolomite A nitrogen adsorption/desorption isotherms

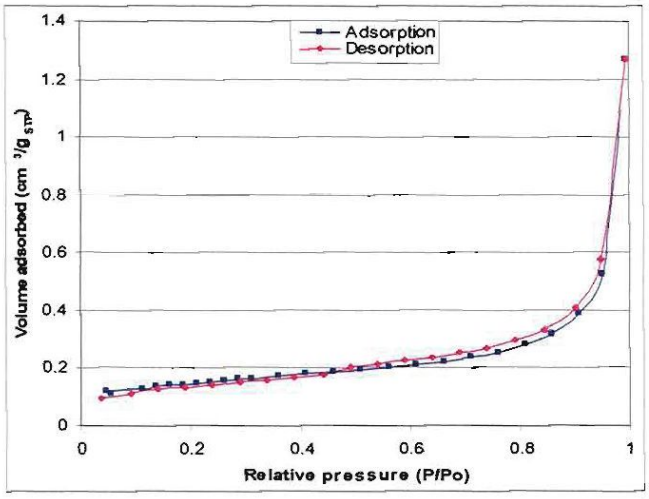

Figure 4.7: Dolomite B nitrogen adsorption/desorption isotherms

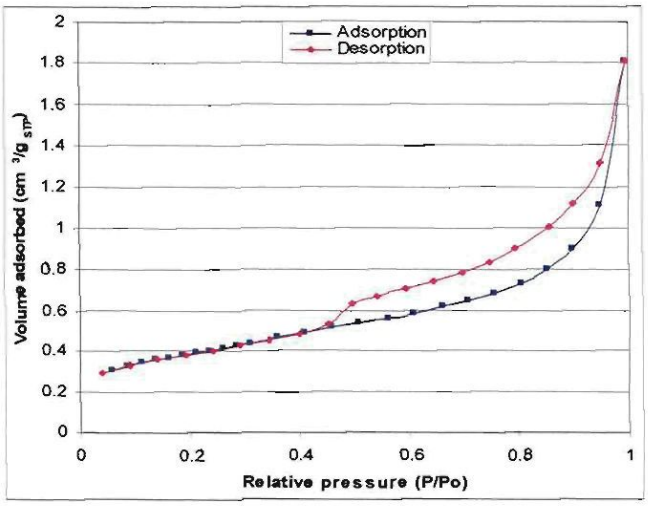

Figure 4.8: Limestone C nitrogen adsorption/desorption isotherms

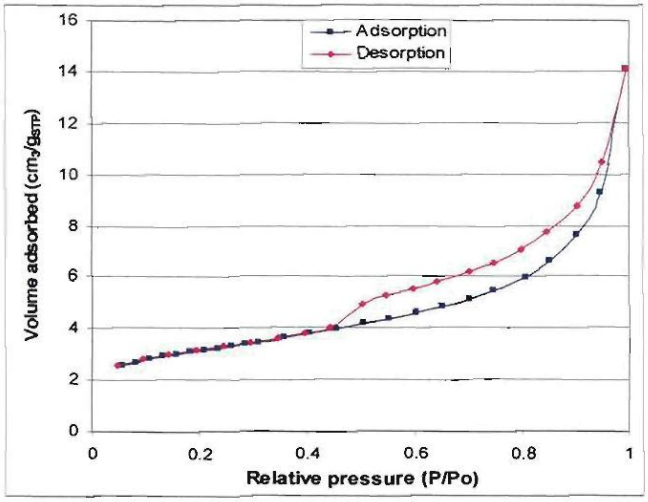

Figure 4.9: Coal ash nitrogen adsorption/desorption isotherms

The adsorption isotherms for these sorbents show class II and IV isotherms as classified by IUPAC (Sing *et al.*, 1982; Gregg and Sing, 1982). The hysteresis loops of the sorbents close at relative pressures between 0.4 and 0.9, meaning that the pore sizes of each sample are confined to the meso-macropore range (Gregg and Sing, 1982; Do, 1998). All the isotherms show type H3 hysteresis, which is associated with slit-shaped pores or the space between parallel plates (Sing *et al.*, 1982; Lowell and Shields, 1984). The rapid rise of the isotherm near relative pressure of one ($p/p^{o}=1$) can be identified in the limit of the large macropores (Sing *et al.*, 1982).

Table 4.4 gives the characterisation parameters obtained from nitrogen adsorption, using the BET and BJH (Barrett, Joyner and Halenda) analysis. The parameters

obtained are BET surface area, pore volume (of pores up to 300nm diameter) and BET average pore diameter.

Table 4.4: BET surface areas, BJH pore volumes and average BET pore diameters

Sorbent	Preparation conditions	BET surface area (m^2/g)	BJH volume of pores 1.7-300nm diameter (cm^3/g)	BET average pore diameter (μm)
Dolomite A	Raw	0.608	0.00316	0.0098
	Partially calcined at 800°C	1.852	0.02857	0.0219
	Fully calcined at 800°C	16.219	0.13686	0.0168
Dolomite B	Raw	0.477	0.00205	0.0070
	Partially calcined at 800°C	6.312	0.08525	0.0259
	Fully calcined at 800°C	15.677	0.14314	0.0147
Limestone C	Raw	1.033	0.00952	0.0210
	Partially calcined at 800°C	0.921	0.00917	0.0176
	Fully calcined at 800°C	10.066	0.08480	0.0848
Coal ash	Coal combusted at 900°C	11.077	0.01508	0.0402

The BET surface area of raw limestone C decreases by 11% on half calcination whilst it increases threefold and thirteen fold for dolomite A and dolomite B respectively. This can be attributed to pore growth due to CO_2 release as $MgCO_3$ calcines. This trend on surface area with partial calcination shows a correlation with sorbent $MgCO_3$ content (refer to Table 4.3), meaning that the higher the $MgCO_3$ content, the higher the increase in surface area of sorbent. On full calcination the surface area of raw sorbent increases about ten fold for limestone C and twenty-seven and thirty-two fold for dolomite A and dolomite B respectively.

4.4.2 Mercury porosimetry

Micromeritics Auto Pore III Analyser was used for the determination of pore volume, pore area and porosity. The method is suitable for pores in the approximate range of diameter 0.003-400μm (Stanley-Wood and Lines, 1992; Webb, 2001), which is porosity and pore size distribution in the meso–macro pore size range. The results obtained from mercury intrusion are presented in Table 4.5. The total intrusion volume per unit mass of raw limestone C marginally decreased by 0.2% on partial calcination whilst it increased twofold and two and half times for dolomite A and dolomite B respectively. This trend is similar to that of BET surface area, the higher the $MgCO_3$ content, the higher the increase in surface area of sorbent on half

calcination. On full calcination the total intrusion volume per unit mass of limestone C increases about two fold and five fold each for the two dolomites.

Table 4.5: Parameters of sorbent characterisation using mercury intrusion

Sorbent	Preparation condition	Total Hg intrusion volume (cm^3/g)	Total pore area (m^2/g)	Average pore diameter (μm)	Porosity (-)
Dolomite A	Raw	0.0832	1.337	0.249	0.190
	Half calcined at 800°C	0.1633	4.900	0.133	0.300
	Fully calcined at 800°C	0.4206	2.091	0.805	0.357
Dolomite B	Raw	0.0754	0.991	0.304	0.172
	Half calcined at 800°C	0.1958	12.029	0.065	0.352
	Fully calcined at 800°C	0.3945	0.019	0.851	0.265
Limestone C	Raw	0.2035	0.951	0.856	0.236
	Half calcined at 800°C	0.2031	1.221	0.665	0.226
	Fully calcined at 800°C	0.3936	2.647	0.595	0.297
Coal Ash	Coal combusted at 900°C	0.4719	1.162	1.623	0.315

4.4.3 Particle density- Helium pycnometry

Table 4.6 shows the sorbent densities obtained, these are skeletal densities. The values are comparable to results obtained by Zevenhoven *et al.* (1998a,b).

Table 4.6: Skeletal densities of the sorbents

Sorbent	Preparation conditions	Skeletal density (kg/m^3)
Dolomite A	Raw	2845
Dolomite B	Raw	2480
Limestone C	Raw	2908
Coal Ash	Coal combusted at 900°C	2790

4.4.4 Integration of nitrogen adsorption and mercury porosimetry data

The characterisation results from nitrogen adsorption and mercury intrusion complement each other and can thus be used to deduce meaningful information which neither methods can supply alone (Lowell and Shields, 1984). The physical parameters as obtained by the integration of results from helium pycnometry, nitrogen adsorption and mercury porosimetry are presented in Table 4.7.

Table 4.7: Physical properties of sorbents

Sorbent	Preparation conditions	BET surface area (m^2/g) [a]	Particle porosity (-) [b]	Average pore diameter (μm) [b]	Particle density (kg/m^3) [c]	Molar density of $CaCO_3$ in sorbent (mol/m^3) [d]
Dolomite A	Raw	0.608	0.191	0.249	2845	19074
	Half calcined at 800°C	1.852	0.300	0.133	2560	
	Fully calcined at 800°C	16.219	0.357	0.805	2151	
Dolomite B	Raw	0.477	0.171	0.304	2908	11492
	Half calcined at 800°C	6.312	0.265	0.065	2300	
	Fully calcined at 800°C	15.677	0.352	0.851	1731	
Limestone C	Raw	1.033	0.236	0.856	2480	18596
	Half calcined at 800°C	0.921	0.226	0.665	2590	
	Fully calcined at 800°C	10.066	0.297	0.595	1970	
Coal ash	Coal combusted at 900°C	11.077	0.315	1.620	2790	3683

[a] – from nitrogen BET surface analysis

[b] – from mercury porosimetry

[c] – from helium pycnometry

[d] – calculated from chemical composition and particle density

Half calcined means the sorbent has been calcined under condition of temperature and pressure where $CaCO_3$ does not calcine but only $MgCO_3$ calcines. The half calcination conditions for the tested dolomites are 800°C, total pressure 15 bar, 20% CO_2, this means a CO_2 partial pressure of 3 bar and the rest is N_2.

4.5 Scanning electron microscope micrographs of the sorbents

A scanning electron microscope (Quanta 200) was used to analyse structural changes taking place on the surface of the material under various conditions of temperature, pressure and chemical reaction. The structural modifications that are a direct result of the physical and chemical changes in the solid are sintering, swelling, softening and cracking (Szekely *et al.*, 1976) some of which have been observed for the sorbents used here as seen in Figures 4.10-4.12 The scanning was done at a high magnification of 5000x and intensively shows surface developments on the particle surface.

Figures 4.10 (a)–(c) show the photo micrographs of raw dolomite B and sulphated dolomite B at 750°C and 900°C respectively, all at atmospheric pressure. Raw dolomite B shows a smooth crystalline surface, which intensively cracks with reaction at 750°C, whilst at 900°C the micrographs show extensive cracking and surface reforming. This could be due to a highly porous structure formed as sorbent calcines, giving way to cracks at 750°C with reaction combined with continuous heating resulting in a combination of cracks and reforming at 900°C. Figures 4.10 (e) and (f) show surface development on sulphating dolomite B at 15 bar pressure, at 750°C the surface remains intact with slight reforming as reaction occurs but open pores can be seen on the surface, whilst at 900°C the surface remains intact but very large pores can be seen, this could be due to sintering and surface reforming at 900°C. The pores are from CO_2 released from direct sulphation at 15 bar sulphation.

On Figures 4.11 (a)-(c) raw limestone C surface shows a rough crystalline surface structure, photographs show an intact structure with smaller pores at 750°C atmospheric sulphation, this is because of lower CO_2 loss on full calcination creating an intact calcine relative to dolomite B (refer to Table 4.3). At 900°C, atmospheric sulphation, surface reformation can be observed with major cracks as sorbent sinters. Figures 4.11 (d) and (e) show sulphation of limestone C at 15 bar total pressure, at 750°C there is visible surface reformation and small pores on the surface whilst at 900°C there is significant surface reformation and sintering with larger open pores on the surface, the pores are possibly a result of CO_2 released from sulphation.

Figure 4.12 (a) and (b) show no significant change on the morphology of coal ash, for sulphation at 900°C.

SEM photo micrographs of Dolomite B

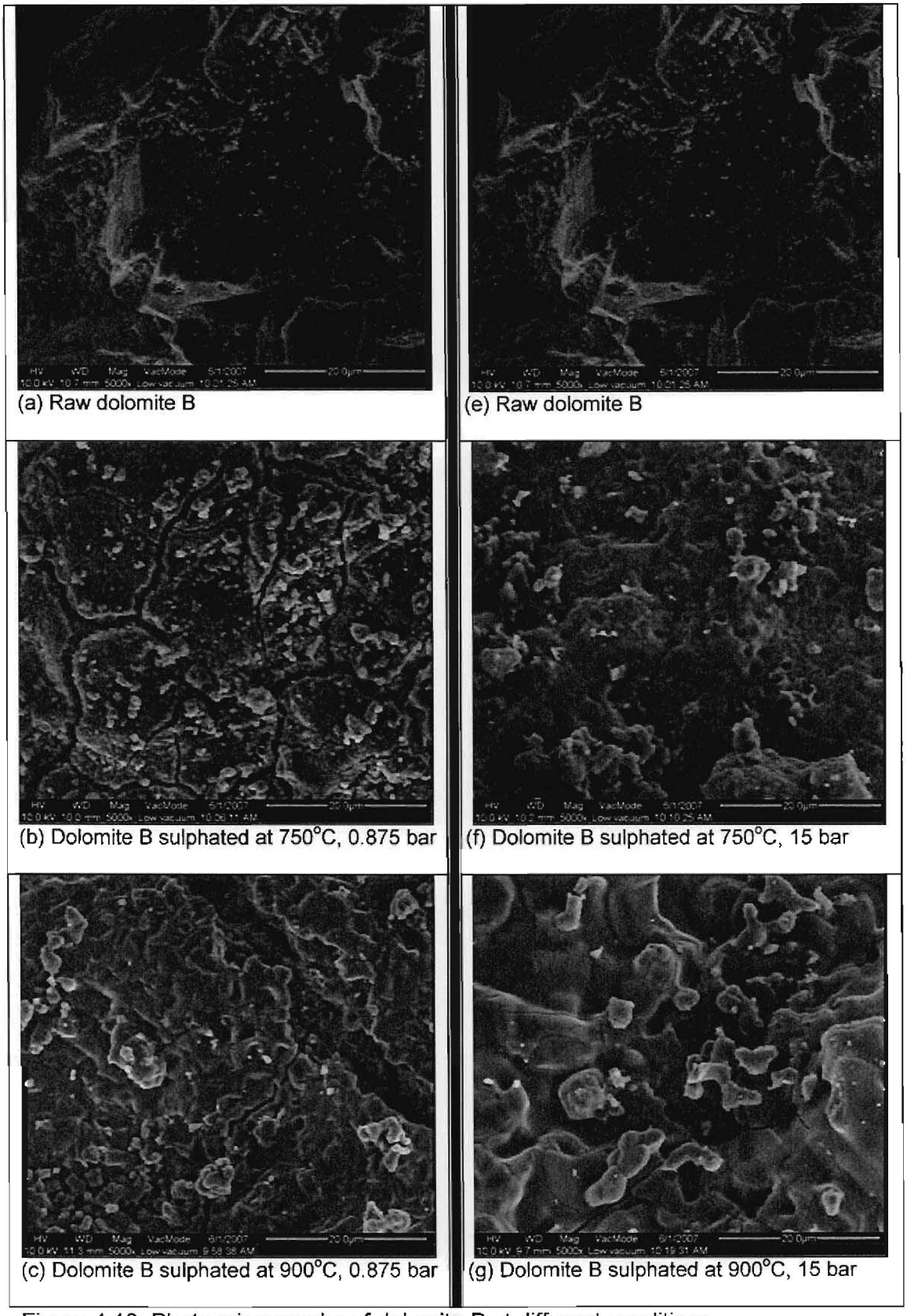

(a) Raw dolomite B

(e) Raw dolomite B

(b) Dolomite B sulphated at 750°C, 0.875 bar

(f) Dolomite B sulphated at 750°C, 15 bar

(c) Dolomite B sulphated at 900°C, 0.875 bar

(g) Dolomite B sulphated at 900°C, 15 bar

Figure 4.10: Photo micrographs of dolomite B at different conditions

SEM photo micrographs of Limestone C

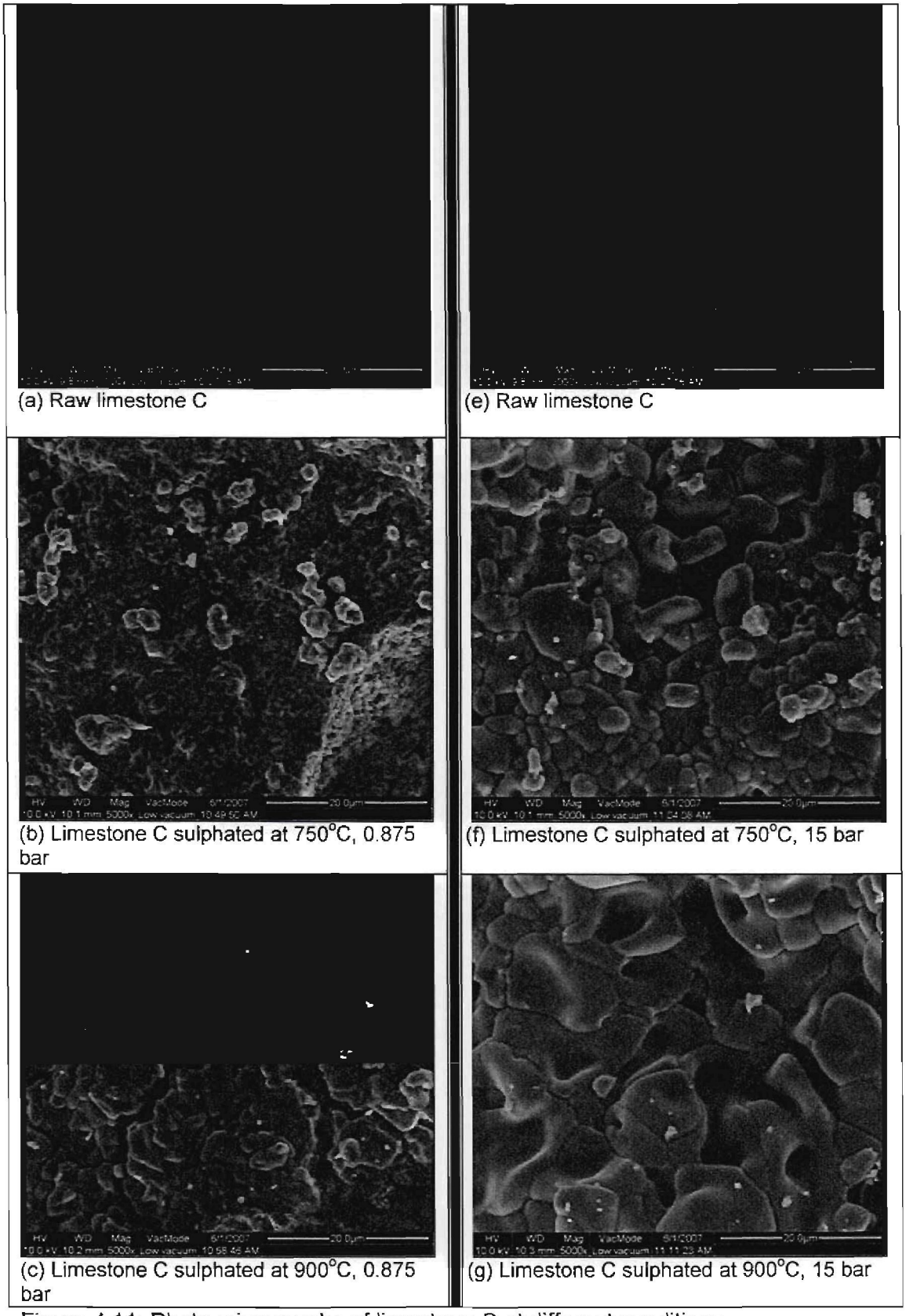

(a) Raw limestone C

(e) Raw limestone C

(b) Limestone C sulphated at 750°C, 0.875 bar

(f) Limestone C sulphated at 750°C, 15 bar

(c) Limestone C sulphated at 900°C, 0.875 bar

(g) Limestone C sulphated at 900°C, 15 bar

Figure 4.11: Photo micrographs of limestone C at different conditions

SEM photo micrographs of coal ash

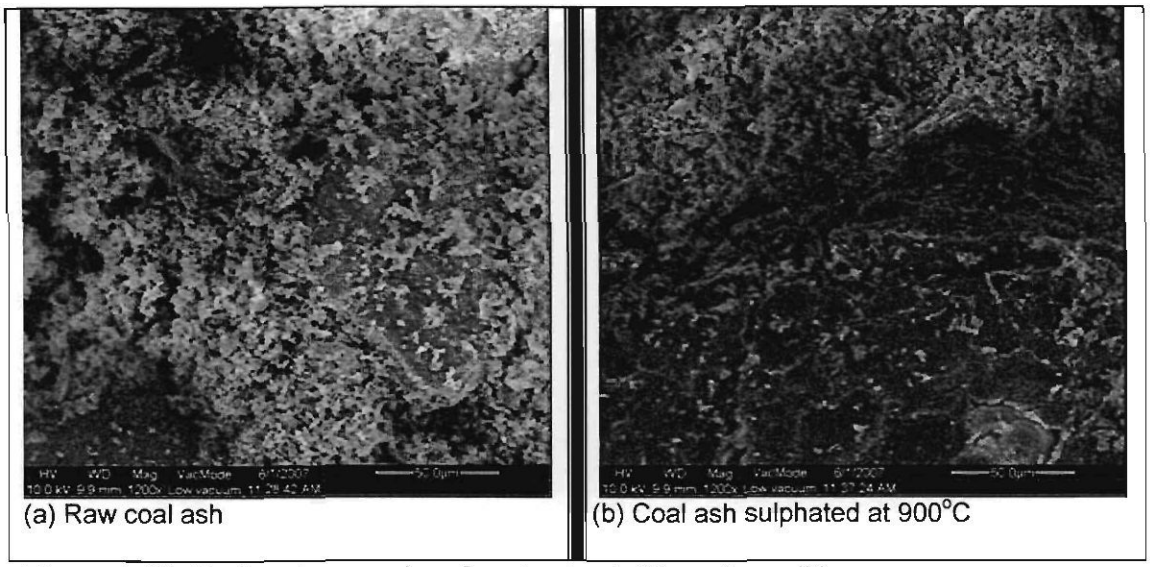

(a) Raw coal ash (b) Coal ash sulphated at 900°C

Figure 4.12: Photo micrographs of coal ash at different conditions

4.6 Conclusions: Characterisation results

Characterisation using nitrogen and mercury intrusion showed that dolomite A and dolomite B exhibit an increase in pore volume, porosity and specific surface area on half and full calcination. The increase in surface area on half calcination shows a direct correlation to the $MgCO_3$ content of the sorbent. The change in porosity due to full calcination of the two dolomites and the limestone seem to be correlated to the combined composition of $MgCO_3$ and $CaCO_3$. The total effect of surface area and porosity change on full calcination is linked to the total loss of CO_2 on calcination.

For limestone C there was a slight decrease in pore volume, porosity and specific surface area on half calcination and an increase on full calcination. The slight surface area loss on half calcination of limestone C could be due to the low $MgCO_3$ content denoting a marginal opening of pores to the little CO_2 loss, which is overwhelmed by the loss in porosity and surface area (sintering) due to calcination temperature, hence the overall effect determined by temperature effect.

Combining results from both nitrogen adsorption and mercury porosimetry show that dolomite A, dolomite B and limestone C are predominantly meso-macroporous with an increase in porosity and surface area on partial and full calcination. The very low internal surface area of raw sorbents dolomite A, dolomite B and limestone C show

that the raw sorbent have very low micro porosity meaning that the greater part of the surface area is external surface area. The internal surface area and porosity of the sorbents increase on calcination through the release of CO_2.

It can be deduced from ash and coal characterisation that the coal ash has already captured 31.2% of the sulphur in the coal during combustion. This capture corresponds to calcium utilisation of about 23% in inherent sulphur retention.

As shown on Table 4.7 the coal ash exhibit larger surface area, pore volume and porosity compared to the dolomite and limestone but the calcium content is much lower such that it is not likely to compete with dolomite and limestone as a commercial sorbent. The physical and chemical parameters of coal ash show good sulphur dioxide capture capability.

The SEM photo micrographs show that there is considerable change to sorbents surface and structure with reaction under different conditions. Therefore there is need for a thorough study to quantify and link the changes and effects of pressure on sorbents' various conversion levels and heating times.

CHAPTER 5

RESULTS AND DISCUSSION: CALCINATION AND SO_2 REMOVAL UNDER FBC CONDITIONS

5.1 Introduction

In this Chapter results on calcination and sulphur dioxide removal capacities of the sorbents under FBC conditions are presented. In Section 5.2 the sorbent preparation results are presented. In Section 5.2.1 and 5.2.2, sorbent preparation results under atmospheric and under high pressure are presented respectively. In Section 5.3 the sorbent sulphation results are presented. In Section 5.3.1 and 5.3.2 the sulphation results under atmospheric and under pressurised conditions are discussed. In Section 5.4 the main conclusions drawn from the experimental findings are presented.

5.2 Sorbent preparation

5.2.1 Atmospheric pressure calcination

Preparation of the four sorbents studied was carried out in a TGA under the conditions given in Table 3.1 with a gas composed of 10% CO_2 and 90% N_2. Under atmospheric pressure conditions, full calcination (calcination of both $CaCO_3$ and $MgCO_3$ components) occurs. The phase equilibria as presented by Figure 3.4 shows that at the experimental temperatures and CO_2 partial pressure both $CaCO_3$ and $MgCO_3$ calcine to CaO and MgO respectively. The full calcination is presented by equation 5.1:

Note: Calcination as used in this report refers to the heating of a sorbent in specific gas composition that results in decarbonation reaction only.

$$CaCO_3.MgCO_{3(s)} \text{-----} > CaO_{(s)} + MgO_{(s)} + 2CO_{2(g)} \quad (5.1)$$

Thermal decomposition of dolomite and limestone had been found to be controlled by a number of factors such as temperature, heating time and gas atmosphere above the sample (Stefaniak *et al.*, 2002), these factors significantly influence changes in the physicochemical properties of the raw sorbent (Chen *et al.*, 2007).

Figures 5.1-5.4 show the mass time curves for calcination of dolomite A, dolomite B, limestone C and coal ash at atmospheric pressure.

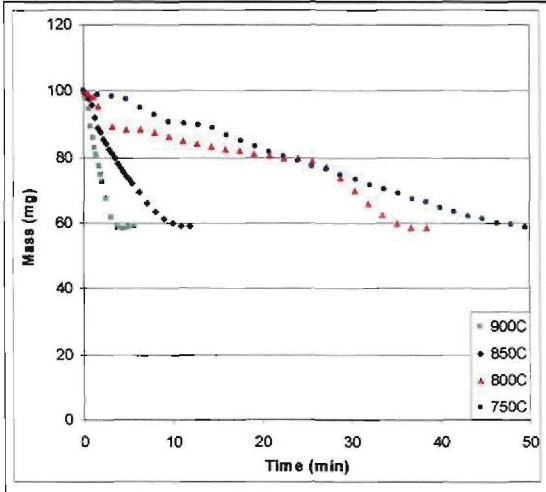

Figure 5.1: Dolomite A calcination at 0.875 bar , 10% CO_2, 90% N_2

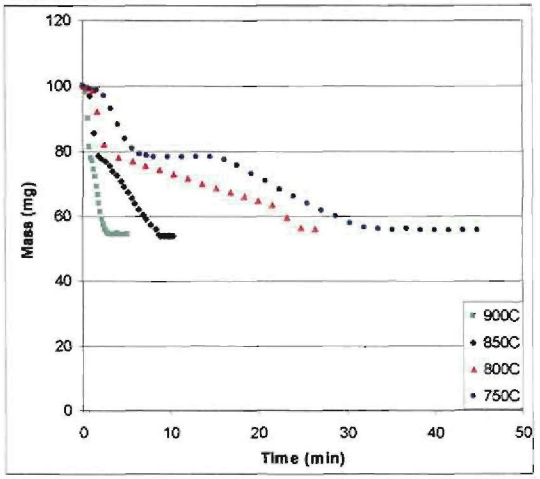

Figure 5.2: Dolomite B calcination at 0.875 bar, 10% CO_2, 90% N_2

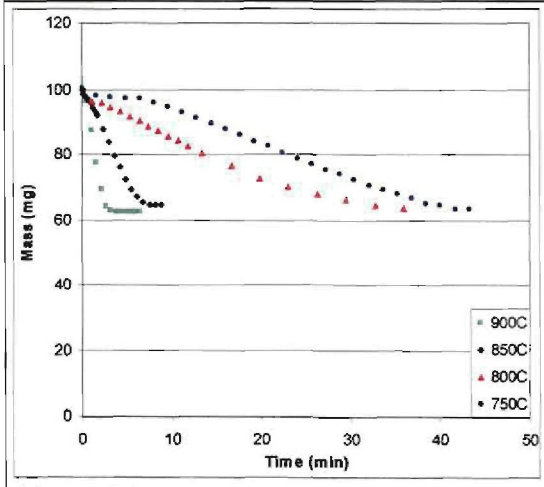

Figure 5.3: Limestone C calcination at 0.875 bar, 10% CO_2, 90% N_2

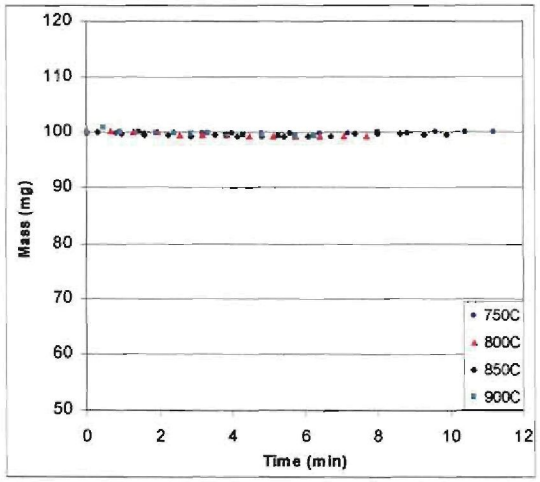

Figure 5.4 Coal ash calcination at 0.875 bar, 10% CO_2, 90% N_2

Calcination rates increased with temperature for dolomite A, dolomite B and limestone C. Coal ash did not react under atmospheric preparation conditions depicting that the calcium in the ash is in the CaO state. The calcination of dolomite B was faster than dolomite A, followed by limestone C, this can possibly be attributed to a lower amount of $CaCO_3$ in dolomite B (50.50%) compared to that in dolomite A (67.30%) and limestone C (75.05%). The calcination of both dolomite A and dolomite B at 750 and 800°C under atmospheric pressure shows two distinct stages, with the first stage faster than the second stage. This behaviour was also observed by other researchers (Dennis and Hayhurst, 1987; Stefaniak *et al.*, 2002; Samtani *et al.*, 2001) in their work. A comparison of Figures 5.1 and 5.8 of dolomite A at atmospheric and 15 bar pressure respectively and Figures 5.2 and 5.9 of dolomite B at atmospheric

and 15 bar pressure respectively, shows that the mass at end of the first stage of atmospheric calcination is the same as the mass at the end of calcination at 15 bar pressure. The first stage observed at atmospheric preparation of dolomite A and dolomite B corresponds to the calcination of $MgCO_3$ whilst the second stage corresponds to the calcination of $CaCO_3$. Equation 5.2 shows the calcination regime at the distinct first stage of dolomite calcination.

$$CaCO_3.MgCO_{3(s)} \text{ ------> } CaCO_3.MgO_{(s)} + CO_{2(g)} \quad (5.2)$$

The first stage of atmospheric calcination of dolomite concurs with the characterised $MgCO_3$ content of the sorbent. Equation 5.3 shows the second stage of atmospheric calcination.

$$CaCO_3.MgO_{(s)} \text{ ------> } CaO_{(s)} + MgO_{(s)} + CO_{2(g)} \quad (5.3)$$

The calcination of dolomite A and dolomite B at 850 and 900°C took place in a single stage. At all tested temperatures between 750-900°C the calcination of limestone C occurred in a single stage as well. Figures 5.5-5.7 give the conversion against time graphs for the sorbents at atmospheric pressure until full calcination is achieved.

The calcination/decarbonisation conversion of the sorbents was calculated using equation 5.4.

$$Calcination\ conversion = \frac{(W_0 - M_t)}{(W_0 - W_a)} \quad (5.4)$$

Where M_t is the weight of sample at any calcination (conversion) time, W_a is the final weight of sample after completion of calcination and W_0 is the weight of oven dried sample before calcination.

The $MgCO_3$ in the sorbent calcines much faster at atmospheric pressure compared to the $CaCO_3$, therefore the $CaCO_3$ content could be the rate determining factor in full calcination.

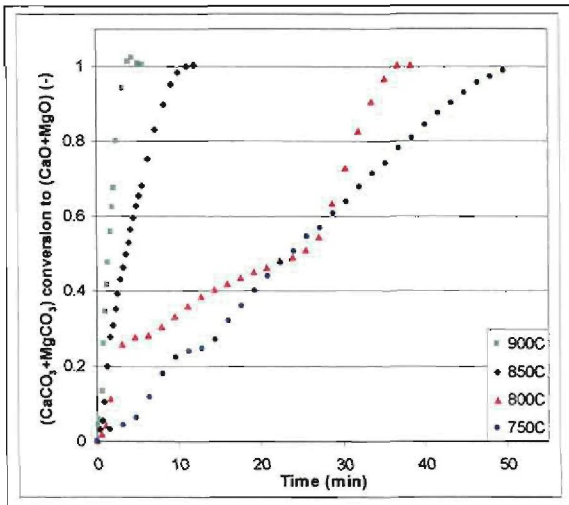

Figure 5.5: Dolomite A calcination conversion at 0.875 bar, 10% CO_2, 90% N_2

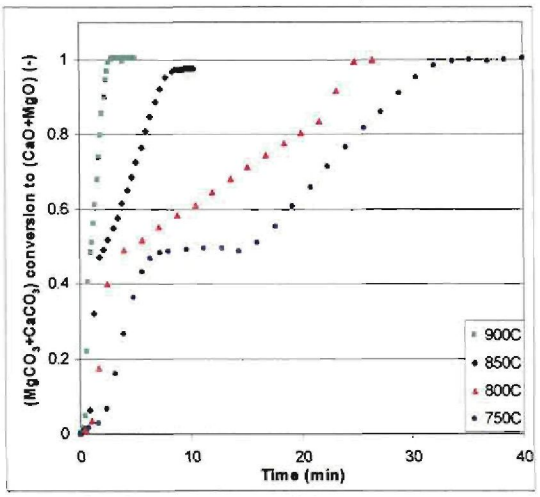

Figure 5.6: Dolomite B calcination conversion at 0.875 bar, 10% CO_2, 90% N_2

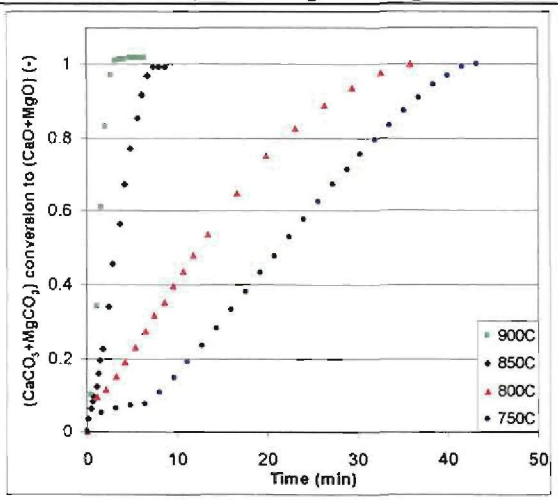

Figure 5.7: Limestone C calcination conversion at 0.875 bar, 10% CO_2, 90% N_2

There is good agreement between experimentally determined calcination mass loss with the characterised $CaCO_3$ and $MgCO_3$ composition of sorbent as presented in Table 5.1. Deviation of mass loss from characterised CO_2 is between 1-3% for full calcination. This supports the fact that the raw sorbents, dolomite A, dolomite B and limestone C are mainly carbonates as characterised whilst the active part of the coal ash is CaO. Table 5.1 summarises the calcination times at different temperatures for the sorbents at atmospheric pressure and gives the loss on calcination of sorbents.

Table 5.1: Calcination times for the sorbents at atmospheric pressure.

Sorbent	Calcination conditions					CO_2 in sorbent (wt%) [a]	Loss on calcination (wt%) [b]
	Pressure (bar)	Calcination time (minutes)					
		750°C	800°C	850°C	900°C		
Dolomite A	0.875	49.6	36.7	11.9	3.9	39.8	41.1
Dolomite B	0.875	35.2	24.8	8.4	3.0	43.2	44.4
Limestone C	0.875	43.2	35.8	8.1	3.2	33.7	35.3

[a] – taken from table 4.3 (characterisation table)

[b] – obtained from calcination experiments in TGA

5.2.2 Pressurised calcination

Pressurised experimental preparation of sorbent was done at 10 and 15 bar under conditions given in Table 3.2, with a gas composed of 20% CO_2 and 80% N_2. From Figure 3.4, it can be presumed that under pressurised conditions and CO_2 partial pressure of 20% used, $CaCO_3$ will not calcine, CaO will carbonate to $CaCO_3$ and $MgCO_3$ will calcine to MgO. Sorbent partial calcination (calcination of $MgCO_3$ content only) is given by equation 5.5.

$$CaCO_3.MgCO_{3(s)} \text{ -----> } CaCO_3.MgO_{(s)} + CO_{2(g)} \quad (5.5)$$

From sorbent characterisation presented in Chapter 4 it has been deduced that the calcium and magnesium in the dolomite and limestone are predominantly in the carbonate state, though existence of free CaO can not be ruled out. In pressurised sorbent preparation, $MgCO_3$ is undergoing calcination and CaO is undergoing carbonation. Calcium in coal ash has been characterised to be predominantly CaO so the preparation of coal ash under pressurised conditions is carbonation of the CaO content of the sorbent to $CaCO_3$ as given by equation 5.6.

$$CaO_{(s)} + CO_{2(g)} \text{ ----> } CaCO_{3(s)} \quad (5.6)$$

Figures 5.8-5.11 show mass against time graphs for calcination/carbonation under pressurised conditions for dolomite A, dolomite B, limestone C and coal ash.

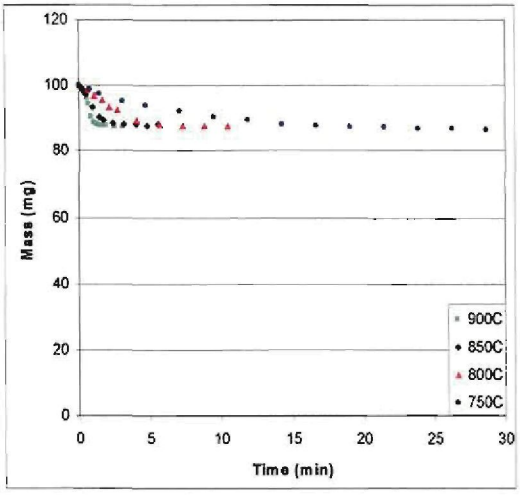

Figure 5.8: Dolomite A calcination/ carbonation at 15 bar, 20% CO_2, 80% N_2

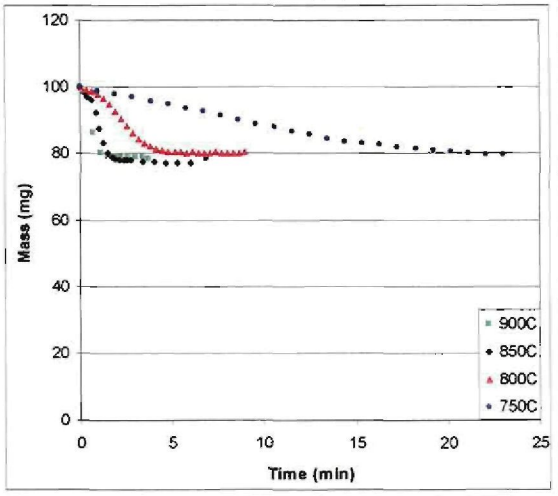

Figure 5.9: Dolomite B calcination/carbonation at 15 bar, 20% CO_2, 80% N_2

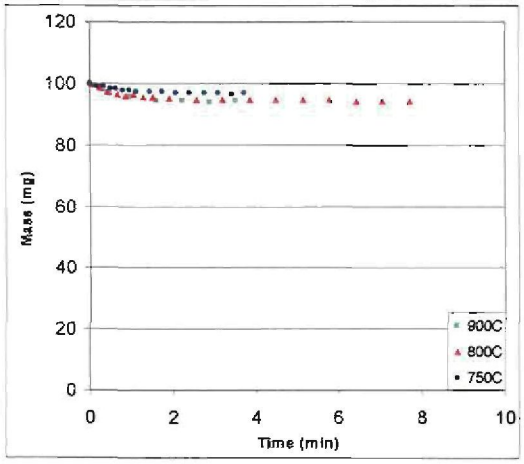

Figure 5.10: Limestone C calcination/ carbonation at 15 bar, 20% CO_2, 80% N_2

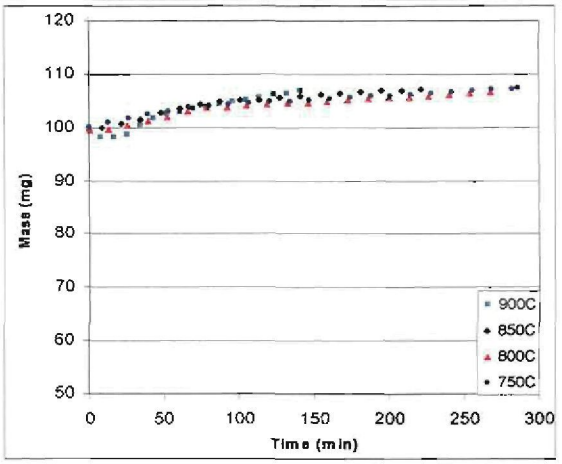

Figure 5.11: Coal ash carbonation at 15 bar, 100% CO_2

The mass loss on calcination/carbonation of sorbents as shown by Figures 5.8-5.11 shows that the equilibrium state of sorbents under pressurised conditions is linked to the CO_2 in $MgCO_3$. This concurs well with the theory that under pressurised combustion conditions, only $MgCO_3$ calcines. Coal ash carbonation links well with the CaO content which confirms the assumption that under these conditions only CaO is carbonated to $CaCO_3$.

Figures 5.12-5.15 show the conversion of dolomite A, dolomite B, limestone C and coal ash respectively. The $MgCO_3$ calcines to MgO whilst CaO is carbonated to $CaCO_3$ under the conditions as given in Table 3.2.

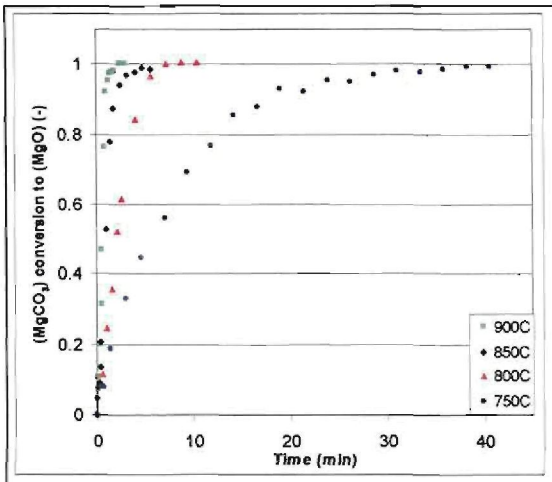

Figure 5.12: Dolomite A conversion (calcination/carbonation) at 15 bar, 20% CO_2, 80% N_2

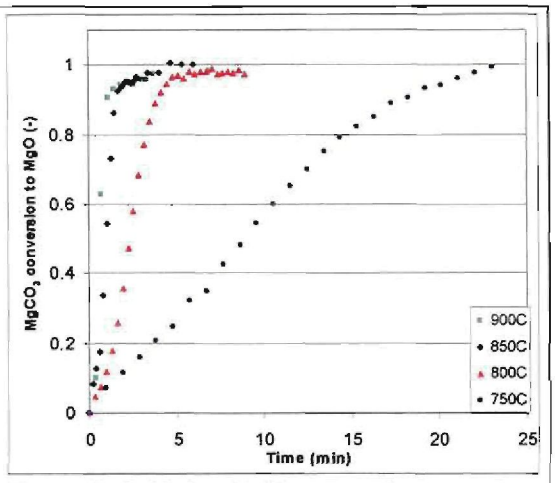

Figure 5.13: Dolomite B conversion (calcination/carbonation) at 15 bar, 20% CO_2, 80% N_2

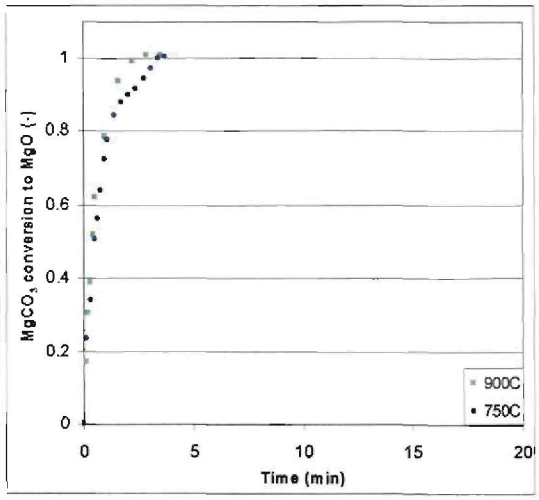

Figure 5.14: Limestone C conversion (calcination/carbonation) at 15 bar, 20% CO_2, 80% N_2

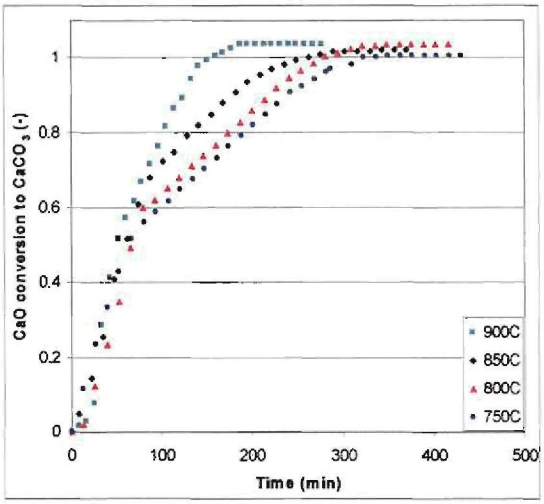

Figure 5.15: Coal ash conversion (carbonation) at 15 bar, 100% CO_2

The time taken for calcination of dolomite A, dolomite B and limestone C to reach equilibrium state under pressurised conditions is much shorter than that observed under atmospheric conditions, this is because under pressurised conditions the CO_2 partial pressure allows only the $MgCO_3$ component of the sorbent to calcine. If any CaO is present in the dolomite and limestone, under pressurised conditions, it gets carbonated. Coal ash carbonation of CaO to $CaCO_3$ has proved to be a very slow process taking between 180 and 300 minutes at temperatures between 900°C and 750°C respectively. Recarbonation of calcined dolomite and limestone is normally a very fast process (Ngeleka, 2005; Tullin and Ljungstrom, 1989). The slow carbonation of coal ash could be due to the spatial distribution of calcium in the ash grain that may make it very difficult and slow for the CO_2 to penetrate to all calcium and achieve 100% carbonation. The fact that the coal ash has already been involved in inherent sulphur capture during combustion process may mean that the CaO in the

ash is already wrapped-up in a product layer of SO_2 hindering easier diffusion of CO_2 to the unreacted grains.

Table 5.2 summarises the preparation times of the sorbents at 10 and 15 bar under the conditions given in Table 3.2. As presented in Table 5.2 there is a good relation between mass loss on calcination of sorbent and characterised $MgCO_3$ in sorbent; the deviation is between 2-8%.

Table 5.2: Calcination/carbonation times at 10 and 15 bar pressure.

Sorbent	**Calcination/carbonation conditions**					**CO_2 in $MgCO_3$ (wt%) [a]**	**Loss on calcination (wt%) [b]**
	Pressure (bar)	Calcination time (minutes)					
		750°C	800°C	850°C	900°C		
Dolomite A	10	22.3	7.4	3.7	2.3	10.2	11.0
	15	38.3	7.3	4.8	2.5	10.2	11.1
Dolomite B	10	19.9	5.2	3.3	1.7	21.0	20.1
	15	23.1	7.0	4.7	3.0	21.0	20.6
Limestone C	15	3.5	3.1	2.9	2.8	0.7	1.3
Coal ash	10	312	274	291	238	-	-
	15	286	267	235	141	-	-

[a] – taken from Table 4.3 (characterisation)

[b] – obtained from calcination experiments in TGA

The calcination data of the different sorbents show different rates at different conditions, this has an impact on physical characteristics of sorbents (Dennis and Hayhurst, 1987; Stefaniak *et al.*, 2002; Samtani *et al.*, 2001) and may influence the sulphation behaviour of the sorbents.

5.3 Sorbent sulphation

5.3.1 Sorbent reactivity under atmospheric pressure conditions

In this section the results of isothermal sulphation of the sorbents under conditions given in Table 3.1 at atmospheric pressure are presented. All the experiments given in Table 3.3 conducted at total pressure of 0.875 bar are presented. The gas composition was 2000ppm SO_2, 5.3% O_2, 10% CO_2 and 84.5% N_2. Figure 3.4 shows that under atmospheric conditions the sorbent is in the CaO/MgO state. Sulphur self-retention in coal ash has been successfully modelled by assuming that the reaction between SO_2 and CaO occurs in the form of uniformly distributed grains in the ash

particle (Manovic *et al.*, 2002) and this will also be assumed in this investigation. The sulphation reaction of sorbent under atmospheric condition is given by equation 5.7:

$$CaO_{(s)} + SO_{2(g)} + ½\ O_{2(g)} \text{----> } CaSO_{4(s)} \qquad (5.7)$$

The mass increase against time is used to calculate conversion. Since mass increase is due to SO_2 adsorption in the presence of O_2, for calculation purposes mass increase is thus assumed to be because of SO_3 (SO_2 + ½ O_2) adsorption by sorbent (Dennis and Hayhurst, 1990), resembling conversion of CaO only (Ar and Balci, 2002). Equation 5.8 given below shows the mathematical formula used for calculating conversion (Ar and Balci, 2002).

The conversion of CaO to $CaSO_4$ is designated as X_{CaO}

$$X_{CaO} = \frac{moles\ of\ CaSO_4\ formed}{total\ moles\ of\ CaO\ in\ sample}$$

$$= \frac{(W_t - W_a)/M(SO_3)}{(x_{CaO}W_0)/M(CaO)} \qquad (5.8)$$

Where W_t is the weight of sample at any sulphation (conversion) time, W_a is the weight of sample after calcination and W_0 is the weight of oven dried sample before calcination. x_{CaO} *is* the CaO weight fraction of the dried sorbent, $M(SO_3)$ is the molar mass of SO_3 (SO_2 + ½ O_2) and $M(CaO)$ is the molar mass of calcium oxide.

5.3.1.1 Effect of temperature on sulphation

The conversion results are shown in Figures 5.16-5.19 for dolomite A, dolomite B, limestone C and coal ash respectively. Experiments were carried out for periods ranging from 180 to 200 minutes. Most sulphation results given in literature vary between 10 and 120 minutes (Yrjas *et al.*, 1995; Ersoy-Mericboyu and Kucukbayrak, 1995; Dam-Johansen and Ostergaard, 1991). The sulphation times applied in this investigation are therefore long enough to give a good insight into atmospheric sulphation.

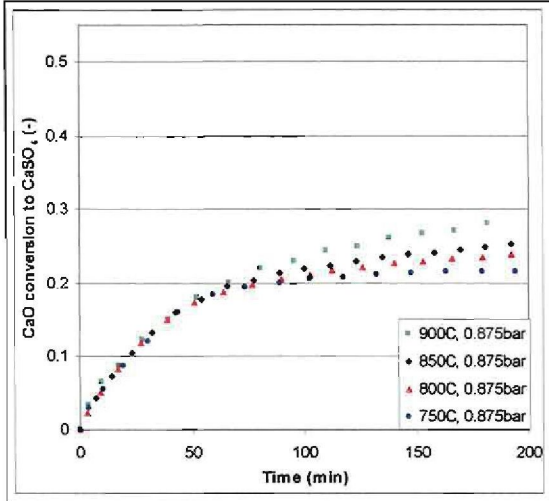

Figure 5.16: Dolomite A sulphation between 750-900°C at 0.875 bar

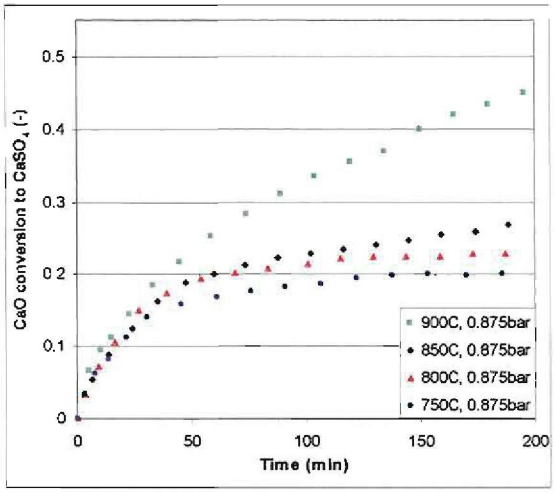

Figure 5.17: Dolomite B sulphation between 750-900°C at 0.875 bar

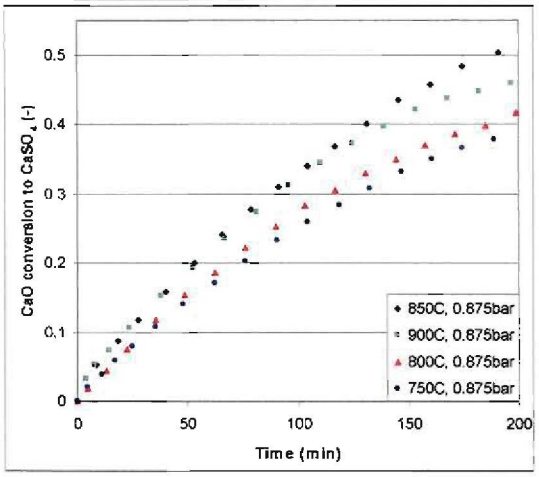

Figure 5.18: Limestone C sulphation between 750-900°C at 0.875 bar

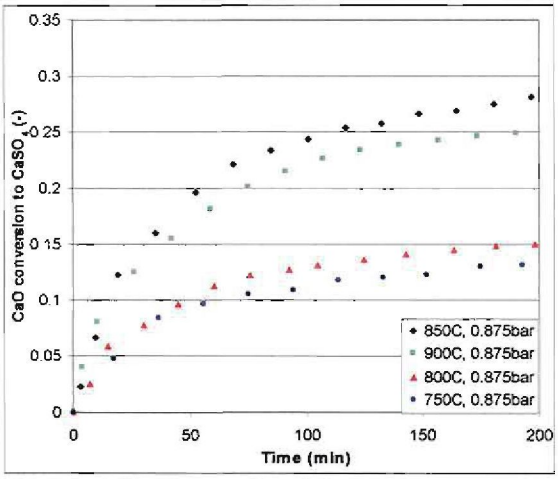

Figure 5.19: Coal ash sulphation between 750-900°C at 0.875 bar

It can be seen from Figures 5.16-5.19 that sulphation of dolomite A, dolomite B and coal ash samples started at a remarkable rate. Conversion increased with increasing temperature at all temperatures up to 900°C for the dolomites, this could mean that there is not much sintering of dolomites up to the maximum temperature used. In approximately 50 minutes dolomite A and dolomite B had achieved 16-20% conversion of CaO to $CaSO_4$ followed by a sharp decrease in the conversion rate. Up to the plateau the conversion rate seems to be independent of temperature between 750-900°C; all the conversion curves at different temperatures are superimposed up to about 16-20% CaO conversion. The time it takes to reach the plateau shows dependence on internal surface area of material, meaning that the fast first stage under atmospheric conditions could be surface area controlled. After the reaction plateau the temperature effect becomes noticeable, conversion was higher for higher temperatures from 750-900°C. Ulerich *et al.* (1980) found out that the rate of reaction varies the most with temperature at higher than 30% CaO conversion. This behaviour

could mean that there is a sudden change in controlling regime after 16-20% conversion. The gradual decline in conversion after plateau can be attributed to product layer development (Iisa and Hupa, 1990; Qiu and Lindquivst, 2000; Trikkel and Kuusik, 2003). Because the molar volume of $CaSO_4$ is 2.72 times that of CaO, the sorbent swells due to sulphation (Ar and Balci, 2002) forming non-porous protective layer, thus preventing easy contact of unreacted CaO with reaction gas (Ersoy-Mericboyu and Kucukbayrak, 1998). Conversion of CaO for dolomite A measured after 180 minutes of reaction ranges from 22-29%, whilst for dolomite B the conversion ranges from 20-44%, these results are within the range obtained by other researchers (Trikkel and Kuusik, 2003; Ersoy-Mericboyu and Kucukbayrak 1995; Ar and Balci, 2002; Dam-Johansen and Ostergaard, 1990). The temperature influence varied considerably between different sorbents (see Figures 5.16-5.19). Differences in product layer structure may be the cause of this behaviour. Iisa and Hupa (1990) in similar research, also found that atmospheric sulphation declines earlier between 10-20% conversion whilst for pressurised sulphation conversion gradually improves.

For limestone C, the sulphation reactions at different temperatures started at relatively similar conversion rates with a distinction based on temperature becoming apparent after about 50 minutes. Conversion of limestone C shows a temperature based maximum at 850°C. The conversion rates increased with temperature from 750-850°C, the conversion at 900°C was lower than that at 850°C but higher than that at 800°C. This behaviour was observed by other researchers (Ulerich *et al.*, 1980; O'Neill *et al.*, 1976; Ghardashkhani and Cooper, 1990), and can be attributed to sorbent calcination conditions that may lead to sintering (O'Neill *et al.*, 1976). Figure 5.18 for limestone C sulphation shows that the 850°C conversion rate started surpassing the 900°C conversion after 50 minutes, as the reaction progresses the difference becomes more pronounced. This can be attributed to the change in morphology of the sorbent caused by high temperature sintering, which in turn leads to a loss in surface area. The conversion obtained after 180 minutes of reaction is between 37-49%, with the peak conversion having been attained at 850°C, conversion at 900°C was 44%.

Figure 5.19 shows that coal ash conversion varies between 13-28%. The reaction rates increase with temperature up to 850°C, the 900°C conversion is lower than that at 850°C. Manovic *et al.* (2006) working at temperatures between 750 and 850°C also noticed a maximum sulphur dioxide capture by coal ash particles at 800°C.

There could be structural modifications with temperature as there is a distinct change from the 750-800°C zone to 850-900°C zone. The CaO content in coal ash is only 10 wt%, therefore its distribution in the coal ash could be quite heterogeneous.

Sorbents used in FBC will have residence times of 12 hours (Ulerich *et al.*, 1980), the longer residence times could cause sintering of the sorbents changing the pore structure and reactivity towards SO_2. Of the four sorbents the detrimental effect of increased temperature and residence time has been noticed for limestone C and coal ash whose conversion rate decreased as temperature was increased beyond 850°C.

5.3.1.2 Comparison of sorbent CaO conversion at atmospheric pressure

Figures 5.20-5.21 show comparisons of CaO conversion of the different sorbents at atmospheric pressure for the 800 and 850°C (optimum temperature range) under FBC conditions. Limestone C has the highest CaO utilisation of 40 and 49% at 800 and 850°C respectively measured after 180 minutes of sulphation. At the optimum FBC temperatures selected for sorbent comparison, conversion of dolomite A and dolomite B were almost similar achieving 24 and 26% conversion at 800 and 850°C respectively. Dolomite A conversion increased from 25% at 850°C to 29% at 900°C. At 900°C dolomite B conversion increased to 44% from 26% at 850°C. Coal ash shows greater dependence on temperature although calcium conversion is comparable to that of the dolomites ranging from 15% at 800°C to 28% at 850°C. Dolomite A and limestone C showed little dependence of conversion on temperature compared to dolomite B and coal ash.

It is interesting to note that calcium conversion curves for different sorbents at 850°C are superimposed on one curve up to 20%. This is most probably because the available surface area initially controls the reaction. Since the internal surface areas of the fully calcined sorbents are comparable there is no distinction based on sorbent up to 20% conversion.

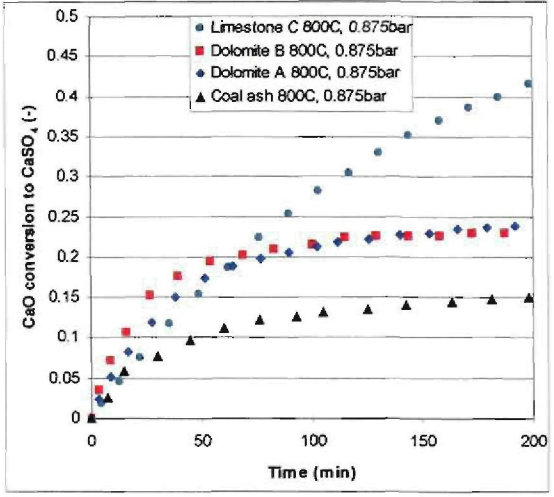

Figure 5.20: Sorbents conversion comparison at 800°C and 0.875 bar

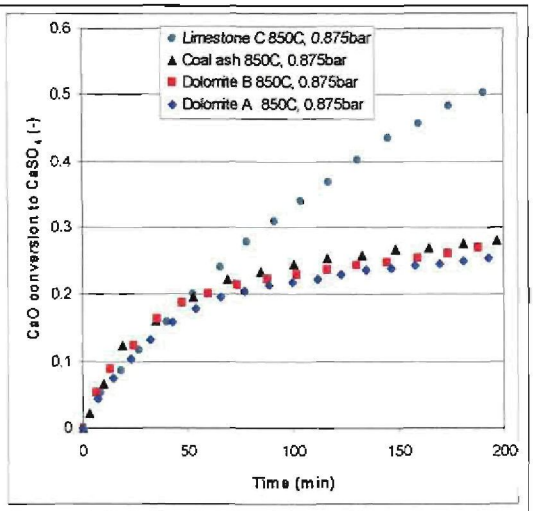

Figure 5.21: Sorbents conversion comparison at 850°C and 0.875 bar

5.3.1.3 Comparison of sorbent adsorption capacities at atmospheric pressure

One of the main purposes of the investigation was to rate SO_2 adsorption of the sorbents under different simulated FBC operating conditions. The sulphur adsorption capacities of various sorbents with different compositions cannot be rated using calcium conversion alone, the composition of the material is taken into consideration. The calcium conversion of a sorbent combined with the chemical composition can be used to calculate the adsorption capacity or sorbent sulphation capacity as this gives mass of SO_2 captured per mass of raw sorbent (O'Neill *et al.*, 1976; Ersoy-Mericboyu, 1998; Trikkel and Kuusik, 2003). Equation 5.9 was used to calculate the adsorption capacity per 100 mg of the sorbents:

$$Adsorption\ capacity = \frac{mass\ of\ SO_2\ captured}{total\ mass\ of\ sample}$$

$$= \frac{((W_t - W_a)(M(SO_2)/M(SO_3))x100}{W_0} \qquad (5.9)$$

Where W_t is the weight of sample at any sulphation (conversion) time, W_a is the weight of sample after calcination and W_0 is the weight of oven dried sample before calcination. $M(SO_3)$ is the molecular mass of SO_3 (SO_2 + ½ O_2) and $M(SO_2)$ is the molecular mass of SO_2. Overall effectiveness of a sorbent can be expressed as the amount of SO_2 or SO_3 (SO_2 + ½ O_2) captured per unit mass of raw sorbent. The effective adsorption capacity determines the relative amount of sorbent needed to

capture a certain amount of SO_2. Since the gain in mass due to sulphation is equivalent to gain in SO_3, to calculate the mass of SO_2 captured, the molecular weight ratio of SO_2 to SO_3 is used.

The average ranking of SO_2 adsorption capacity correlates to the calcium content of the sorbent even though conversion does not follow the same rank. Figure 5.22a shows the sulphur dioxide adsorption achieved by the sorbents under atmospheric conditions. Dolomite A SO_2 adsorption after 180 minutes between 750-900°C was between 9.47-12.49 mg SO_2/100 mg sorbent (11.8-15.6 mg SO_3/100 mg sorbent). Dolomite B sulphur adsorption capacity ranged between 6.47-14.22 mg SO_2/100 mg sorbent (8.1-17.8 mg SO_3/100 mg sorbent) and limestone C SO_2 adsorption was much higher than that of the dolomites as it adsorbed between 17.77-23.54 mg SO_2/100 mg sorbent (22.2-29.4 mg SO_3/100 mg sorbent). Comparable results as achieved for limestone C were obtained by Trikkel and Kuusik (2003) adsorbing from 15.5-33.9 mg SO_2/100 mg sorbent under similar conditions of time and pressure .

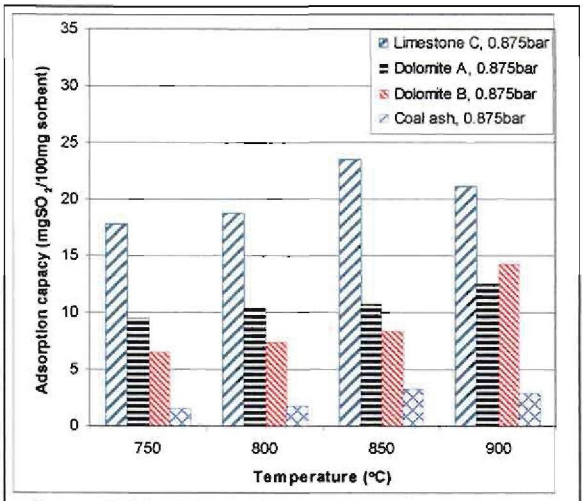

Figure 5.22: Adsorption capacities at 0.875 bar after 180 minutes (based on 100mg raw sorbent)

Figure 5.22 shows that SO_2 adsorption capacity of limestone C is higher than that of both dolomite A and dolomite B up to 180 minutes at atmospheric pressure for all temperatures. At atmospheric pressure, up to 850°C, dolomite A has higher sulphation capacity compared to dolomite B, but at 900°C dolomite B is a better sorbent. Coal ash adsorption capacity is lower than that for the other three sorbents.

5.3.2 Sorbent reactivity under pressurised conditions

Pressurised sulphation experiments were done at 10 and 15 bar under conditions as given in Table 3.2. The gas composition was 2000ppm SO_2, 5.3% O_2, 20% CO_2 and 74.5% N_2. From sorbent preparation results and from Figure 3.4 it can be deduced that under these conditions the most effective sorbent is $CaCO_3$, considering that MgO does not react (Dennis, 1985, Fuertes *et al.*,1995).

The sulphation reaction of sorbent under pressurised conditions is given in equation 5.10 shown below

$$CaCO_{3(s)} + SO_{2(g)} + ½\ O_{2(g)} \text{ ----> } CaSO_{4(s)} + CO_{2(g)} \qquad (5.10)$$

Mass against time data is used to calculate conversion. For calculation purposes, the mass increase is assumed to be because of SO_3 (SO_2 + ½ O_2) adsorption by sorbent, meaning conversion of $CaCO_3$ only, with release of CO_2. Equation 5.11 below show the mathematical formula used for calculating sorbent conversion:

The conversion of $CaCO_3$ to $CaSO_4$ designated as X_{CaCO3} is calculated as follows

$$X_{CaCO3} = \frac{moles\ of\ CaSO_4\ \ formed}{total\ moles\ of\ CaCO_3\ in\ sample}$$

$$= \frac{(W_t - W_a)/M(SO_3)}{(x_{CaCO3}W_0)/M(CaCO_3)} \qquad (5.11)$$

Where W_t is the weight of sample at any sulphation (conversion) time, W_a is the weight of sample after calcination and W_0 is the weight of oven dried sample before calcination. x_{CaCO3} is the $CaCO_3$ composition of the sorbent, $M(SO_3)$ is the molecular mass of SO_3 (SO_2 + ½ O_2) and $M(CaCO_3)$ is the molar mass of calcium carbonate.

The conversion results for pressurised sulphation are shown in Figures 5.23-5.30 for dolomite A, dolomite B, limestone C and coal ash. Conversion is calculated on the basis of the experimentally determined $CaCO_3$ composition of each sorbent as presented in Table 4.3. Experiments were carried out for periods ranging between 180 and 200 minutes. The sulphation times applied in the investigation are long enough to give a good sulphation profile with time. Up to the maximum time of 200

minutes considered the sorbents under pressurised sulphation are still quite reactive compared to those at atmospheric sulphation, this suggests that with time the conversion is likely to be much higher as there is no sign of sudden deactivation.

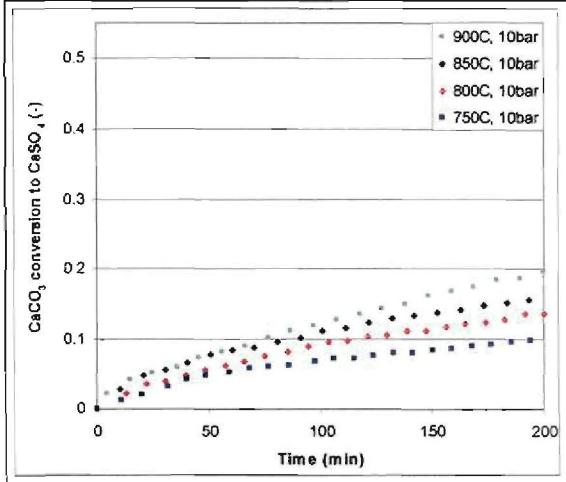

Figure 5.23: Dolomite A sulphation at 10 bar

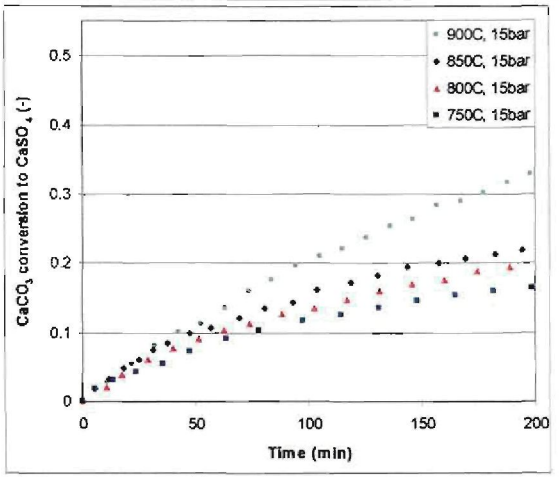

Figure 5.24: Dolomite A sulphation at 15 bar

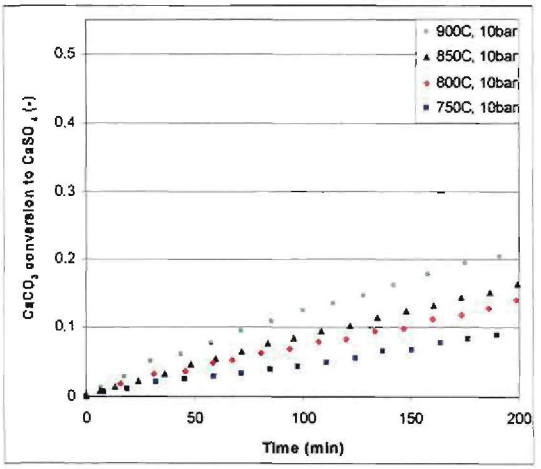

Figure 5.25: Dolomite B sulphation at 10 bar

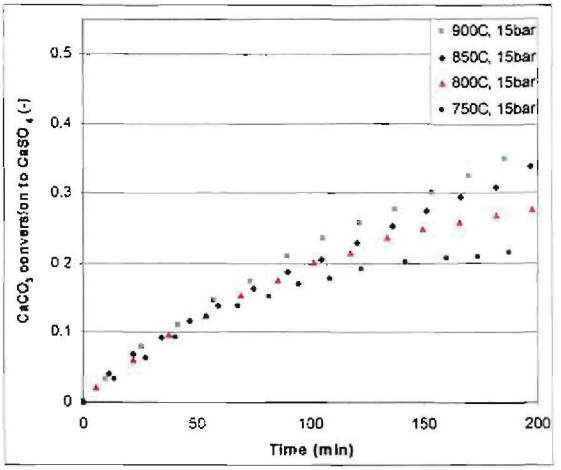

Figure 5.26: Dolomite B sulphation at 15 bar

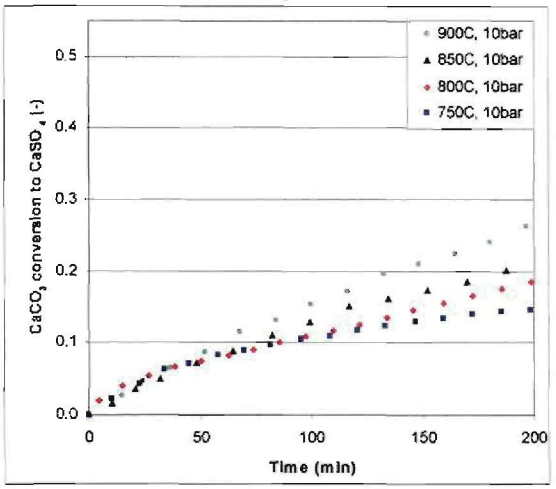

Figure 5.27: Limestone C sulphation at 10 bar

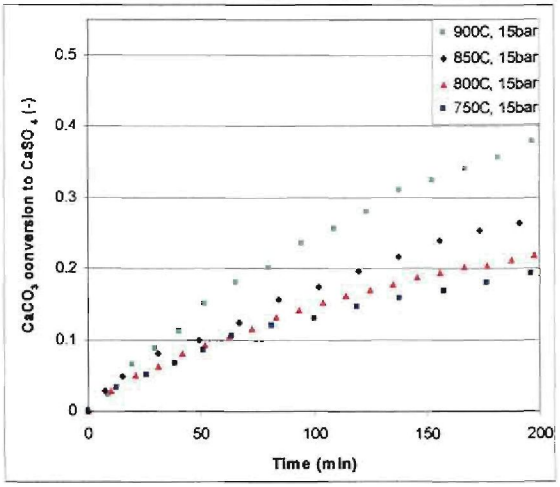

Figure 5.28: Limestone C sulphation at 15 bar

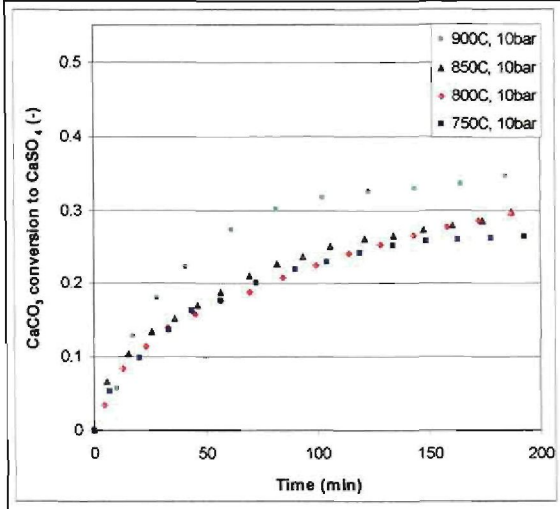

Figure 5.29: Coal ash sulphation at 10 bar

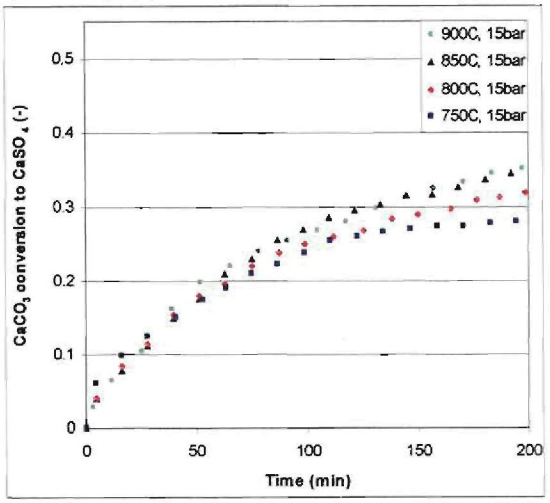

Figure 5.30: Coal ash sulphation at 15 bar

5.3.2.1 Effects of temperature on sulphation

It can be seen from Figures 5.23-5.30 that sulphation of dolomite, limestone and coal ash started at relatively constant rates. There was no sharp decrease in the conversion rates of dolomites as observed at the atmospheric pressure sulphation. The reaction at 10 bar and 15 bar initiated relatively much slower than the atmospheric sulphation for the dolomites and limestone while for coal ash calcium conversion rate did not change much. After 50 minutes of sulphation the dolomites and limestone had achieved about 3-5% calcium conversion at 10 bar and 8-10% calcium conversion at 15 bar compared to 16-20% calcium conversion achieved after same sulphation time at atmospheric pressure. The conversion rates show a direct dependence on temperature, conversion rates increased with temperature for all the samples from 750-900°C at 10 and 15 bar. The fact that limestone C and coal ash which show a temperature maximum at 850°C and 800°C respectively under atmospheric conditions do not behave likewise at 10 and 15 bar may mean that the $CaCO_3$ does not sinter as fast as the CaO. This effect was also observed by (Alvarez and Gonzalez, 1999; Zhong, 1995; Fuertes *et al.*, 1995; Iisa, 1992; Qiu and Lindqvist, 2000). At 15 bar pressure, conversion of dolomite A was 16-32%, conversion of dolomite B was 21-34% and limestone C conversion was 18-36% after 180 minutes of sulphation. At 10 bar the conversion of dolomite A was 9-18%, dolomite B was 8-19% and limestone C was 14-24%. Coal ash conversion at 10 and 15 bar did not increase much with increasing temperature as for the atmospheric conditions. Conversions after 180 minutes increased about twofold by increasing temperature from 750 to 900°C at both 10 and 15 bar. Yrjas *et al.* (1995) noticed the same effect and suggested this could be the effect of product layer structure.

5.3.2.2 Effects of pressure on sulphation

The conversions of dolomite A, dolomite B and limestone C at 10 bar were lower than those obtained at 15 bar pressure. Changing total gas pressure from 15 bar to 10 bar while maintaining gas composition changes the partial pressures of the gases. The effect of decreasing total pressure at a fixed gas composition has shown to be a decrease in sorbent conversion. Dolomite A conversion after 180 minutes at 15 bar was 16-32% whilst at 10 bar it was 9-18% at temperatures between 750-900°C. Dolomite B conversion was 21-34% at 15 bar and 8-19% at 10 bar for temperature between 750-900°C. Limestone C conversion was 18-36% at 15 bar and 14-24% at 10 bar pressure after 180 minutes of sulphation for temperature between 750-900°C. For dolomite A and dolomite B, increase in pressure from 10 to 15 bar resulted in a twofold increase in conversion whilst for limestone the increase was one and half times. Iisa and Hupa, 1990 using limestone obtained conversions between 10-45% after 3 hours of sulphation for temperature between 700-900°C, they observed that for pressures from 10-20 bar sulphation rate increases. This could be the effect of product layer formation. Dolomites show a higher effective conversion due to pressure than limestone, this could be due to a partially open half calcined structure owing to $MgCO_3$ calcination. This pressure related behaviour as shown by dolomite A, dolomite B and limestone C was also observed by Iisa, (1992) and Alvarez and Gonzalez, (1999). Conversion of $CaCO_3$ in coal ash due to sulphation did not change much between 10 and 15 bar pressure, $CaCO_3$ conversion was 26-35% at 10 bar and 28-35% at 15 bar pressure and temperatures between 750-900°C.

5.3.2.3 Comparison of pressure effects on calcium conversion of each sorbent

A temperature of 850°C (optimum temperature for FBC) has been chosen for comparison of sorbent calcium conversion behaviour at different pressures. Figures 5.31 and 5.32 showing conversion of dolomite A and dolomite B respectively at 0.875, 10 and 15 bar pressure and 850°C show that the atmospheric sulphation started off faster but levelled off with time compared to the 10 and 15 bar. It is important to understand that the reaction with SO_2 at atmospheric pressure involves CaO while at 10 and 15 bar it is $CaCO_3$ which is reacting. Figure 5.32 shows that after 130 minutes dolomite B conversion at 15 bar surpassed that of atmospheric sulphation. From Figures 5.31 and 5.32 it can be deduced that the pressurised sulphation of dolomite A and dolomite B will exhibit higher conversion with sulphation

times longer than those used in this research hence higher pressure would exhibit higher conversion. Yrjas *et al.* (1995) made a similar observation.

For limestone C there is no convergence of pressurised and atmospheric calcium conversion with time contrary to what was observed for the dolomites. Figure 5.34 shows that coal ash calcium conversion has a marginal dependence on pressure. This could be due to a spatial calcium distribution in coal particles and a highly open structure, both of which may not be dependent on pressure considering that $CaCO_3$ in ash is a product of carbonation of CaO.

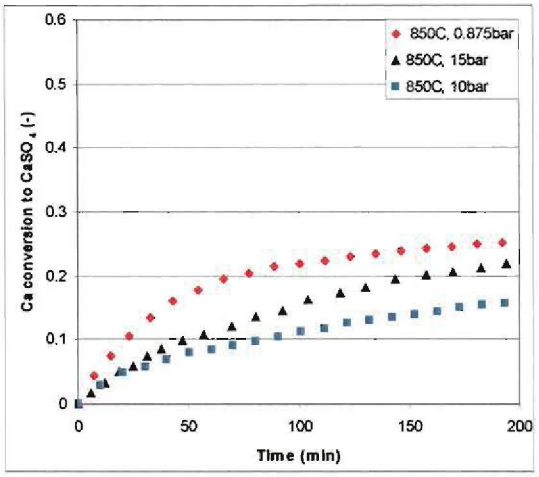

Figure 5.31: Dolomite A sulphation at 0.875, 10 and 15 bar

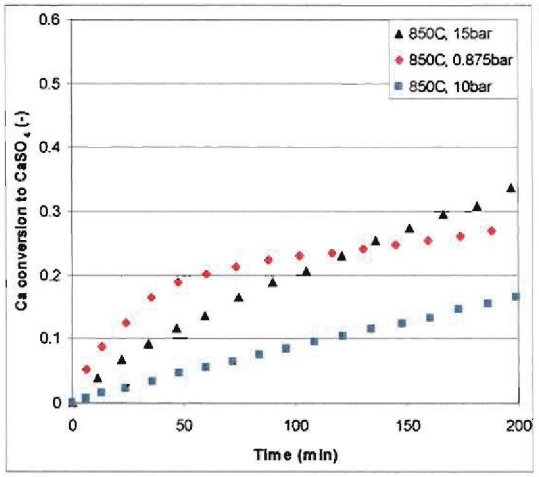

Figure 5.32: Dolomite B sulphation at 0.875, 10 and 15 bar

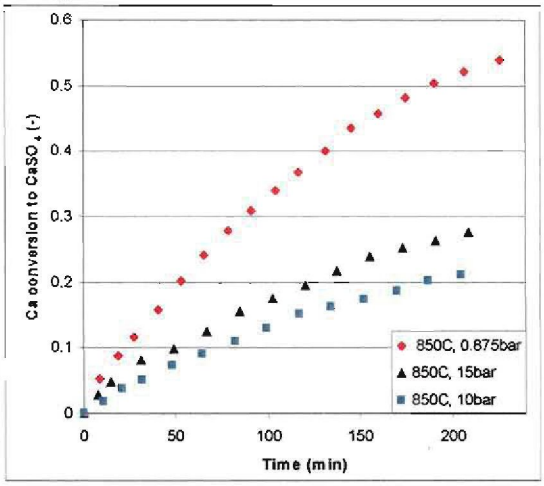

Figure 5.33: Limestone C sulphation at 0.875, 10 and 15 bar

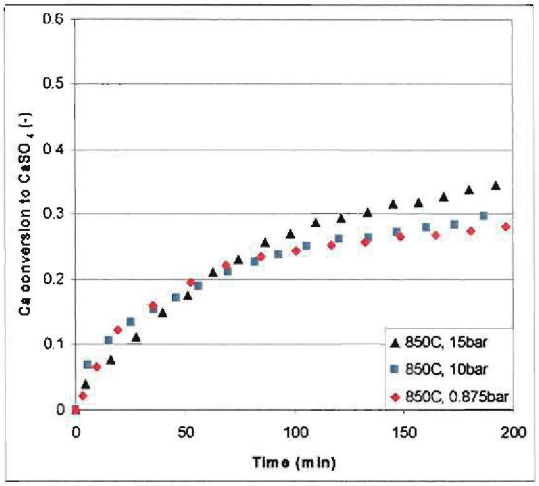

Figure 5.34: Coal ash sulphation at 0.875, 10 and 15 bar

The reaction at atmospheric pressure and atmospheric pressure effectively involve a different material as proven in the sorbent preparation section of this research.

5.3.2.4 Comparison of different sorbents on calcium conversion under similar conditions.

Comparison of calcium conversion of different sorbents at different pressures was done at 800 and 850°C (optimum temperature) under FBC conditions. Figures 5.35-5.38 show conversion of the different sorbents under similar conditions. There is consistence between 800 and 850°C in ranking sorbent conversion for sulphation times up to 200 minutes. Coal ash conversion showed little dependence on pressure although calcium conversion is comparable to that of dolomite B at 15 bar. At 10 and 15 bar pressures, coal ash shows the highest conversion rates of between 30 and 35%. At 10 bar the calcium conversion ranking is higher for limestone C followed by dolomite A and lastly dolomite B, the sequence changes at 15 bar pressure to dolomite B, limestone C and dolomite A. This change in pattern of calcium conversion ranking of sorbents between 10 and 15 bar could be due to the effects of pressure on calcination (conversion of $CaCO_3$ to CaO) and its influence on activity of calcines formed by the same sorbent at different pressures.

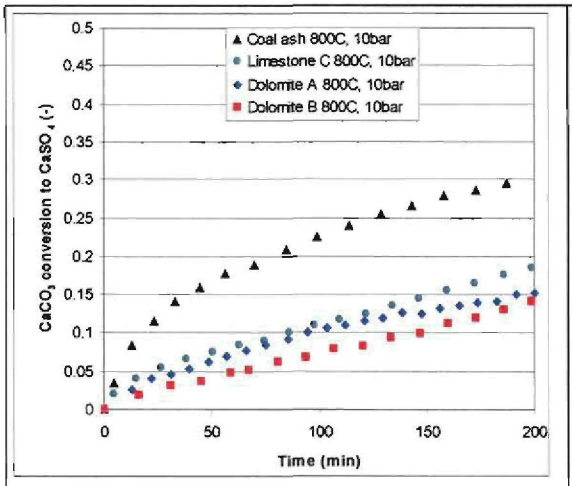

Figure 5.35: Sorbents conversion comparison at 800°C and 10 bar

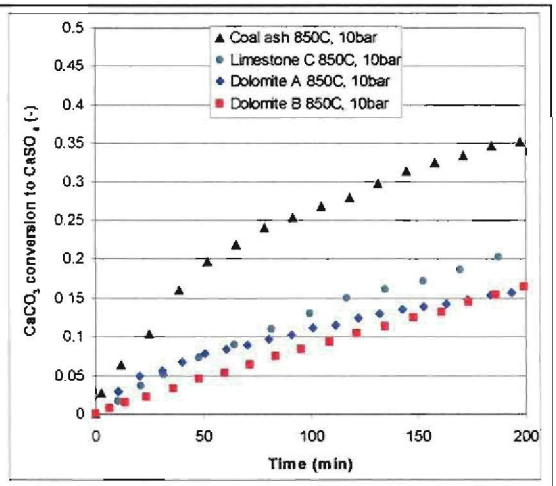

Figure 5.36: Sorbents conversion comparison at 850°C and 10 bar

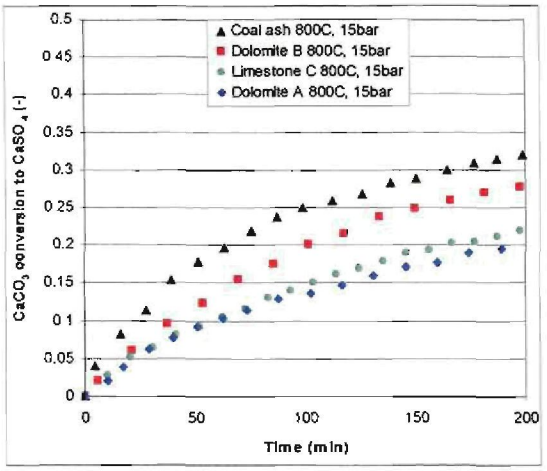

Figure 5.37: Sorbents conversion comparison at 800°C 15 bar

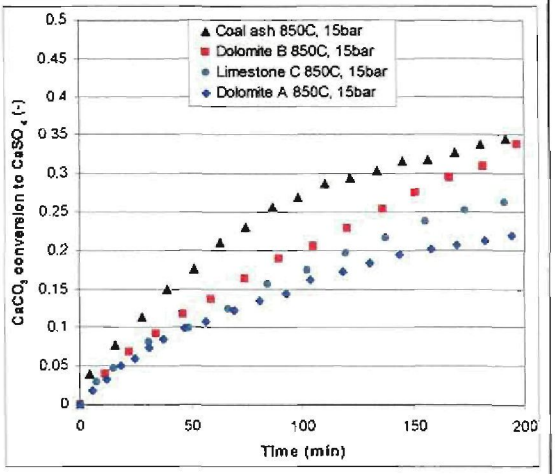

Figure 5.38: Sorbents conversion comparison at 850°C 15 bar

5.3.2.5 Sulphur dioxide adsorption capacities of sorbents

Equation 5.8 was used to calculate the adsorption capacities of the sorbents under pressurised conditions. Figures 5.39 and 5.40 show the sulphur dioxide adsorption achieved by the sorbents under pressurised conditions.

Figure 5.39-5.40 give the sorbents adsorption capacities at 10 and 15 bar pressure whilst keeping all other conditions constant. It can be seen from Figure 5.39a and 5.40a that SO_2 adsorption capacity of limestone C was higher than that of dolomite A and dolomite B up to 200 minutes at both 10 and 15 bar pressure. At 15 bar, dolomite B is a better sorbent than dolomite A up to 850°C but at 900°C dolomite A is a better sorbent. Coal ash adsorption capacity is lower than that of the other three sorbents. Figures 5.39b and 5.40b show that the calcium conversion of coal ash is the highest at 10 and 15 bar pressure compared to the other sorbents unlike at atmospheric pressure where it has the least calcium conversion relative to the other three sorbents.

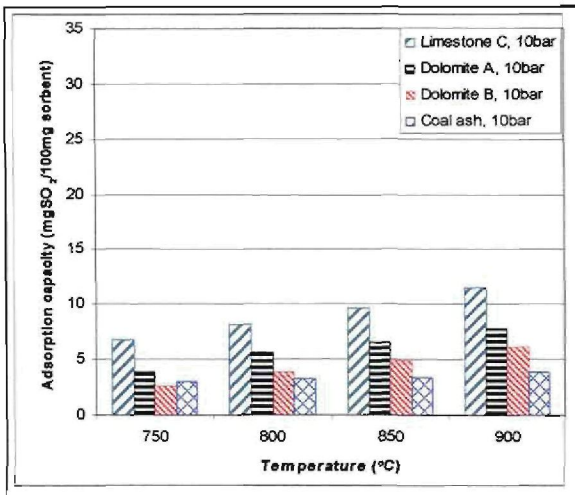

Figure 5.39a: Adsorption capacities at 10 bar (based on 100mg raw sorbent)

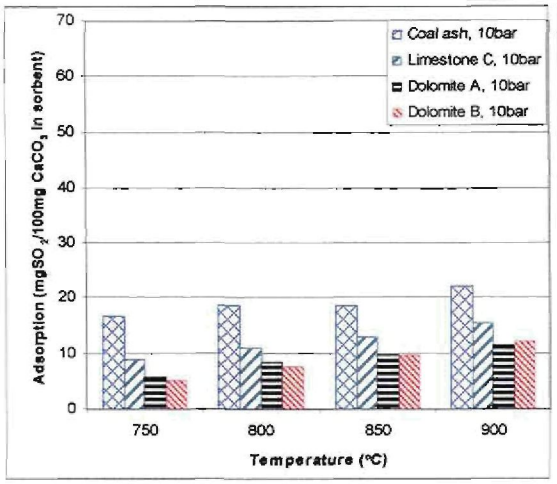

Figure 5.39b: Adsorption capacities at 10 bar (based on 100mg $CaCO_3$ in sorbent)

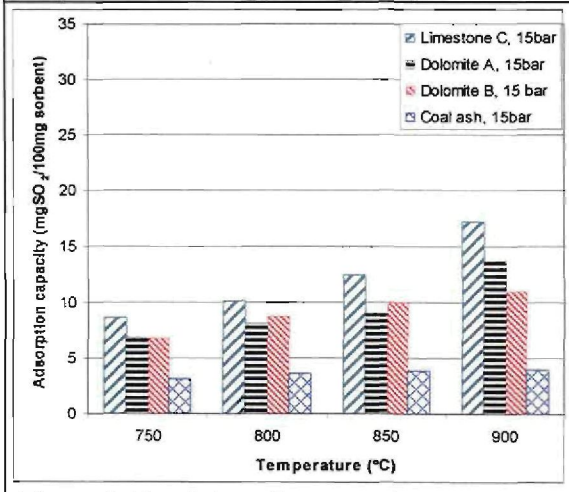

Figure 5.40a: Adsorption capacities at 15 bar (based on 100mg raw sorbent)

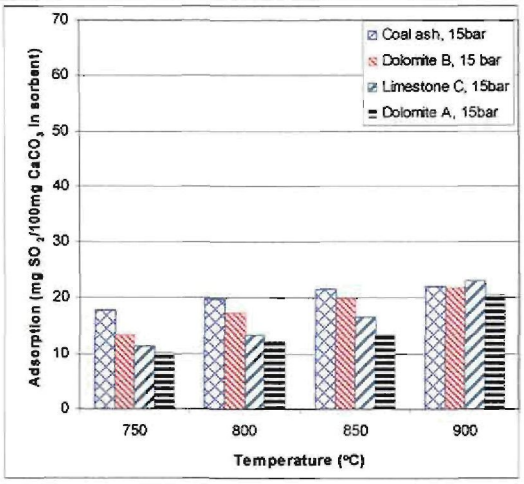

Figure 5.40b: Adsorption capacities at 15 bar (based on 100mg $CaCO_3$ in sorbent)

Dolomite A SO_2 adsorption after 180 minutes at 15 bar were between 6.89-13.78 mg SO_2/100 mg sorbent (8.6-17.2 mg SO_3/100 mg sorbent). Dolomite B SO_2 adsorption capacity after 180 minutes at 15 bar were 6.79-10.99 mg SO_2/100 mg sorbent (8.5-13.7 mg SO_3/100 mg sorbent). Limestone C SO_2 adsorption after 180 minutes at 15 bar was much higher than that of the dolomites, at 15 bar adsorption was between 8.65-17.29 mg SO_2/100 mg sorbent (10.8-21.6 mg SO_3/100 mg sorbent). Comparable range of results as achieved in this research for limestone C were obtained by Trikkel and Kuusik (2003) adsorbing from 15.5-33.9 mg SO_2/100 mg sorbent under similar conditions of time and pressure.

O'Neill *et al.* (1976) attributed high CO_2 partial pressure and its related calcination effects to the increase in sulphation potential of sorbent as pressure and temperature were increased. The increase in conversion with pressure could be because of the increase in SO_2 partial pressure due to system pressurisation. The effect of pressure

should not affect the sulphation rate (O'Neill *et al.*, 1976) so the major change in SO_2 adsorption by changing pressure could be because of differences in the effective calcines and surface morphology due to change in pressure.

Figures 5.41a and 5.41b give sorbents' SO_2 averaged (750-900°C) adsorption at 0.875, 10 and 15 bar pressure.

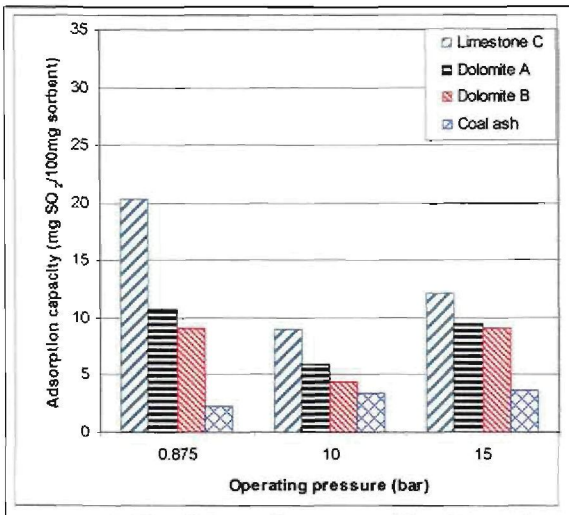

Figure 5.41a: Adsorption capacities (based on 100mg raw sorbent)

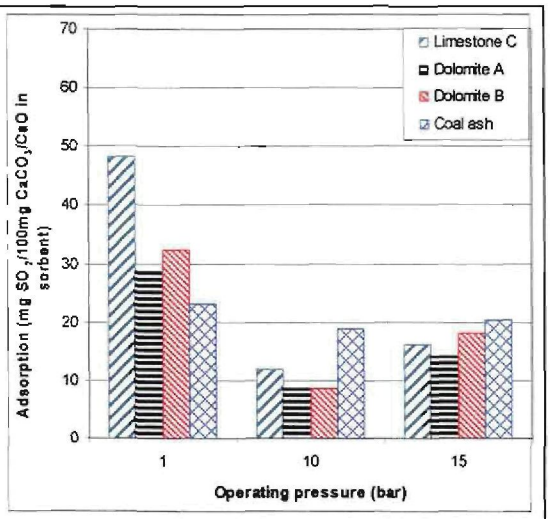

Figure 5.41b: Adsorption capacities (based on 100mg $CaO/CaCO_3$ in sorbent)

For the different sorbents considered here, limestone C SO_2 capture per unit mass of sorbent is the highest, followed by dolomite A, dolomite B and lastly coal ash as presented on Figure 5.41a. From Figure 5.41b the calcium conversion of coal ash under pressurised conditions at 10 and 15 bar is higher than for the other three sorbents unlike at atmospheric pressure where coal ash conversion is the least.

5.4 Conclusions: Sorbent calcination and sulphation results

Calcination of dolomite A, dolomite B and limestone C under atmospheric and pressurised conditions concurs well with characterised calcium and magnesium content of sorbent, which shows that sorbent is predominantly $CaCO_3$ and $MgCO_3$, coal ash calcium is in the CaO state. By carefully controlling the CO_2 partial pressure, the effective sorbent at atmospheric pressure is CaO and that at pressurised conditions is $CaCO_3$.

The calcination and carbonation rates of sorbents under both atmospheric and pressurised conditions increases with increased temperature and higher $CaCO_3$

content except for some sorbents which sinter and lose reaction surface area because of higher temperature, usually above 850°C.

For the pressurised conditions calcination rates of dolomite A, dolomite B and limestone C decrease by increasing pressure from 10 to 15 bar for all temperatures between 750-900°C whereas carbonation rates increase with increasing pressure for the coal ash.

Sorbent chemical and physical properties and operation conditions affect SO_2 capture from simulated flue gas. The conversion of the different sorbents under similar conditions is different, though the behaviour of the two dolomites is comparable unlike with the limestone and coal ash.

At atmospheric pressure dolomite conversion rates and adsorption capacities increase from 750-900°C. Limestone C and coal ash increase with temperature and show a maximum reactivity at 850°C then decreases at 900°C. This means that the sintering and loss of surface reactivity of dolomite A and dolomite B is lower as compared to that of limestone C.

The sudden decline in conversion of dolomite A, dolomite B and coal ash under atmospheric conditions mean that reaction takes place in two proceeding mechanisms due to surface controlled reaction whilst a product layer develops and changes chemical composition of the solid surface followed by diffusion through the product layer. At atmospheric pressure CaO is the effective reactant in the calcined sorbent. Under pressurised conditions the sulphation of all the sorbents started at a gradual rate and no decline in reaction rate was observed depicting that the reaction is diffusion controlled. At higher pressures of 10 and15 bar, $CaCO_3$ is the effective constituent in the sorbent.

Under pressurised conditions, all sorbents' reactivity increased with temperature between 750-900°C, this means $CaCO_3$ has less sintering properties compared to CaO. Increasing sulphation pressure from 10 to 15 bar with all the other parameters unchanged gave an increase in conversion by about 50%, this can be due to the SO_2 partial pressure and the effect of pressure on calcination conditions.

Sorbent ranking shows that limestone C has higher adsorption capacity than dolomite A, dolomite B and coal ash at both atmospheric and pressurised conditions. The lowest adsorption capacity was measured for coal ash.

It can be concluded that dolomite and limestone can be used as sorbents under atmospheric and pressurised fluidised bed combustion conditions. If residence time of sorbents is long enough (more that 200 minutes), higher conversions can be achieved for the dolomite under pressurised conditions since the reaction is still active up to 180 minutes and does not level off so early as noticed for the atmospheric conditions.

Since coal ash is a waste product of combustion the fact that it has some sulphur adsorption capacity means this will assist in alleviating the SO_2 pollution problem when using high ash poor quality coal with reasonable calcium content.

Circulating FBC requires Ca/S ratio of 1.5-2.0 whilst bubbling FBC requires Ca/S ratio 2.0-3.5 for 90% sulphur capture (Basu, 2006). The Ca/S ratio of the other sorbents can be increased to the right ratio by adding more sorbent depending on the sulphur content of the coal. A coal with good Ca/S ratio may stand alone as a sorbent. The coal ash used in this investigation had Ca/S ratio of 1.2 therefore it may not stand alone as a sorbent, it may need to be augmented by additional sorbent to increase the Ca/S ratio to the required ratio.

CHAPTER 6

MODELLING OF EXPERIMENTAL RESULTS

6.1 Introduction

In this Chapter modelling results of the sulphation experiments are presented. A detailed description and derivation of the model as used by Zevenhoven *et al.* (1998a) has been considered and presented in Section 6.2. In Section 6.3 the evaluation procedure is described. Model results for atmospheric experiments are presented in Section 6.4 whilst in Section 6.5 model results for pressurised sulphation are presented. Comparisons of model results are presented in Section 6.6. A summary of the results obtained in this Chapter is given in Section 6.7.

6.2 Model description and evaluation

The unreacted shrinking core model with variable effective diffusivity (Zevenhoven *et al.,* 1998a) was adapted for experimental results modelling. The unreacted shrinking core (USC) time-conversion model equations, combining the two rate determining steps, reaction kinetics and intra-particle gas diffusion, relating time to overall conversion is expressed as described by equations 6.1-6.6 (refer to Nomenclature for symbols definition).

6.2.1 Model parameters

The independent model parameters were obtained from characterisation experiments while some parameters like molecular and Knudsen diffusivities which are more difficult to determine through separate work were deduced from studies by other researchers. Particle density (ρ) was determined using helium pycnometry and sorbent chemical composition (x_{CaCO3}) was done using ICP analysis, a combination of these two parameters was used to calculate an input parameter, molar density of particle ($\rho_{mol,CaCO3}$). Particle radius (R_p) for the dolomites and limestone was calculated as the average of the upper and lower screen size used (212-300μm). Coal ash particle radius was deduced from particle size distribution characterisation. Molar ratio of products to molar ratio of reactants (Z) was calculated using equation

6.6 taking molar volume of 16.9 cm^3/mol, 36.9 cm^3/mol, and 46 cm^3/mol for CaO, $CaCO_3$ and $CaSO_4$ respectively (Gullet and Bruce, 1989). Products to reactants ratios (Z) of 2.72 and 1.25 were obtained for atmospheric (0.875 bar) and pressurised (10 and 15 bar) experiments respectively. Porosity (ε) and average pore radius (r_p) were obtained from mercury intrusion porosimetry. The tortuosity (γ) of the material was taken as 3 (Szekely *et al.*, 1976; Zevenhoven *et al.*, 1998a,b). The concentration of SO_2 in the gas mixture was calculated using the ideal gas equation. Molecular diffusivity (D_{mol}) was determined from equation 6.13 which is the Fuller, Schettler and Giddings relationship (Perry *et al.*, 1984). Knudsen diffusivity was obtained from equation 6.14. The time against conversion (t, X) data was calculated from the data obtained from thermogravimetric sulphation experimental work.

Table 6.1 gives a summary of the fixed measured parameters used in the model, chemical composition parameters are found on Table 4.3. Common parameters calculated using other correlations are given in the Appendices in Section A.1.

Table 6.1: Fixed model parameters

Sorbent	Particle Porosity (ε) (-)	A (-)	Average pore diameter (μm) [b]	Particle density (kg/m^3) (ρ)	Molar density of $CaO/CaCO_3$ in sorbent (mol/m^3) ($\rho_{mol,CaCO3}$)
Dolomite A	0.191	1.801	0.249	2845	19074
Dolomite B	0.171	4.848	0.304	2908	11492
Limestone C	0.297	2.367	0.856	2480	18596
Coal ash	0.315	2.175	1.620	2790	3683

6.2.2 Model description

Chemical kinetics

Assuming first order reaction with respect to SO_2.

$$\tau_{kin} = \frac{\rho_{mol,CaCO_3} R_p}{b k_s C_{SO_2}} \tag{6.1}$$

$$F_{kin}(X) = 1 - (1 - X)^{1/3} \tag{6.2}$$

Intra-particle diffusion

$$\tau_{dif} = \frac{\rho_{mol,CaCO_3} R_p^2}{6bD_{dif}C_{SO_2}} \tag{6.3}$$

$$F_{dif}(X) = 1 - 3(1-X)^{2/3} + 2(1-X) \ldots for\ Z = 1 \tag{6.4}$$

$$F_{dif}(X) = 3\left[\frac{Z - (Z + (1-Z)(1-X))^{2/3}}{Z-1} - (1-X)^{2/3}\right] \ldots if\ Z \neq 1 \tag{6.5}$$

$$Z = \frac{V_{mol\ product}}{V_{mol\ rectant}} \tag{6.6}$$

In cases where all these mechanisms are rate controlling, the total time will be the sum of all the mechanisms, i.e. additive reaction times (Levenspiel, 1999). Time to achieve a certain degree of conversion can be expressed as given in equation 6.7.

$$t = \tau_{kin} F_{kin}(X) + \tau_{dif} F_{dif}(X) \tag{6.7}$$

A modified version of the USC model, called the unreacted shrinking core with variable effective diffusivity (USC-VED) has been developed and used in modelling sulphation data (Zevenhoven *et al.,* 1998a,b; Alvarez and Gonzalez, 1999; Trikkel and Kuusik, 2003). The USC-VED model takes into consideration diffusion inside the sorbent particle being conversion dependent: which covers diffusion both in the pores and in the product layer given as a function of conversion and structural parameters of the sorbent.

Effective diffusivity D_{dif} includes two sequential processes: Diffusion in pores D_{pore} and diffusion through product layer D_{pl} which are combined as shown in equation 6.8 below:

$$\frac{Vol_{pore} + Vol_{pl}}{D_{dif}} = \frac{Vol_{pl}}{D_{pl}} + \frac{Vol_{pore}}{D_{pore}} \tag{6.8}$$

$$Vol_{pore} = \varepsilon = \varepsilon_0 - (1-\varepsilon_0)(Z-1)X \tag{6.9}$$

$$Vol_{pl} = (1-\varepsilon_0)XZ \tag{6.10}$$

$$V_{unreacted\ solid} = (1-\varepsilon_0)(1-X) = 1 - V_{pore} - V_{pl} \tag{6.11}$$

The volume of pores (Vol_{pore}) and product layer (Vol_{pl}) changes along with conversion as shown in equations 6.9 and 6.10.

$$D_{pore} = D_{mol+Kn}\frac{\varepsilon}{\gamma} = D_{mol+Kn}\frac{\varepsilon_0 - (Z-1)(1-\varepsilon_0)X}{3} \tag{6.12}$$

$$D_{mol} = \frac{10^{-3}T^{1.75}\left[(M_{N_2} + M_{SO_2})/(M_{N_2} + M_{SO_2})\right]^{1/2}}{P\left[(V_{N_2})^{1/3} + (V_{SO_2})^{1/3}\right]^2} \tag{6.13}$$

$$D_{Kn} = 97 r_{av}\sqrt{\frac{T}{M_{SO_2}}} \tag{6.14}$$

$$\frac{1}{D_{mol+Kn}} = \frac{1}{D_{mol}} + \frac{1}{D_{Kn}} \tag{6.15}$$

Diffusion of gas in a porous sorbent with porosity ε and tortuosity γ can be expressed as a function of conversion by equation 6.12, where D_{Kn} gives Knudsen diffusivity (calculated from equation 6.14) for an average pore radius r_{av}. Molecular diffusivity of SO_2 in N_2 (D_{mol}) is calculated using Fuller, Schettler and Giddings relationship (Perry *et al.*, 1984) where parameters V_{N2} and V_{SO2} are empirical parameters and M_{N2} and M_{SO2} are molecular weights of N_2 and SO_2. D_{mol+Kn} gives the combined molecular and Knudsen diffusivity in the gaseous phase inside the porous solid. Where D_{mol+Kn} is the combined molar Knudsen diffusivity for the reactant gas at a certain average pore radius. In these calculations tortuosity (γ) has been taken equal to 3 (Zevenhoven *et al.*, 1998a; Szekely *et al.*, 1976).

Combining equation 6.12-6.15 gives conversion-dependent effective diffusivity

$$D_{dif} = \frac{\varepsilon_0 + (1-\varepsilon_0)X}{\frac{3}{D_{mol+Kn}} + \frac{Z(1-\varepsilon_0)X}{D_{pl}}} \tag{6.16}$$

To obtain a simple expression for the variable effective diffusivity D_{dif}, the last equation can be rewritten using parameters *A* (equation 6.17) and *B* (equation 6.18), where *A* depends only on the initial porosity of the solid and *B* must be derived from (t-X) data set.

$$A = \frac{1-\varepsilon_0}{\varepsilon_0} \tag{6.17}$$

$$B = \frac{Z(1-\varepsilon_0)D_{mol+Kn}}{3D_{pl}} = \frac{AZD_{dif,0}}{D_{pl}} \tag{6.18}$$

$$D_{dif} = D_{dif,0}\frac{1+AX}{1+BX} \tag{6.19}$$

$$D_{dif,0} = D_{pore,0} = D_{mol+Kn}\frac{\varepsilon_0}{\gamma} \tag{6.20}$$

$$D_{pl} = \frac{AZD_{dif,0}}{B} \tag{6.21}$$

Having determined the value for *B*, it is possible to calculate also the product layer diffusivity D_{pl} using equation 6.21.

The basic equation for the USC - VED model can be expressed as equation 6.22. Equation 6.2 gives $F_{kin}(X)$ which is the relation between conversion and time for reaction control. Equation 6.4 gives $F_{dif}(X)$, which is the relationship between conversion and time for diffusion control meanwhile equation 6.7 gives A which is a dimenstionless parameter based on initial porostity. $\tau_{dif,0}$ which is the diffusion time scale before reaction starts is given by equation 6.3. This leaves B and τ_{kin} (reaction time scale) as the only uknowns, which can be obtained through curve fitting procedure, this was done with Excel Solver.

$$t = \tau_{kin} F_{kin}(X) + \tau_{dif,0} \frac{1+BX}{1+AX} F_{dif}(X) \qquad (6.22)$$

6.3 Model fitting procedure

Experimental results were modelled using a non-linear least sum of squares procedure. A Microsoft Excel built in program, Solver was used to model the results. Effective diffusivity of sorbent before reaction ($D_{dif,0}$) was calculated from equation 6.20, $\tau_{dif,0}$ (diffusion time scale before reaction starts) was calculated using equation 6.3. Parameter A was calculated from sorbent initial porosity (ε_0) using equation 6.17. Sulphation effectively started off with a calcined or half calcined sorbent, hence initial porosity for atmospheric reaction was taken to be that of fully calcined sorbent whereas for the high pressure experiments that of half calcined sorbent was considered. $F_{dif}(X)$ and $F_{kin}(X)$ which are the conversion functions for diffusion and reaction control respectively were calculated using equation 6.4 and 6.2 respectively. Parameter B and τ_{kin} (reaction time scale) were obtained from the curve fitting routine of the experimental results (t, X) using equation 6.22. Reaction constants ($k_{s,CaO}$ and $k_{s,CaCO3}$) and product layer diffusivity (D_{pl}) were calculated from the regressed values obtained from curve fitting using equations 6.1 and equation 6.21 respectively.

6.4 Modelling of atmospheric experimental results

6.4.1 Model results and discussion

Figures 6.1-6.4 show the modelling results of dolomite A, dolomite B, limestone C and coal ash under atmospheric conditions. Table 6.2 presents the parameters obtained from modelling (fitting). The sulphation process for dolomite A and dolomite B started at a relatively high rate with little dependence of conversion on temperature from 750-900°C. The relatively fast first stage is followed by a sudden decline in conversion rate after CaO conversion ranging between 16-20%. The model results show good closeness of fit to experimental results. The first stage of atmospheric reaction was found to be controlled by reaction kinetics which changes sharply to product layer control. Product layer diffusivities showed higher dependence on temperature compared to the reaction constants. Rate constants for sulphation were between 2.85-3.35x10^{-3} m/s for dolomite A and 2.43-3.12x10^{-3} m/s for dolomite B

between 750-900°C. Product layer diffusivities ranged from 0.334-8.23x10^{-10} m^2/s for dolomite A and 0.549-53.7x10^{-10} m^2/s for dolomite B.

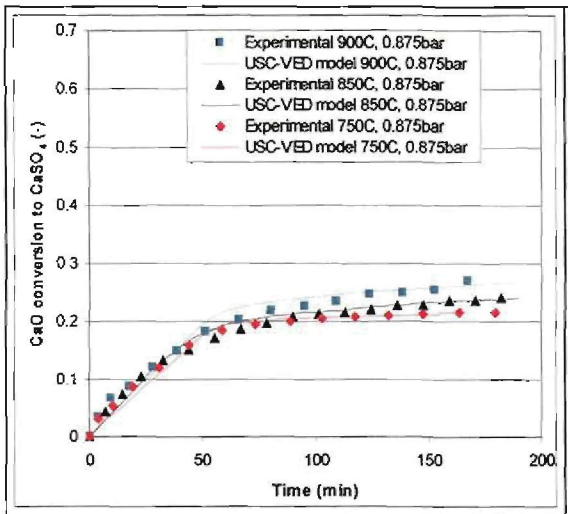

Figure 6.1: Dolomite A sulphation modelling at 0.875 bar

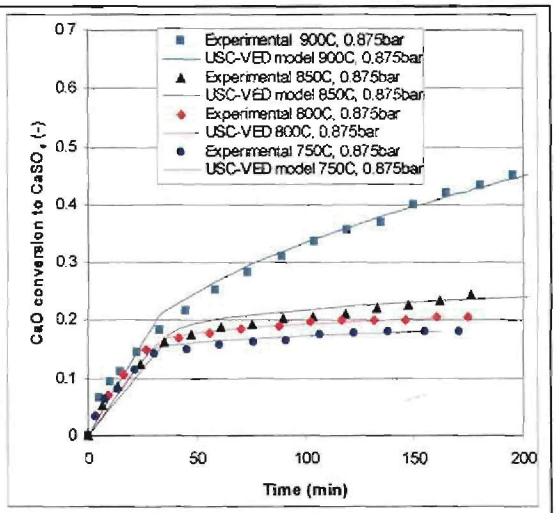

Figure 6.2: Dolomite B sulphation modelling at 0.875 bar

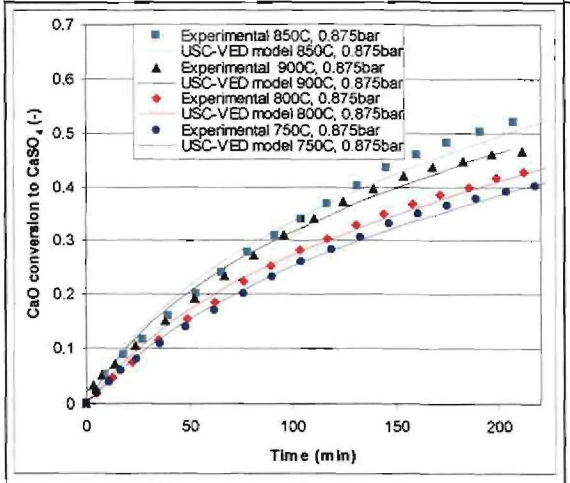

Figure 6.3: Limestone C sulphation modelling at 0.875 bar

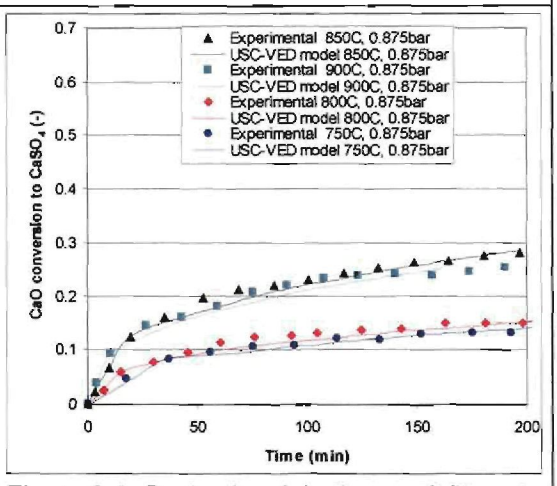

Figure 6.4: Coal ash sulphation modelling at 0.875 bar

Figure 6.4 show that sulphation reaction for coal ash also initiated at a relatively fast rate followed by a sharp reduction in reaction rate after conversions between 10-20% at temperatures between 750-900°C. There was a significant increase in reaction rate constant from 1.95-8.57x10^{-4} m/s as temperature increases from 750-900°C unlike in dolomite sulphation. The product layer diffusivities for coal ash sulphation show greater dependence on temperature at 1.54-11.03x10^{-10} m^2/s from 750-900°C respectively. The diffusivities obtained correlate well with ultimate coal ash sulphation at temperatures between 750-900°C.

Figure 6.3 shows that limestone C sulphation at atmospheric pressure occurred at a relatively constant reaction rate with no sharp change in reaction rate. The reaction

rate constants of 2.17-3.91x10^{-3} m/s shows marginal direct dependence of reaction kinetics on temperature in the range 750-900°C. At atmospheric pressure the product layer diffusivities of 7.22-12.40x10^{-8} m^2/s for limestone C sulphation are much higher than those obtained from fitting for dolomite A, dolomite B and coal ash; this explains the relatively higher conversion of limestone C. From Table 6.1 it can be seen that the product layer diffusivity at 900°C is less than that at 850°C; this result concurs well with the fact that peak sulphation for limestone C was obtained at 850°C.

The statistical analysis of the linear regression parameters showed a statistical error of < 10% for all cases, relative to the regression parameters D_{pl} and k_s. Correlation coefficients were between 0.84-0.99 which shows good closeness of fit of the model to the experimental data.

D_{pl} and $k_{s,CaCO3}$ were calculated from fitted parameters, B and τ_{kin} so are directly correlated to the value. τ_{kin} was calculated using model and experimentally deduced parameters.

Table 6.2: Model parameters for atmospheric pressure sulphation

Sorbent	Temperature (°C)	τ_{kin} (10^3 s)	B (10^3)	D_{pl} (10^{-10} m^2/s)	$k_{s,CaO}$ (10^{-4} m/s)
Dolomite A 0.875 bar	750	37.8	1270	0.33	31.5
	800	44.1	138	3.25	28.3
	850	39.1	56.6	8.24	33.5
	900	43.2	58.8	8.23	31.6
Dolomite B 0.875 bar	750	32.8	743	0.55	24.3
	800	32.2	300	1.43	26.0
	850	37.3	127	3.52	23.5
	900	29.3	8.71	53.7	31.2
Limestone C 0.875 bar	750	46.6	0.511	722	21.7
	800	38.9	0.497	783	27.2
	850	28.7	0.337	1210	38.8
	900	29.7	0.414	1040	39.1
Coal ash 0.875 bar	750	74.2	342	1.54	1.95
	800	45.5	280	2.01	3.34
	850	26.5	53.0	11.3	5.99
	900	19.4	61.0	10.4	8.57

The typical parameter values obtained for pore diffusion (1-10x10^{-7} m^2/s), product layer diffusion (1x10^{-10} m^2/s) and reaction kinetics (1x10^{-3} m/s) show that pore

diffusion is not reaction controlling since it is much larger than product layer diffusion. The conversion switches from chemical control to product layer diffusion control once a certain product layer has been formed (in this case at conversion between 16-20% for the dolomite and between 10-20% for the coal ash).

Trikkel and Kuusik, (2003) found values of D_{pl} ranging between 2.89-8.29x10^{-10} m^2/s at atmospheric pressure. Wang and Bjerle (1998) found that the surface reaction was controlling during first stages of reaction, and then the product layer diffusion took over. For dolomite A, dolomite B and limestone C the product layer diffusivities show greater dependence on temperature between 750-900°C than does the reaction constant. For coal ash, both reaction constant and product layer diffusivities show about fourfold increase for temperature increases from 750 to 900°C.

6.5 Modelling of pressurised experimental results

6.5.1 Model results and discussion

Sulphation at 10 and 15 bar as presented in Figures 6.5-6.12 started at a slower rate than observed for the atmospheric results shown in Figures 6.1-6.4 for all temperatures from 750-900°C. The sorbent conversion started and progressed at relatively constant rates with no sharp changes.

The gradual reaction rate under pressurised conditions could be due to the nature of product layer formed under pressurised sulphation conditions relative to that at atmospheric conditions. Under pressurised conditions release of CO_2 occurs at the same time with SO_2 reaction and this gives rise to a product layer that is different from the one at atmospheric pressure where there is no gas release on sorbent surface; hence control by intraparticle diffusion was dominant at early stages of reaction unlike at atmospheric pressure.

Figures 6.5-6.12 show the modelling results for dolomite A, dolomite B, limestone C and coal ash at 10 and 15 bar pressures and temperatures between 750-900°C. The modelling results show a very good closeness of fit to the experimental results meaning that the model describes the reaction well.

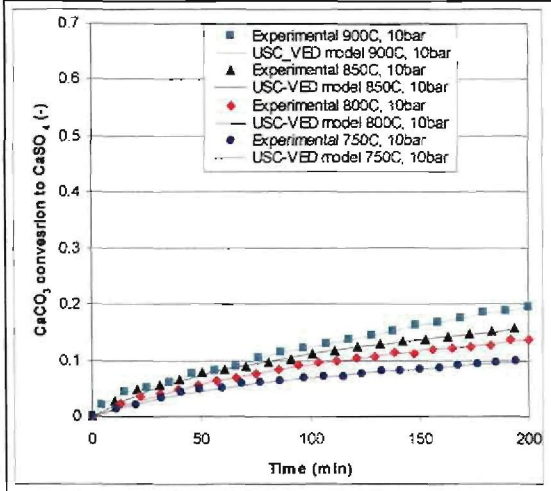

Figure 6.5: Dolomite A sulphation modelling at 10 bar

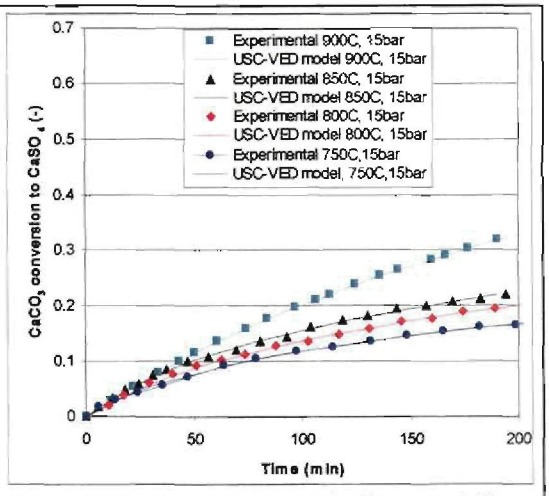

Figure 6.6: Dolomite A sulphation modelling at 15 bar

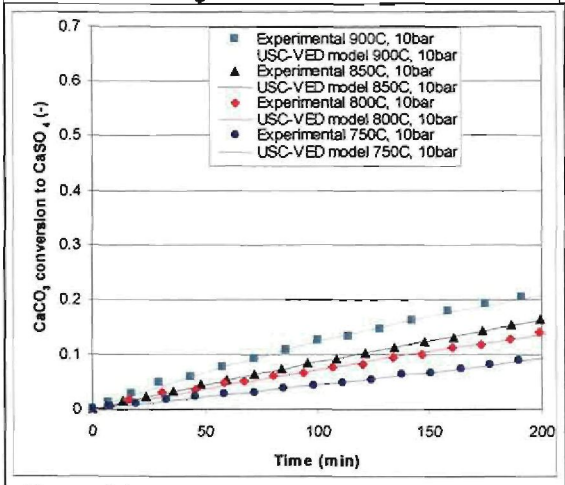

Figure 6.7: Dolomite B sulphation modelling at 10 bar

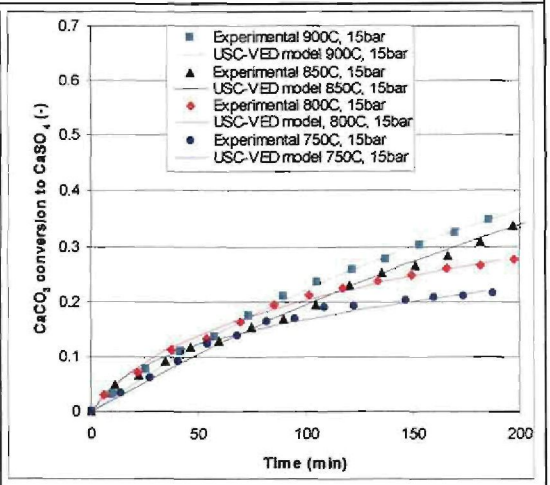

Figure 6.8: Dolomite B sulphation modelling at 15 bar

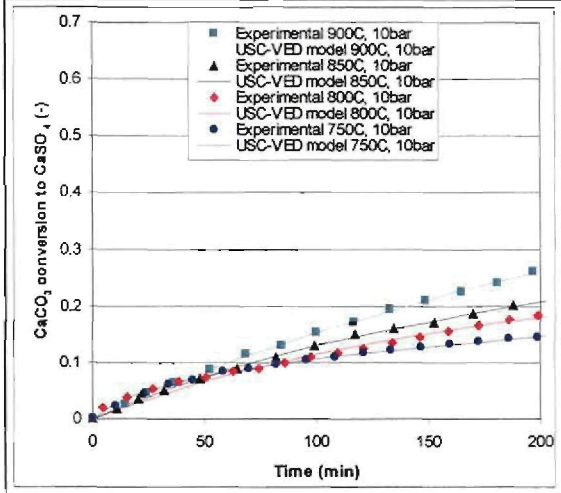

Figure 6.9: Limestone C sulphation modelling at 10 bar

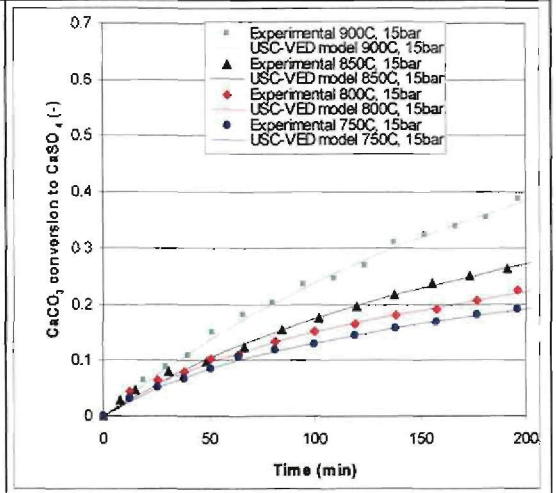

Figure 6.10: Limestone C sulphation modelling at 15 bar

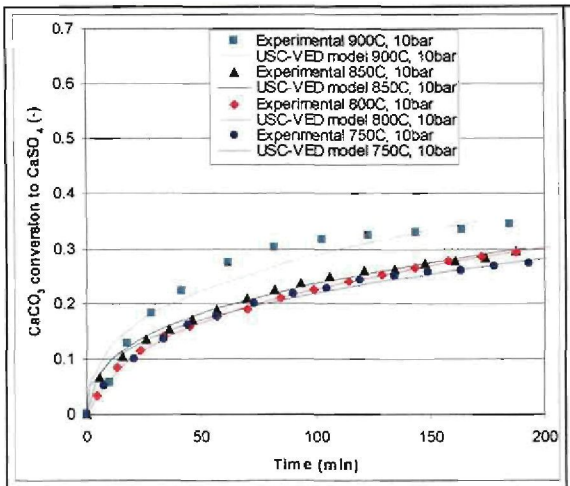

Figure 6.11: Coal ash sulphation modelling at 10 bar

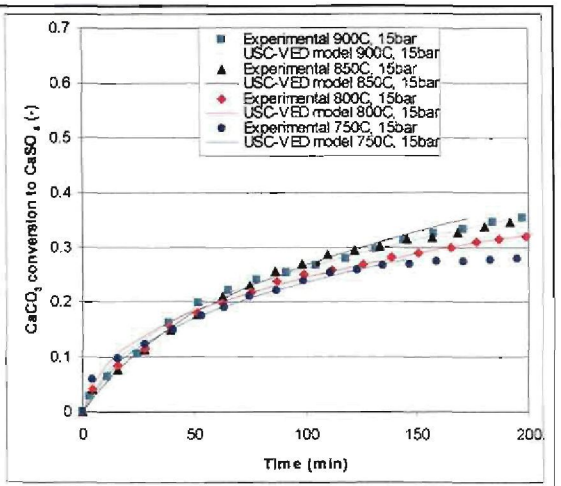

Figure 6.12: Coal ash sulphation modelling at 15 bar

Table 6.3 lists the model parameters obtained from modelling of sulphation reaction for dolomite A, dolomite B, limestone C and coal ash at 10 and 15 bar pressure. Some sulphation experiments were repeated at 10 and 15 bar pressure and non linear regression analysis was separately done for each of the repeated experiments to test for reproducibility of sulphation reaction. Tests for sulphation under same conditions at 10 and 15 bar pressure showed good reproducibility of between 90-95%.

The statistical analysis of the linear regression parameters showed a statistical error of < 10% for all cases, relative to the regression parameters D_{pl} and k_s. Correlation coefficients were between 0.96-0.99 which shows good closeness of fit of the model to the experimental data.

The regression statistic results shows that the regression coefficients are significant and thus useful in predicting the dependent variables. The regression parameters as obtained from the model using the non linear curve fitting are presented on Table 6.3.

Table 6.3: Model parameters for the pressurised sulphation

Sorbent	Pressure	Temperature (°C)	τ_{kin} (10^3 s)	B (10^3)	D_{pl} (10^{-10} m²/s)	$k_{s,CaCO3}$ (10^{-4} m/s)
Dolomite A	10bar	750	151	73.8	0.32	0.69
		800	129	25.2	0.98	0.85
		850	841	21.3	1.23	1.36
		900	106	7.9	3.51	1.13
	15bar	750	818	19.2	0.90	0.85
		800	78.8	10.5	1.76	0.92
		850	64.9	3.82	2.37	1.18
		900	71.2	1.43	14.7	1.12
Dolomite B	10bar	750	400	-	-	0.20
		800	235	2.69	7.23	0.36
		850	197	1.58	12.90	0.45
		900	1250	3.25	6.61	0.74
	15bar	750	28.2	11.2	1.30	1.89
		800	359	5.29	2.93	1.56
		850	811	0.586	28	0.72
		900	671	0.800	21.60	0.91
Limestone C	10bar	750	625	33.5	0.95	1.62
		800	119	10.1	3.63	0.89
		850	108	6.60	6.02	1.03
		900	101	2.17	19.70	1.15
	15bar	750	805	12.8	1.82	0.84
		800	70.2	8.86	2.86	1.01
		850	72.9	3.99	6.85	1.02
		900	58.8	1.10	26.70	1.32
Coal ash	10bar	750	-	126	0.25	-
		800	20.1	86.0	0.40	0.77
		850	4.1	102	0.36	3.94
		900	-	65.1	0.62	-
	15bar	750	21.6	70.9	0.30	0.46
		800	12.8	78.2	0.30	0.81
		850	32.0	40.0	0.68	0.34
		900	21.7	55.1	0.49	0.52

The kinetic constants ($k_{s,CaCO3}$) for all the sorbents show marginal increase as sulphation temperatures were increased between 750-900°C. Zevenhoven *et al.* (1998a) found reaction rates of 1.1×10^{-5} and 2.2×10^{-5} m/s for 850 and 950°C respectively; these values are slightly lower than values obtained in this investigation.

Hajaligol *et al.* (1988) reported values of $k_{s,\ CaCO3}$ ranging from 0.96-1.76x10^{-3} m/s between 850 and 950°C, these compare well with the results obtained in this research. Trikkel and Kuusik (2003) obtained wide ranging values of $k_{s,CaCO3}$ from 0.0259 -7x10^{-2} m/s.

The product layer diffusivities for dolomite A, limestone C and coal ash generally show a marked increase with temperature from 750-900°C. Dolomite B sulphation showed a surprisingly different behaviour as the product layer diffusivity decreases from 7.23-6.61x10^{-10} m^2/s at temperatures from 800-900°C. Zevenhoven *et al.* (1998a) reported product layer diffusivity values from 0.0081-1.02x10^{-8} m^2/s for various limestones and dolomites. They obtained the lowest values of D_{pl} for dolomites and this was also observed in this research between dolomite A and limestone C. Iisa and Hupa, 1990 obtained values of D_{pl} values between 0.6-2x10^{-10} m^2/s, whilst Trikkel and Kuusik found values from 3.26-8.22x10^{-10} m^2/s for different sorbents under conditions similar to those used in this research, these compare well with value obtained in this research.

6.6 Comparison of results

The kinetic constants under atmospheric pressure sulphation for all the sorbents used are higher than for pressurised conditions by a factor of above 20-30 for dolomite A, dolomite B and limestone C and by a factor of about 5 for coal ash. This is mainly attributable to the fact that the reaction of CaO with SO_2 is much faster than the reaction of $CaCO_3$ with SO_2.

There is no significant difference in the kinetic constants for 10 and 15 bar pressure for all the sorbents which indicates 1st order kinetics.

At atmospheric pressure, coal ash exhibits the lowest kinetic constants compared to the other sorbents by a factor of about four. The reason for this could be due to the spatial distribution of the reactive surface area in the ash and the fact that the coal ash has already inherently captured some SO_2 in the process of coal combustion.

For dolomite A and dolomite B the product layer diffusivity at atmospheric pressure and at 10 and 15 bar pressure are in the same ranges. This could mean that the

product layer resistance at the decline stage of the dolomite is the same as that encountered for pressurised sulphation. For limestone C the product layer diffusivity at atmospheric pressure is much higher than that at 10 and 15 bar; this could mean that the resistance of product layer diffusion is much lower owing to surface cracks at atmospheric pressure compared to an intact surface under pressurised conditions as observed in Figure 4.10. The average BET pore diameter of limestone C is about four times that of the other sorbents, meaning, diffusion resistance is low such that there is relatively no pore closure in limestone C up to the 200 minutes time considered.

6.7 Conclusions: Sorbent sulphation modelling results

The experimental results obtained in this investigation fitted well to the unreacted shrinking core model with variable effective diffusivity.

The parameter values found for pore diffusion, product layer diffusion and reaction kinetics show that pore diffusion is not controlling. This agrees well with the range of pore diameter obtained showing meso-macro porosity hence unlikely to offer much resistance to flow of gas to reaction surface. Reaction and product layer diffusion can thus be considered to be controlling.

The reaction kinetic constant at atmospheric pressure was higher ($1x10^{-3}$ m/s), compared to ($1x10^{-4}$ m/s) under pressurised conditions. This most probably mean that the reaction between SO_2 and CaO is faster than the reaction between SO_2 and $CaCO_3$ in the presence of O_2.

It can be observed from Table 6.2 and 6.3 that reaction constants showed marginal dependence on temperature for the range 750-900°C whilst the product layer diffusivities show substantial dependence on temperature. However this is not often observed in heterogenous reactions, a similar observation was found by Zevenhoven *et al.* (1998a, b) and Ngeleka (2005). A definite explanation of this phenomenon can not be given.

The effect that causes an increasing conversion as pressure increased from 10 to 15 bar could not be exactly explained, however effects of pressure on calcination conditions could be the cause and also the effective increase in SO_2 partial pressure.

The temperature effect on diffusivity could be considered not as an effect on gas diffusion but rather an effect on structure of product layer (Qiu and Lindqvist, 2000).

CHAPTER 7

CONCLUSIONS AND RECOMMENDATIONS

7.1 Conclusions

The conclusions made from the investigation on the characterisation, calcination, sulphation and modelling of sulphation results are given below:

1. From the characterisation results of the four sorbents the following conclusions were made:
   - the particle size distribution of the dolomite and limestone showed a normal distribution with an average particle diameter 260μm. Coal ash has a skewed particle size distribution owing to fragmentation during combustion of a coal of normal particle size distribution and 260μm diameter, average coal ash particle diameter was 140μm.
   - dolomite A, dolomite B and limestone C contained similar elements, their major difference was in calcium, magnesium and silicon composition, limestone C had the highest calcium, followed by dolomite A, then dolomite B. Coal ash contained much less calcium and further contained higher aluminium, silicon and iron content relative to dolomite and limestone.
   - it can be deduced from ash and coal characterisation that the coal ash had already captured 31.2% of the 1.7% sulphur by weight in the coal during combustion. This capture corresponds to calcium utilisation of about 23% in inherent sulphur retention before the ash was used in the laboratory sulphation experiments. this gives an indicator of how much the coal ash contribute to inherent sulphur capture.
   - the sorbents showed bimodal pores size distribution in the meso-macropore size range. The greater part of the internal surface area was in the mesopore range. The macropore surface area was relatively small.
   - there is pore growth on calcination. Average pore diameter for half calcined dolomite is higher than that of fully calcined dolomite and porosity follows the same trend. There is considerable change to sorbent structure with calcination and sulphation temperature.

2. Calcination of dolomite A, dolomite B and limestone C under atmospheric and pressurised conditions concurs well with characterised Ca content of sorbent, which support the chemical characterisation results that raw sorbent are predominantly composed of $CaCO_3$ and $MgCO_3$. Coal ash calcium is in the CaO state. By carefully controlling the CO_2 partial pressure, the effective sorbent at atmospheric pressure is CaO and that at pressurised conditions is $CaCO_3$ whilst $MgCO_3$ calcines to MgO under both atmospheric and pressurised conditions.

3. Sorbent chemical and physical properties and reaction operation conditions affect SO_2 capture from flue gas. The conversion of the different sorbents under similar conditions is different, though the behaviour of the two dolomites is quite comparable relative to the limestone and coal ash.

4. At atmospheric pressure dolomite conversion rates and adsorption capacities increased for temperatures from 750-900°C. Limestone C and coal ash conversion increased with temperature and showed a maximum reactivity at 850°C then declined at 900°C. This means that the sintering and loss of surface reactivity of dolomite A and dolomite B is lower as compared to that of limestone C. Under pressurised conditions, all sorbents' reactivity increased with temperature between 750-900°C, this indicate that $CaCO_3$ has lower sintering properties compared to CaO. Increasing sulphation pressure from 10 to 15 bar with all the other parameters unchanged gave an increase in conversion of about 50%, this can be attributed to the SO_2 partial pressure and the effect of pressure on calcination.

5. Sulphation at atmospheric pressure showed calcium conversion between 22-44% for dolomites, 37-49% for limestone and 13-28% for coal ash after 180 minutes. At atmospheric pressure, dolomites and coal ash reactivity started off relatively fast followed by a sudden decline after 16-20% conversion, limestone did not show decline in reactivity up to 200 minutes. The sudden decline in conversion implies that reaction takes place in two sequential mechanisms due to surface controlled reaction whilst a product layer develops and changes chemical composition of the solid surface followed by diffusion through the product layer.

6. Under pressurised conditions the sulphation of all the sorbents started at a relatively slow and gradual rate and no decline in reaction rate was observed between 750-900°C. Sulphation at 15 bar was higher than at 10 bar. At 15 bar

dolomite calcium conversion ranged between 16-34% and limestone was between 18-36% and coal ash conversion was higher at 28-35% calcium conversion.

7. Sorbent adsorption capacities show that limestone C had higher adsorption capacity than dolomite A, followed by dolomite B and lastly coal ash at both atmospheric and pressurised conditions. The lowest adsorption capacity was measured for coal ash. It can be concluded that dolomite and limestone can be used as sorbents under atmospheric and pressurised fluidised bed combustion conditions. If residence time of sorbents is long enough (greater than 200 minutes), higher conversions can be achieved for the dolomite under pressurised conditions since the reaction is still active up to 180 minutes and does not decline so early as noticed for the atmospheric condition.

8. Dolomite A SO_2 adsorption after 180 minutes was between 9.47-12.49 mg SO_2/100 mg sorbent. Dolomite B SO_2 adsorption capacity ranged between 6.47-14.22 mg SO_2/100 mg sorbent and limestone C SO_2 adsorption was much higher than that of the dolomites as it adsorbed between 17.77-23.54 mg SO_2/100 mg sorbent. Comparable results as achieved by limestone C were obtained by Trikkel and Kuusik (2003) adsorbing from 15.5-33.9 mg SO_2/100 mg sorbent under similar conditions of time and pressure. According to sorbent ranking in Basu (2006) suggested by Westinghouse (Keairns and Newby, 1981) the SO_2 capture capacities obtained for the limestone means that it can be ranked as medium-high rank sorbent while dolomite can be ranked as average sorbent and coal ash can be ranked as low ranked sorbent (Basu, 2006).

9. Since coal ash is a waste product of combustion, the fact that it has some sulphur adsorption capacity means this will assist in alleviating the SO_2 pollution problem when using high ash poor quality coal with reasonable calcium content.

10. The experimental results obtained in this investigation fitted well to the unreacted shrinking core model with variable effective diffusivity. The model shows a shift in reaction control from surface reaction kinetics to product layer diffusion as the reaction progresses. The parameter values found for pore diffusion, product layer diffusion and reaction kinetics show that pore diffusion is not controlling, this agrees well with the range of pore diameters obtained showing meso-macro porosity hence unlikely to offer much resistance to flow of gas to reaction surface.

7.2 Recommendations

The research was limited to sulphation of two dolomites, limestone and coal ash under atmospheric and pressurised conditions with a fixed particle size and fixed gas concentration under isothermal conditions. It is recommended for the betterment of the understanding of the sorbents to broaden the results obtained by:

1. Increasing the number of dolomites, limestones and coal ashes to ascertain the effect of various chemical compositions on sulphation.
2. Including mineralogical composition analysis and ascertain the existence of different mineral forms in the sorbents and the coal ash.
3. Considering the study on the effect of temperature on structural parameters and pore development during calcination and consider the sintering effect of temperature on the sorbents.
4. Considering the effect of time of continuous heating on internal structure of sorbent under atmospheric and pressurised conditions.
5. Considering the quantitative effect of particle size on sulphation of these dolomites and limestone.
6. Looking at the effect of SO_2 gas composition on sulphation and determination of reaction order.
7. Using a more detailed pore size distribution model for determination of the structural parameters that can be used with pore models like the random pore model and experimentally obtaining structural parameters.
8. Comparing the results obtained from the TGA with the results obtained from Eskom's pilot plant using the same sorbents.

REFERENCES

ALVAREZ, E., GONZALEZ, J.F. 1999. High pressure thermogravimetric analysis of the direct sulphation of Spanish calcium-based sorbents. Fuel, 78:341-348.

ANTHONY, E.J, GRANATSTEIN, D.L. 2001. Sulphation phenomena in fluidised bed combustor systems. Progress in energy and combustion science, 27:215-229.

ANTHONY, E.J, IRIBARNE, A.P., IRIBARNE, J.V., JIA, L. 1997. Reuse of land filled FBC residues. Fuel, 76:603-609.

AR, I., BALCI, S. 2002. Sulphation reaction between SO_2 and limestone: application of deactivation model. Chemical engineering and processing, 41:179-188.

BARRET, E.P., JOYNER, L.G., HALENDA, P.P. 1951. The determination of pore volume area distributions in porous substances. Journal of American Chemical Society, 73:373–380.

BASU, P. 2006. Combustion and gasification in fluidized beds. CRC Press – Taylor and Francis group. 473p.

BHATIA, K.S., PERLMUTTER, D.D. 1980. A random pore model for fluid-solid reactions. American Institute of Chemical Engineers journal, 26(3):379-385.

BHATIA, K.S., PERLMUTTER, D.D. 1983. Unified treatment of structural effects in fluid-solid reactions: isothermal kinetic control. American Institute of Chemical Engineers journal, 29(2):281-289.

BORGWARDT, R.H., BRUCE, R.C. 1987. An investigation of product layer diffusivity for CaO sulphation. Industrial and engineering chemistry research, 26:1993-1998.

BORGWARDT, R.H., ROACHE, K.R., BRUCE, R.C. 1986. Method for variation of grain size in studies of gas solid reaction involving CaO. Industrial and engineering chemistry research, 25:165-169.

BOSKOVIC, S., REDDY, B.V., BASU, P. 2002. Effect of operating parameters on sulphur capture in a pressurized circulating fluidised bed combustor. International journal of energy research, 26:173-183.

BP. 2005. Statistical Review of World Energy. BP, London
http://www.bp.com/genericsection.do [Date of access: 10 April 2006]

BUZEK, J., JASCHIK, M., PODKAN'SKI, J., WASILEWSKI, W., MROZOWSKI, J.1998. A non-isothermal model of thermal desorption with chemical reaction in the liquid phase. Chemical engineering and processing, 37:233–247.

CARPENTER, A.M. 1998. Switching to the cheaper coals for power generation. IEA Coal Research.
https://www.iea.org/textbase/nppdf/free/1990/elecpower99.pdf [Date of access: 08 September 2006]

CHEN, C., ZHAO, C., LIANG, C., PANG, K., 2007. Calcination and sintering of limestone under O_2/CO_2 combustion atmosphere. Fuel processing technology, 88:171-178.

CHRISTMAN, P.G., EDGAR, T.F. 1983. Distributed pore-size model for sulphation of limestone. American Institute of Chemical Engineers journal, 29:388-394.

CONN, R.E., TAYLOR, T.E., TANG, J. 1993. Evaluation of inherent sulphur capture from low rank coals in circulating fluidised beds. Proceedings of the 12th International Conference of fluidised bed combustion. American Society of Mechanical Engineers, San Diego, USA, pp 273-281.

CURRAN, R.A., TANF, J.T., CAPAN, S.F., FIORITI, G.A., TAYLOR, T.E. 1995. Fluidized bed combustion. American Society of Mechanical Engineers journal, 2:851–857.

DAM-JOHANSEN, K., OSTERGAARD, K. 1991. High temperature reaction between sulphur dioxide and limestone-I: Comparison of limestones in two laboratory reactors and pilot plant. Chemical engineering science, 46 (3):827-837.

DAVINI, P. 1995. Thermogravimetric study of the characteristics and reactivity of CaO formed in presence of small amounts of SO_2. Fuel, 74:995–998.

DENNIS, J.S., HAYHURST, A.N. 1985. The effect of temperature on the kinetics and extent of SO_2 uptake by calcareous materials during the fluidised bed combustion of coal. Proceedings of The Twentieth International Symposium on Combustion, The Combustion Institute, Pittsburgh: pp1347-1355.

DENNIS, J.S., HAYHURST, A.N. 1990. Mechanism of the sulphation of calcined limestone particles in combustion gases. Chemical engineering science, 45(5):1175-1187.

DENNIS, J.S., HAYHURST, A.N. 1987. The effect of CO_2 on the kinetic and extent of calcination of limestone and dolomite particles in fluidised beds. Chemical engineering science, 42:2361-2372.

DENNIS, J.S., HAYHURST, A.N. 1984. The effect of temperature on the kinetics and extent of SO_2 uptake by calcareous materials during fluidised bed combustion. Proceedings of the 20th International Symposium on combustion. The combustion institute, pp1347-1355.

DO, D. 1998. Adsorption analysis equilibria and kinetics, Imperial College Press. 892p.

ENERGY INFORMATION ADMINISTRATION (EIA). 2004b. Country analysis briefs – Energy and environmental issues.
http://www.eia.doe.gov/emeu/cabs/safrica.html [Date of access: 23 November 2006]

ERSOY-MERICBOYU, A., KUCUKBAYRAK, S. 1998. Modelling of the isothermal sulphation reactions of natural sorbents. Thermochimica acta, 319:163-170.

ERSOY-MERICBOYU, A., KUCUKBAYRAK, S. 1995. The isothermal sulphation reactions of natural sorbents. Thermochimica acta, 260:45-50.

ESKOM HOLDINGS ANNUALLY REPORT, 2005.
http://www.eskom.co.za/publications [Date of access: 03 March 2006]

ESKOM HOLDINGS ANNUALLY REPORT, 2007.
http://www.eskom.co.za/publications [Date of access: 03 September 2007]

FUERTES, A.B., VELASCO, G., ALVAREZ, T., FERNANDEZ, M.J. 1995. Sulphation of dolomite at high CO_2 partial pressures. Thermochimica acta, 254:63-78.

FUERTES, A.B., ARTOS, V., PI, J.J., MRBAN, G., PALACIOS, J.M. 1992. Sulphur retention by ash during fluidised bed combustion of bituminous coals. Fuel, 71:507-511.

FUKASAWA, K. 1997. Low cost, retrofit FGD systems. IEA Coal Research.
http://www.iea-coal.org.uk/catalogues/coalonline [Date of access: 11 August 2006]

GARCIA-LABIANO, F.J. 1992 Doctoral thesis. Instituto de Carboquimica, Zaragoza.

GHARDASHKHANI, S., COOPER, D.A. 1990. A thermogravimetric study of the reaction between sulphur dioxide and calcium oxide. Thermochimica acta, 161:327-337.

GRAY, V.R. 1986. Retention of sulphur by laboratory prepared ash from low rank coal. Fuel, 65:1618-1619.

GREGG, S.W., SING, K.W. 1982. Adsorption, surface area and porosity. Academic Press, London, 303p.

GRUBOR, B., MANOVIC, V. 2002. Influence of non uniformity of coal and distribution of active calcium on sulphur self-retention by ash – a case study of lignite of Kolubara. Energy and fuels, 16;951-955.

GRUBOR, B., MANOVIC, V., OKA, S. 2003. An experimental and modelling study of the contribution of coal ash to SO_2 capture in fluidised bed combustion. Chemical engineering journal, 96:157-159.

GULLET, B.K., BRUCE, K.R. 1989. Identification of $CaSO_4$ formed by reaction of CaO and SO_2. American Institute of Chemical Engineers journal, 35:1739-1741.

HAJALIGOL, M., LONGWELL, J.P., SAROFIM, A.F. 1988. Analysis and modelling of the direct sulphation of $CaCO_3$. Industrial and engineering chemistry research, 27:2203-2210.

HARTMAN, M., COUGHLIN, R.W. 1976. Reaction of sulphur dioxide with limestone and the grain model. American Institute of Chemical Engineers journal, 22(3):490-498.

HARTMAN, M., COUGHLIN, R.W. 1974. Reaction of sulphur dioxide with limestone and the influence of pore structure. Industrial and engineering chemistry process design and development, 16(3):248-253.

HARTMAN, M., HEJNA, J., BERAN, Z. 1979. Application of the reaction kinetics and dispersion model to gas solid reactors for removal of sulphur dioxide from flue gas. Chemical engineering science, 34: 475-483.

HORSFALL, D.W. 1993. Coal Preparation and Usage, volume 3. Coal Publication (Pty) Ltd, SA. Chapter 21-28.

IISA, K., HUPA, M. 1990. 23rd Symposium (international) on combustion: The Combustion Institute, Pittsburgh. pp943-948

IISA, K. 1992. Sulphur capture under pressurised fluidised bed combustion conditions. Academic dissertation – Abo Akademi University: Department of Chemical Engineering.

ILIC, M., GRUBOR, B., MANOVIC, V. 2003. Sulphur retention by ash during coal combustion – Part 1. A model of char particle combustion. Journal of the Serbian Chemical Society, 68:137-145.

INTERNATIONAL ENERGY AGENCY (IEA): 2003. COAL INDUSTRY ADVISORY BOARD. 2003. Meeting with IEA Governing Board: Clean coal technologies, pp3-4 http://www.iea-coal.org.uk/content/default.asp [Date of Access: 31 May 2006]

INTERNATIONAL ENERGY AGENCY (IEA). 2004. World Energy Outlook, 2004 OECD/IEA, Paris
http://www.worldenergyoutlook.org { Date of access: 21 September 2006]

INTERNATIONAL ENERGY AGENCY (IEA). 2005. Electricity Information 2005. OECD/IEA, Paris
http://www.worldenergyoutlook.org [Date of access: 21 September 2006]

IRIBARNE, A.P., IRIBARNE, J.V., ANTHONY, E.J. 1997. Reactivity of calcium sulphate from FBC systems. Fuel, 76:321.

KAITANO, R. 2006. Characterisation and reaction kinetic of high ash chars derived from inertinite-rich coal discards. Doctoral thesis – North-West University: Department of Chemical Engineering.

KOCAEFE, D., KARMAN, D., STEWARD, F.R. 1987. Interpretation of the sulphation rate of CaO, MgO and ZnO with SO_2 and SO_3. American Institute of Chemical Engineers journal, 33(11):1835-1843

LEVENSPIEL, O. 1999. Chemical Reaction Engineering. John Wiley and Sons, Inc. 668p.

LINDNER, B., SIMONSSON, D. 1981. Comparison of structural models for gas solid reactions in porous solids undergoing structural changes. Chemical engineering science, 36(9):1519-1527.

LJUNGSTROM, E., LINDQUIVST, O. 1982. Proceedings of the 7th International Conference of Fluidised Bed Combustion, pp465-472.

LOWELL, S., SHIELDS, J.S. 1984. Powder surface area and porosity. Chapman and Hall Limited, London. 234p.

MANOVIC, V., GRUBOR, B., LONCAREVIC, D. 2006. Modeling of inherent SO_2 capture in coal particles during combustion in fluidised bed. Chemical engineering science, 61:1676-1685.

MANOVIC, V., GRUBOR, B., ILIC, M. 2002. Sulphur self retention in ash - a grain model approach. Thermal science, 6:29-26.

MCCAULEY, R.A., JOHNSON, L.A. 1991. Decrepitation and thermal decomposition of dolomite. Thermochimica acta, 185:271-280.

NATIONAL ENERGY LABORATORY TECHNOLOGY. 2006. Combustion – fluidized bed combustion.
http://www.netl.doe.gov/Combustion Technologies.htm /index.html [Date of access: 04 December 2006]

NGELEGA, P.,K. 2005. Sulphur dioxide capture under fluidised bed combustion. Masters dissertation – North-West University: Department of Chemical Engineering

NJAPHA, D. 2003. Determination of the kinetic models and associated parameters for the low temperatures combustion and gasification of high-ash coal chars. Doctoral thesis – North-West University: Department of Chemical Engineering.

NOLAN P. S. 2000. Flue gas desulphurisation technology for China. International Electric Power for China. Babcock and Wilcox Company, a McDermott company. Barberton, Ohio, U.S.A

NYGAARD, H.G., KIIL, S., JOHNSSON, J.E., JENSEN, J.N., HANSEN, J., FOGH, F., DAM-JOHANSEN, K. 2004. Full-scale measurements of SO_2 gas phase concentrations and slurry compositions in a wet flue gas desulphurisation spray absorber. Fuel, 83:1151-1164

O'NEILL E.P., KEAIRNS D.L., KITTLE, F. 1976. A thermogravimetric study of the sulphation of limestone and dolomite: The effect of calcination conditions. Thermochimica acta, 17:209-220.

OZER, A.K., GULABOGLU, M.S., BAYRAKCEKEN, S., WEISWEILER, W. 2002. Flue gas desulphurisation with phosphate rock in a fluidised bed. Fuel, 81:41-49.

PATSIAS, A.A., NIMMO, W., GIBBS, B.W., WILLIAM, P.T. 2005. Calcium based sorbents for simultaneous NOx/SOx reduction in a down fired furnace. Fuel, 84: 1864-1873.

PERRY, R.H., GREEN, D., MARLONEY, J.O. 1984. Chemical engineer's handbook, 6th edition. McGraw-Hill, New York.

PIGFORD, R.L., SLIGER, G. 1973. Rate of diffusion-controlled reaction between a gas and porous solid sphere. Industrial and engineering chemistry process design and development, 12(1):85-92.

PUFF, R., KITA, J.C., LARGE, J.F. FEUGIER, A. 1983. Self desulphurisation of high sulphur high ash Provence coal by the Cerchar FBC process. Proceedings of the first international FBC and applied technology symposium, Beijing, China, pp22-24.

QIU K., LINDQVIST, O. 2000. Direct sulphation of limestone at elevated pressures. Chemical engineering science, 55:3091-3100.

RAASK, E. 1985. Mineral impurities in coal combustion. Hemisphere publishing, Washington , USA, 370p.

RAMACHANDRAN, P.A. 1983. Analytical prediction of conversion-time behaviour of gas-solid non catalytic reaction. Chemical engineering science, 38:1385-1390.

RAMACHANDRAN, P.A., SMITH, J.M. 1977. A single pore-model for gas solid non catalytic reactions. American Institute of Chemical Engineers journal, 23:353-361.

RANADE, P.V., HARRISON, D.P. 1981. The variable property grain model applied to zinc oxide hydrogen sulphide reaction. Chemical engineering science, 36:1079-1089

SAMTANI, M., DOLLIMORE, L., WILBURN, F.W., ALEXENDER. 2001. Isolation and identification of the immediate and final products in the thermal decomposition of dolomite in a atmosphere of carbon dioxide. Thermochimica acta, 368:285-295.

SHAH, C.L., ABBOTT, J., MILES, N.J., XUEJUN, LI., JIANPING, XU. 2002. Sulphur reduction evaluation of selected high sulphur Chinese coals. Fuel, 81:519-529.

SHEAREAR, J., JOHNSON, J., TURNER, C.B. 1979. Effects of sodium chloride on limestone calcination and sulphation in fluidised bed combustion. Environmental science technology, 13:1113-1118.

SHENG, C., XU, M., ZHANG, J., XU, Y. 2000. Comparison of sulphur retention by coal ash in different types of combustors. Fuel processing technology, 64:1-11.

SIMON, G.A., GARMAN, A.R., BONI, A.A. 1987. The kinetic rate of SO_2 sorption by CaO. American Institute of Chemical Engineers journal, 33:211-217.

SIMON, G.A., GARMAN, A.R. 1986. Small pore closure and deactivation of the limestone sulphation reaction. American Institute of Chemical Engineers journal, 32:1491-1499.

SING, K.S.W., EVERETT, D.H., HAUL, R.A.W., MOSCON, L., PIEROTTI, R.A., ROUGUEROL, J., SIEMIENIEWSKA., T. 1982. Reporting physisorption data for gas/solid systems with special reference to the determination of surface area and porosity. Pure applied chemistry, 57(4):603-620.

SOUTH AFRICA. Department of minerals and energy. 2001. National Inventory on discards and duff coal. http://www.dme.gov.za/publications [Date of access: 05 March 2006]

SOUTH AFRICA. 2004.National Environmental Management: Air Quality Act 39 of 2004. Chapter 9 section 63.
http://www.environment.gov.za/Documents/PreviousAnnualReports/2003Apr25/StrategicPlan_apr2003.doc [Date of access: 16 May 2006]

SOUTH AFRICA MINISTRY OF FINANCE. 2006. Budget 2006, the people's guide. http://www.southafrica.info/doing_business/economy/fiscal_policies/budget2005-peoples-guide.htm: [Date of access: 06 June 2006]

SPARTINOS, D., VAYENAS, C. 1991. Kinetics of sulphation of limestone and precalcined limestone. Chemical engineering processing, 30:94-101.

STANLEY-WOOD, N.G., LINES, R.W. 1992. Particle size analysis. Royal Society of Chemistry. London. 538p.

STEFANIAK, E., BILINSKI, B., DOBROWOLSKI, R., STASZCZUK. WOJCIK, J. 2002. The influence of preparation conditions on adsorption properties and porosity of dolomite based sorbents. Colloids and surfaces A: Physicochemical and engineering aspects 208:337-337.

SZEKELY, J., EVANS, J.W. SOHN, Y.H. 1976. Gas-solid reactions. Academic press inc. 400p.

SZEKELY, J., EVANS, J.W. 1970. A structural model for gas-solid reactions with a moving boundary. Chemical engineering science, 25:1091-1107.

THE HEALTHY COUNCIL OF THE NETHERLANDS. 2003. Sulphur dioxide: Health-based recommended occupational exposure limit. http://www. Gr.nl/pdf.php [Date of access: 06 June 2006]

TRIKKEL, A., KUUSIK, R. 2003. Modeling of decomposition and sulphation of oil shale carbonates on the basis of natural limestone. Oil shale, 20(4):491-500.

TRIKKEL, A., ZEVENHOVEN, R., KUUSIK, R. 1999. Estonian calcareous rocks as SO_2 sorbent in AFBC and PFBC conditions. Department of Chemical Engineering: Abo Akademi University. Finland.

TULLIN, C., LJUNGSTROM. 1989. Reaction between calcium carbonate and sulphur dioxide. Energy and fuels, 3:284-287.

ULERICH, N.H., NEWBY, R.A., AND KEAIRNS, D.L. 1980. A thermogravimetric Study of the sulphation of limestone: prediction of pressurised and atmospheric fluidised bed desulphurisation. Thermochimica acta, 36:1-16.

VAN DER RIET, M., BEGG, J.H. 2003. Clean coal technologies for South Africa. ESI Africa2: 43_1.

WANG, W., BJERLE, I. 1998. Modelling of high temperature desulphurisation by Ca based sorbents. Chemical engineering science, 53:1973-1989.

WANG, C., SHEN, X., XU, Y. 2002. Investigation on sulphation of modified Ca based sorbent. Fuel processing technology, 79:121-133.

WEBB, P.A. 2001. An introduction to the physical characterisation of materials by Mercury intrusion porosimetry with emphasis on reduction and presentation of experimental data. Micromeritics Instrument Corporation. Norcross, Georgia.

http://www.pss.aus.net/products/micromeritics/equip_surface_area/2010/2020.html [Date of access: 05 December 2006]

WILLIAMS, P.J. 1999. Use of seawater as makeup water for wet flue gas desulphurisation systems. Presented to: EPRI-DOE-EPA Combined utility air pollutant control symposium. August 16-20, 1999. Atlanta, Georgia, U.S.A.

WORLD COAL INSTITUTE (WCI). 2005a. Coal: Secure energy. 48p. www.worldcoal.org [Date of access: 31 May 2006]

WORLD COAL INSTITUTE (WCI). 2005b. The coal resource: A comprehensive overview of coal. 48p. http://www.worldcoal.org [Date of access: 31 May 2006]

WORLD ENERGY COUNCIL (WEC). 2006. Focus on the optimized fuel use and improvement of the advanced clean coal use technologies. MENÉNDEZ, Emilio (ENDESA), ALEGRÍA, Fernando (CIEMAT-OCICARBON), AVELLANAL, Iñaki (BWE), BALLESTEROS, Juan C. (ENDESA) Spain. http://www.worldenergy.org/wec-geis/publications [Date of access: 08 June 2006]

YANG, R.T. 1997.Gas separation by adsorption. Imperial college press. 352p.

YRJAS, P., IISA, K., HUPA, M. 1995. Comparison of SO_2 capture capacities of limestones and dolomites under pressure. Fuel, 74:395-400

ZEVENHOVEN, C.A.P., YRJAS, K.P., HUPA, M.M. 1998b. Product layer development during sulphation and sulfidation of uncalcined limestone particles at elevated pressures. Industrial and engineering chemistry research, 37: 2639-2646.

ZEVENHOVEN, R., YRJAS, P., HUPA, M. 1998a. Sulphur dioxide capture under PFBC conditions: the influence of sorbent particle. Fuel, 77:285-292.

ZHANG, L., SATO, A., NINOMIYA, Y., AND SASAOKA, E. 2003. In situ desulphurisation during combustion of high sulphur coal added with sulphur capture sorbents. Fuel, 82:255-266.

ZHENG, Y., KIIL, S., JOHNSSON, J.E., ZHONG Q. 2002. Use of spray dry absorption product in wet flue gas desulphurisation plants: pilot-scale experiments. Fuel, 81:1899-1905.

ZHONG, Q. 1995. Direct sulphation reaction of SO_2 with calcium carbonate. Thermochimica acta, 260:125-136.

Appendix A: Fixed parameters used for model calculation

The table below gives parameter values used in the model calculation

Table A.1: Constant parameters used in model calculations

Model Constants	**Value**
Molar mass of SO_2 (kg/kmol)	64.06
Molar mass of $CaCO_3$ (kg/kmol)	100.09
Molar mass of CaO (kg/kmol)	56.08
Molar mass of MgO (kg/kmol)	40.3
Molar mass of $CaSO_4$ (kg/kmol)	136.14
Molar volume $CaCO_3$ (cm^3/mol)	36.9
Molar volume $CaSO_4$ (cm^3/mol)	46
Molar volume CaO (cm^3/mol)	19.3
Molar density $CaCO_3$ (mol/m^3)	27085
Z CaO	2.73
Z $CaCO_3$	1.247
Weight % of SO_2 (mol/mol)	0.002
R (universal gas constant)(J/°C.mole)	8.314
γ (tortuosity)	3
Temperature(C)	750-900
Temperature(K)	1023.15-1173.15
V_{SO2} (empirical constants) Fuller	41.1
V_{N2} (empirical constants) Fuller	17.9
D_{mol}(m^2/s)	$1.15x10^{-4}$